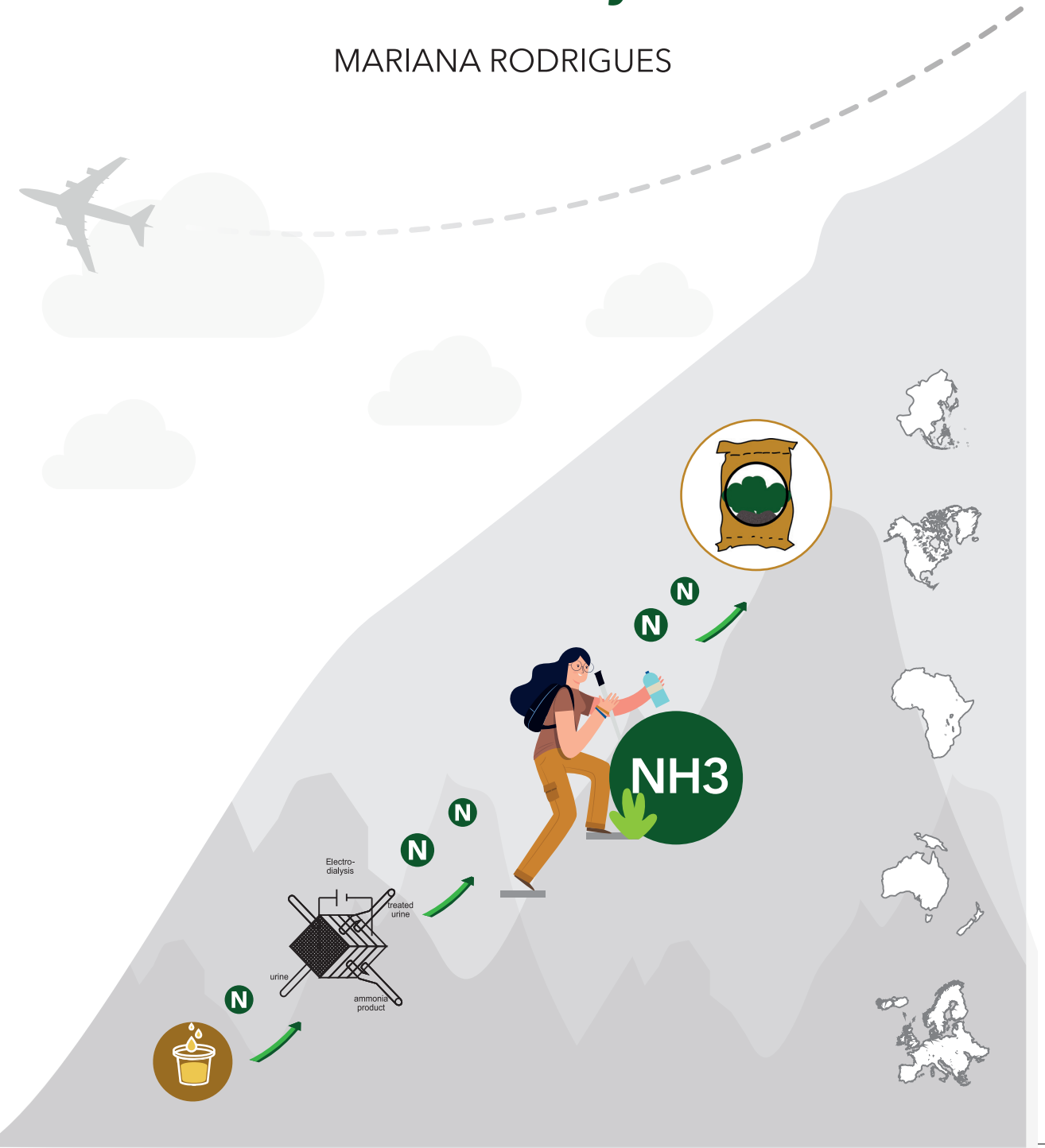


Modeling and Application of Electrochemical Ammonia Recovery

MARIANA RODRIGUES



Propositions

1. Increasing the removal efficiency of an electrochemical system for ammonia recovery costs less energy than other technologies. (this thesis)
2. Up-scaled ammonia recovery should be operated exclusively under pH control. (this thesis)
3. The use of recovered fertilizers is limited due to few agriculture studies on its safety and efficiency.
4. The surpass of several planetary boundaries indicates that environmental challenges need downstream solutions.
5. War drives technological progress faster than any other societal concern.
6. International traveling is crucial for both personal and professional growth.

Propositions belonging to the thesis, entitled

"Modeling and application of electrochemical ammonia recovery"

Mariana Rodrigues

Wageningen, 7th of October, 2022

Modeling and application of electrochemical ammonia recovery

Mariana Rodrigues

Thesis committee

Promotor

Prof. Dr C.J.N. Buisman
Professor of Biological Recovery and Reuse Technology
Wageningen University & Research

Co-promotors

Prof. Dr H.V.M. Hamelers
Special Professor of Electrochemical Resource Recovery
Wageningen University & Research

Dr. P. Kuntke
Lecturer, Environmental Technology
Wageningen University & Research

Other members

Prof. Dr W.M. De Vos, University of Twente, Enschede
Dr. P.F.H. van den Brink, Evides, Rotterdam, The Netherlands
Prof. Dr K.J. Keesman, Wageningen University & Research
Prof. Dr J. Radjenovic, ICREA, Girona, Spain

This research was conducted under the auspices of the Graduate School Wageningen Institute for Environment and Climate Research.

Modeling and application of electrochemical ammonia recovery

Mariana Rodrigues

Thesis

submitted in fulfilment of the requirements for the degree of doctor
at Wageningen University
by the authority of the Rector Magnificus,
Prof. Dr A.P.J. Mol,
in the presence of the
Thesis Committee appointed by the Academic Board
to be defended in public
on Friday 7 October 2022
at 1:30 p.m. in De Harmonie, Leeuwarden.

Mariana Rodrigues

Modeling and application of electrochemical ammonia recovery

180 pages

PhD thesis, Wageningen University, Wageningen, the Netherlands (2022)

With references, with summary in English

ISBN: 978-94-6447-371-1

DOI: <https://doi.org/10.18174/575597>

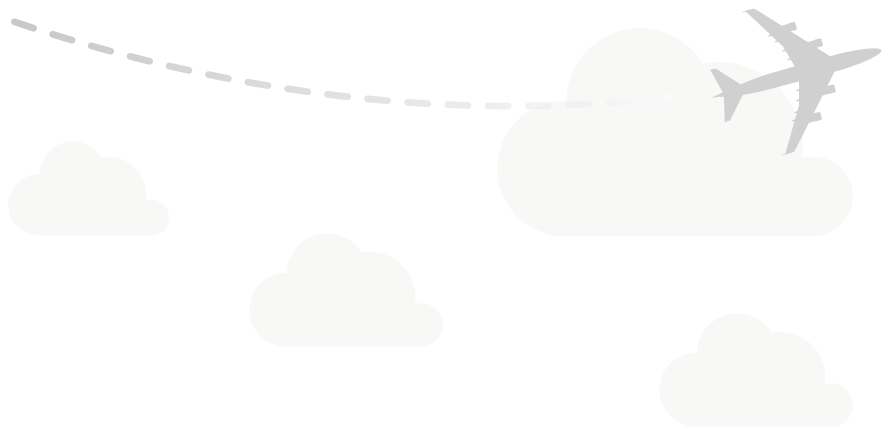
Table of Contents

Chapter 1:	General Introduction	7
Chapter 2:	Exploiting Donnan Dialysis to Enhance Ammonia Recovery in an Electrochemical System	17
Chapter 3:	Donnan Dialysis for scaling mitigation during electrochemical ammonium recovery from complex wastewater	35
Chapter 4:	Minimal bipolar membrane cell configuration for scaling up ammonium recovery	63
Chapter 5:	Effluent pH correlates with electrochemical nitrogen recovery efficiency at pilot scale operation	89
Chapter 6:	Effects of Current on the Membrane and Boundary layer selectivity in Electrochemical systems designed for nutrient recovery	105
Chapter 7:	Critical transport regimes during electrochemical ammonia recovery	127
Chapter 8:	General Discussion	153
Summary		168
Epilogue		
	List of Publications	172
	About the Author	173
	Acknowledgments	174



Chapter 1

General Introduction



A changing perspective on the environment

Fifty years ago, the implementation of measures to protect the environment was only a “developed country” concern. Around this time the EPA (Environmental Protection Agency) was founded in the United States (1970), and the first European environmental policies were discussed at European Council in Paris (1972) ¹⁻³. Although borders are established between countries, our planet works as a whole. Many positive and negative actions occurring in one country affect the environment of the surrounding ones. Therefore, the interest in environmental measures was expanded worldwide, and our young “environmental conscience” is constantly developing.

In 2015, the United Nations (UN) established the 2030 Agenda for Sustainable Development to address this decade’s most challenging environmental issues and accomplish a more equitable use of resources ⁴. According to the UN, we still have a long way to go to solve climate change, air and water pollution, water scarcity, energy transition, overpopulation, etc. As the world population grows, some crucial natural resource reserves are close to depletion. Therefore, the development of sustainable food supply and waste management are urgent.

Framing Nitrogen recovery in nowadays environment challenges

When mentioning both food and waste, two terms are unavoidable: phosphate and nitrogen. Unlike some other organisms that adapted to starvation conditions to survive, mankind developed sophisticated processes to avoid famine. Nitrogen and phosphate fertilizers are essential compounds that allowed our population to increase to more than 7 billion ^{5,6}. Phosphate is extracted from natural resources, yet these are finite. Consequently, we face a phosphate crisis, as the phosphate rock reserves are scarce and its extraction often causes heavy metals pollution ^{7,8}. Nitrogen, however, is abundant in our atmosphere, so the “nitrogen crisis” is often based on the pollution of reactive nitrogen.

The urgent need for nitrogen for both food and explosives production (World War I) in Germany in the 20th century led to the development of the Haber-Bosch process (HB). Here, nitrogen gas (N_2) is converted to a reactive form (NH_4^+ , NH_3) ^{6,9}. Using natural gas as the primary source of hydrogen and energy, HB requires considerable energy to first break the chemical bonds between the carbon and hydrogen atoms and the triple bonds of the nitrogen atoms in a nitrogen gas molecule (N_2). Consequently, HB consumes 2% of the energy produced worldwide, and it represents almost 2% of the world’s carbon emissions due to the energy source, fossil fuels,

used. To change the global energy panorama, two points should be addressed: (i) recycle reactive nitrogen and (ii) change the energy source of HB.

With a growing population the need for reactive nitrogen will increase. Therefore, making ammonia a commodity available through a circular economy is a priority^{10,11}. At first sight, the nitrogen issue might seem an isolated topic. However, addressing nitrogen recovery is key to consume less energy, to emit less greenhouse gases, a sustainable food production, and less water pollution.

So far, nitrogen recovery from wastewater has been explored through different technologies summarized in Figure 1.

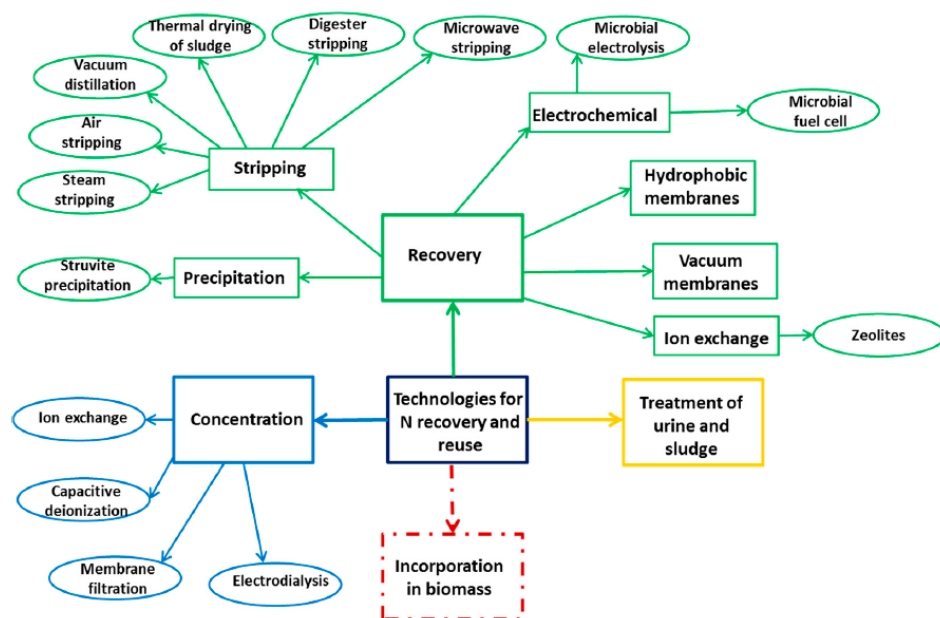


Figure 1. Nitrogen recovery technologies (adapted from ⁹). Within ammonia recovery technologies, the main principles include precipitation, gas permeable membranes (stripping), ion exchange membranes (electrochemical), biological treatment, and concentration electrokinetic processes.

At lab scale, the performance of nitrogen recovery technologies is quite ample for wastewaters with concentrations from 60 to 8000 mgN/L. Nitrogen removal efficiencies from concentrated streams such as urine or digestate often vary from 60 to 95%. However the energy input required fluctuates and it is a bottleneck for implementation. Additionally, for all processes presented in Figure 1, certain advantages and disadvantages can be identified, specifically related to the technical and economic feasibility, sustainability, maturity, or possibility of scaling up^{9,12–15}.

The purity of recovered products also influences the implementation of recovery technologies. Ideally, a recovery technology should yield a contaminant free product, avoid the consumption of extra chemicals and emissions of pollutant substances (greenhouse gases, for example).

Electrochemical systems for ammonia recovery

One viable option for nitrogen recovery from concentrated wastewater streams is the electrochemical systems (ES) ¹⁶. ES was indicated as a promising technology due to its robustness, stability, purification, and concentration capacity, with the promise of being a chemical-free and low energy process ^{11,16}.

Generally, an ES includes an anode and cathode electrodes in a solution connected through an external circuit ¹⁷. When first used for ammonia removal/recovery, the anode and cathode were separated by a cation exchange membrane (CEM) to separate the ammonium ions from other components present in the wastewater. Here, the system works as a concentration process, see Figure 2.

Considering the pKa of NH_4^+ and NH_3 equals 9.25 at 25 degrees, these two nitrogen species can often both be found in solution ^{18,19}. In an ES, the anode produces protons that acidify the ammonia in wastewater ($\text{H}^+ + \text{NH}_3 \rightarrow \text{NH}_4^+$). Once in the ion form, ammonium can be transported over the CEM. On the other side, the cathode reaction generates hydroxide, which reacts with the transported ammonium. Therefore, ammonia is formed ($\text{NH}_4^+ + \text{OH}^- \rightarrow \text{NH}_3$) and the pH in the cathode increases. This allows for further concentration or NH_3 extraction. The NH_3 extraction step aims to even further purify the recovered nitrogen and can be achieved by combining ES with for example ammonia stripping (gas-permeable membranes). Here, the ammonia gas formed at the cathode is extracted and separated from the other cations ^{20,21}, see Figure 2A.

In order to decrease the energy input required to recover ammonia, a few modifications have been introduced in the ES (shown in Figure 2A, see Figure 2B) ^{22,24}. Kuntke et al., 2017 introduced a third compartment (feed) between the anode and cathode which allowed to use other redox reactions at the anode, such as hydrogen gas oxidation. This reaction has a lower electrode potential than for example O_2 evolution. Additionally, wastewater components were separated from the electrode by a membrane electrode assembly (MEA), avoiding the formation of undesired substances (for example, chlorine gas).

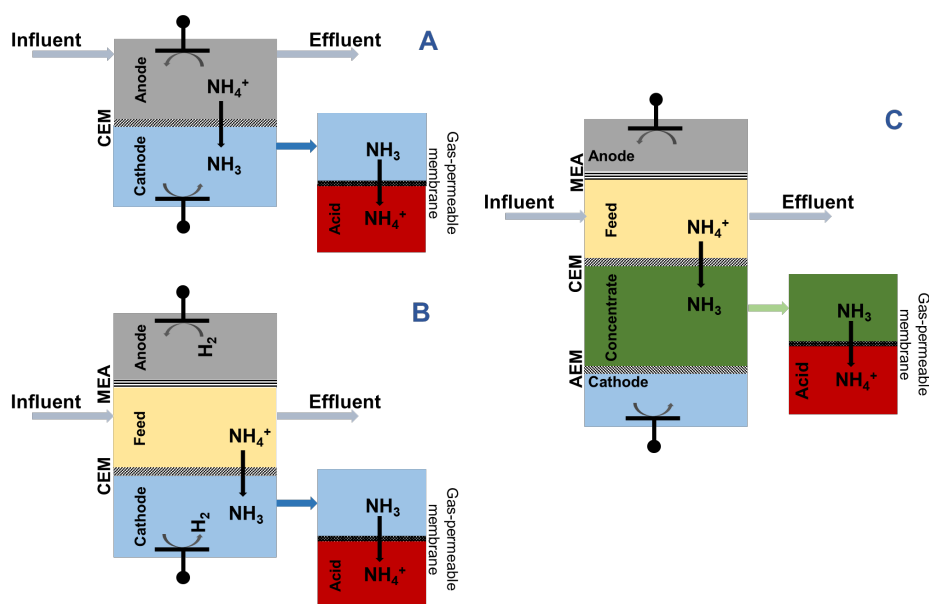


Figure 2. Evolution of ES for ammonia recovery. Initially, it was used a two-compartment cell ^{20,21}(A). The addition of a feed compartment ²²(B) and a concentrate ²³(C) compartment allow to isolate the purification reactions from the electrode reactions.

On the cathode side, water splitting results in the production of hydroxide as well as hydrogen gas. If separated, hydrogen gas can be used as an energy source or re-used in the ES. To separate the hydrogen gas from the ammonia and prevent its loss over the gas-permeable membrane, an anion exchange membrane (AEM) was integrated in between the concentrate and cathode compartment, see Figure 2C ²³. The introduction of AEM and CEM shielding the electrodes also allowed to separate the electrodes reaction from the purification ^{23,25}. This resulted in an extra concentrate compartment where cations are concentrated and a separated cathode where hydroxide and hydrogen are produced. The hydroxide is transported over the AEM, and ammonia gas is formed once the hydroxide reacts with NH_4^+ . As aforementioned, the ammonia gas can be recovered and the hydrogen re-used for the anode reaction, decreasing the overall energy input of the system.

During electrochemical ammonia recovery, the negatively charged functional groups of the CEM block the transport of anions and allow the transport of all cations in wastewater towards the cathode ²⁶. Furthermore, both ammonium ions and protons have a relatively small hydrated ionic size and fast diffusivity, ideal to be transported across the CEM. As a consequence, other cations also accumulate in a concentrated solution from which ammonia is extracted. Being both a diffusion and electrically driven process, the flux of ions through the CEM is influenced by different factors

such as applied current density and ratio among ionic species. Overall, optimizing the ammonium flux over the CEM is crucial in order to increase the performance of an electrochemical system regarding removal, current efficiency and, consequently, energy input.

Overall, the use of ES previously described for nitrogen recovery, yielded 1) an often-limited removal of all nitrogen loaded when supplied with different wastewaters; 2) a variable energy consumption ($>16\text{kJ/gN}$); and 3) were mostly performed at lab-scale (low maturity level – TRL 3-5). Further research should be conducted to study the scalability and improve recovery and energetic performance. These steps are required to future mature the technology and secure sufficient nitrogen availability in the future

Scope and context of the Research

Compared to other technologies, ES is still lagging behind regarding economic, technical, and scale-up feasibility^{9,11,14,16,27,28}. This thesis emerged from the need to bring electrochemical ammonia recovery one step forward towards up-scaling while maintaining a high removal efficiency at a low energy input. ES excels in decentralized applications of concentrated streams. Therefore, the work developed in this thesis focused on electrochemical systems performance using different concentrated streams such as urine, digestate, and blackwater.

Other cations are present in these wastewaters and are transported over the CEM together with ammonium, ending up in the concentrated stream. Chapters 2 and 3 explore how Donnan dialysis can improve the performance of ES once a concentration gradient is formed between both sides of the CEM. First, Donnan dialysis allows the exchange of sodium and potassium with ammonium without extra energy input. Furthermore, the transport of protons is also promoted during Donnan dialysis, creating an environment less favorable for inorganic scaling (calcium precipitates – CaCO_3). The concepts in these chapters were also extended to pilot operation during “intermittent mode” operation (Chapter 5).

Regarding scaling and economic feasibility, it is important to consider that electrodes have considerably high costs compared to membranes²⁹. Chapter 4 explores how ES for ammonia recovery can be scaled by using bipolar exchanges membranes (BPMs) due to their water-splitting ability. Aside from scaling up the membrane area, the treatment capacity can be extended by improving the transport over membrane

area. Also in Chapter 4, the effect of increasing current density on the treatment capacity and performance of ES was explored. The same principles were applied at a pilot scale in Chapter 5. Furthermore, in Chapter 5, we identified that controlling the current and/or the loading was insufficient to achieve high removal efficiency. Therefore, a new operation setting, pH control, was characterized for pilot scale.

Current, nitrogen loading, mode of operation (continuous vs. intermittent), and pH are among the variables that can be controlled when operating ES for ammonia recovery from concentrated streams. Although ES appears to be a simple system, the influence of these parameters is not yet evident, and an equally limited performance is often observed under distinctive operation conditions. Chapters 6 and 7 characterize the transport over the CEM in an ES for ammonia recovery (modeling approach). The behavior between $\text{NH}_4^+/\text{NH}_3$ and the use of a two-step process creates dynamic conditions in the system and further influences ion transport. Moreover, the ES do not behave as an electrodialysis process, and an early limiting current region is observed. In Chapter 7, we identify optimal regions of operation for maximum current efficiency (ammonium transport number equal to one) or maximum removal efficiency.

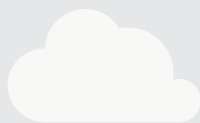
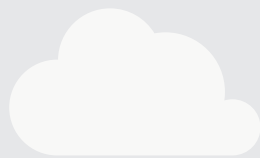
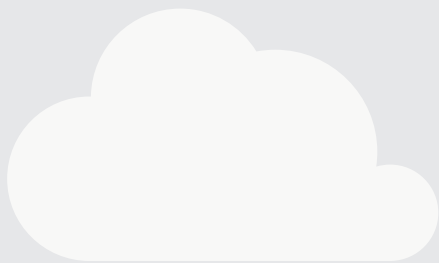
In Chapter 8, a discussion on how the findings of this thesis can lead to the implementation of electrochemical ammonia recovery is provided. Additionally, further challenges and future research are also included in the last chapter. Finally, an overall discussion on nitrogen recovery is presented.

References

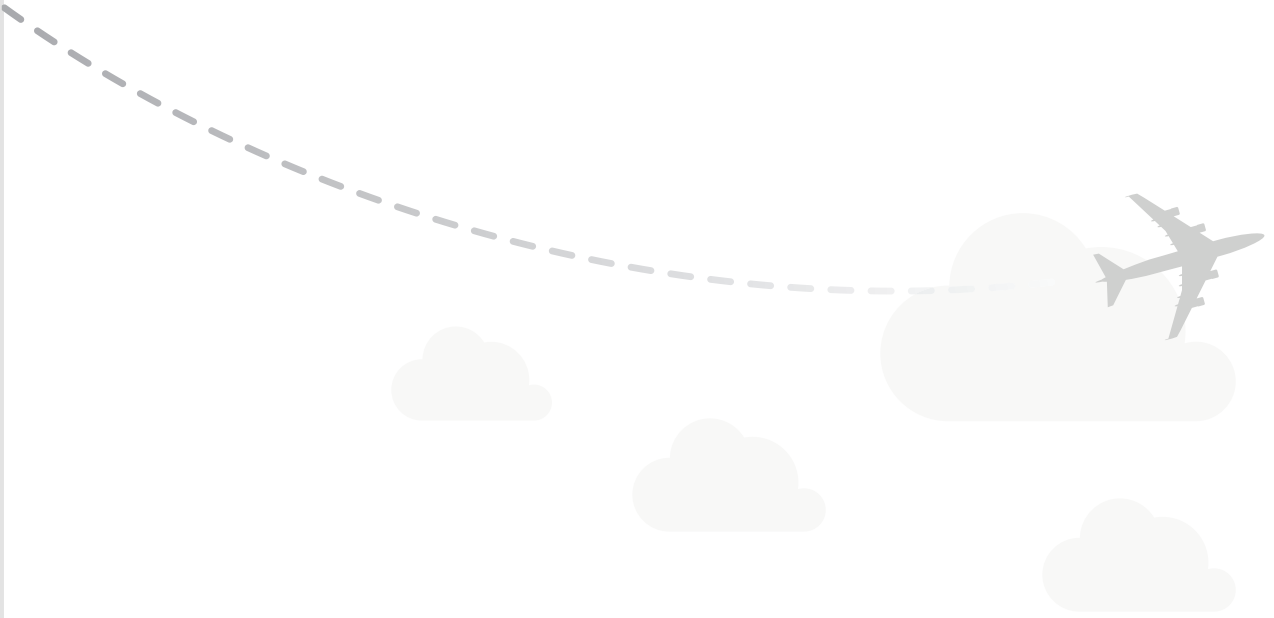
- (1) *The Origins of EPA*. <https://www.epa.gov/history/origins-epa>.
- (2) Jordan, A. *Environmental Policy in the EU*; Routledge, 2012. <https://doi.org/10.4324/9780203109823>.
- (3) Basis, L. *Environment Policy : General*. **2021**, No. 2009, 1–5.
- (4) Iberdrola. *The big global environmental issues we need to resolve by 2030*. <https://www.iberdrola.com/sustainability/most-important-environmental-issues>.
- (5) H. Sabry, A.-K. Synthetic Fertilizers, Role and Hazards. *Fertilizer technology* **2015**, No. November, 111–133. <https://doi.org/10.13140/RG.2.1.2395.3366>.
- (6) Razon, L. F. Reactive Nitrogen: A Perspective on Its Global Impact and Prospects for Its Sustainable Production. *Sustainable Production and Consumption* **2018**, 15, 35–48. <https://doi.org/10.1016/j.spc.2018.04.003>.
- (7) Cordell, D.; Rosemarin, A.; Schröder, J. J.; Smit, A. L. Towards Global Phosphorus Security: A Systems Framework for Phosphorus Recovery and Reuse Options. *Chemosphere* **2011**, 84 (6), 747–758. <https://doi.org/10.1016/j.chemosphere.2011.02.032>.
- (8) Cordell, D.; Drangert, J. O.; White, S. The Story of Phosphorus: Global Food Security and Food for Thought. *Global Environmental Change* **2009**, 19 (2), 292–305. <https://doi.org/10.1016/j.gloenvcha.2008.10.009>.
- (9) van der Hoek, J. P.; Duijff, R.; Reinstra, O. Nitrogen Recovery from Wastewater: Possibilities, Competition with Other Resources, and Adaptation Pathways. *Sustainability (Switzerland)* **2018**, 10 (12). <https://doi.org/10.3390/su10124605>.
- (10) Chang, J.; Havlík, P.; Leclère, D.; de Vries, W.; Valin, H.; Deppermann, A.; Hasegawa, T.; Obersteiner, M. Reconciling Regional Nitrogen Boundaries with Global Food Security. *Nature Food* **2021**, 2 (9), 700–711. <https://doi.org/10.1038/s43016-021-00366-x>.
- (11) Beckinghausen, A.; Odlare, M.; Thorin, E.; Schwede, S. From Removal to Recovery: An Evaluation of Nitrogen Recovery Techniques from Wastewater. *Applied Energy* **2020**, 263 (February), 114616. <https://doi.org/10.1016/j.apenergy.2020.114616>.
- (12) Ledezma, P.; Kuntke, P.; Buisman, C. J. N.; Keller, J.; Freguia, S. Source-Separated Urine Opens Golden Opportunities for Microbial Electrochemical Technologies. *Trends in Biotechnology*. April 2015, pp 214–220. <https://doi.org/10.1016/j.tibtech.2015.01.007>.
- (13) Macura, B.; Johannesdottir, S. L.; Piniewski, M.; Haddaway, N. R.; Kvarnström, E. Effectiveness of Ecotechnologies for Recovery of Nitrogen and Phosphorus from Anaerobic Digestate and Effectiveness of the Recovery Products as Fertilisers: A Systematic Review Protocol. *Environmental Evidence* **2019**, 8 (1), 29. <https://doi.org/10.1186/s13750-019-0173-3>.
- (14) Maurer, M.; Pronk, W.; Larsen, T. A. Treatment Processes for Source-Separated Urine. *Water Research* **2006**, 40 (17), 3151–3166. <https://doi.org/10.1016/j.watres.2006.07.012>.
- (15) Sengupta, S.; Nawaz, T.; Beaudry, J. Nitrogen and Phosphorus Recovery from Wastewater. *Current Pollution Reports* **2015**, 1 (3), 155–166. <https://doi.org/10.1007/s40726-015-0013-1>.
- (16) Liu, Y.; Deng, Y. Y.; Zhang, Q.; Liu, H. Overview of Recent Developments of Resource Recovery from Wastewater via Electrochemistry-Based Technologies. *Science of the Total Environment* **2021**, 757, 143901. <https://doi.org/10.1016/j.scitotenv.2020.143901>.
- (17) Desloover, J.; Abate Woldeyohannis, A.; Verstraete, W.; Boon, N.; Rabaey, K. Electrochemical Resource Recovery from Digestate to Prevent Ammonia Toxicity during Anaerobic Digestion. *Environmental Science and Technology* **2012**, 46 (21), 12209–12216. <https://doi.org/10.1021/es3028154>.

- (18) Darestani, M.; Haigh, V.; Couperthwaite, S. J.; Millar, G. J.; Nghiem, L. D. Hollow Fibre Membrane Contactors for Ammonia Recovery: Current Status and Future Developments. *Journal of Environmental Chemical Engineering* **2017**, 5 (2), 1349–1359. <https://doi.org/10.1016/j.jece.2017.02.016>.
- (19) Kissel, D. E.; Cabrera, M. L. AMMONIA. In *Encyclopedia of Soils in the Environment*; Elsevier, 2005; pp 56–64. <https://doi.org/10.1016/B0-12-348530-4/00177-6>.
- (20) Christiaens, M. E. R.; Gildemyn, S.; Matassa, S.; Ysebaert, T.; de Vrieze, J.; Rabaey, K. Electrochemical Ammonia Recovery from Source-Separated Urine for Microbial Protein Production. *Environmental Science & Technology* **2017**, 51 (22), 13143–13150. <https://doi.org/10.1021/acs.est.7b02819>.
- (21) Rodríguez Arredondo, M.; Kuntke, P.; ter Heijne, A.; Hamelers, H. V. M.; Buisman, C. J. N. Load Ratio Determines the Ammonia Recovery and Energy Input of an Electrochemical System. *Water Research* **2017**, 111 (3), 330–337. <https://doi.org/10.1016/j.watres.2016.12.051>.
- (22) Kuntke, P.; Rodríguez Arredondo, M.; Widyakristi, L.; ter Heijne, A.; Sleutels, T. H. J. A. J. A.; Hamelers, H. V. M.; Buisman, C. J. N. N. Hydrogen Gas Recycling for Energy Efficient Ammonia Recovery in Electrochemical Systems. *Environmental Science & Technology* **2017**, 51 (5), 3110–3116. <https://doi.org/10.1021/acs.est.6b06097>.
- (23) Kuntke, P.; Rodrigues, M.; Sleutels, T.; Saakes, M.; Hamelers, H. V. M.; Buisman, C. J. N. N. Energy-Efficient Ammonia Recovery in an Up-Scaled Hydrogen Gas Recycling Electrochemical System. *ACS Sustainable Chemistry & Engineering* **2018**, 6 (6), 7638–7644. <https://doi.org/10.1021/acssuschemeng.8b00457>.
- (24) Tarpeh, W. A.; Barazesh, J. M.; Cath, T. Y.; Nelson, K. L. Electrochemical Stripping to Recover Nitrogen from Source-Separated Urine. *Environmental Science and Technology* **2018**, 52 (3), 1453–1460. <https://doi.org/10.1021/acs.est.7b05488>.
- (25) Thompson Brewster, E.; Mehta, C. M.; Radjenovic, J.; Batstone, D. J. A Mechanistic Model for Electrochemical Nutrient Recovery Systems. *Water Research* **2016**, 94, 176–186. <https://doi.org/10.1016/j.watres.2016.02.032>.
- (26) Yang, K.; Qin, M. The Application of Cation Exchange Membranes in Electrochemical Systems for Ammonia Recovery from Wastewater. *Membranes (Basel)* **2021**, 11 (7), 494. <https://doi.org/10.3390/membranes11070494>.
- (27) Chang, H.; Lu, M.; Zhu, Y.; Zhang, Z.; Zhou, Z.; Liang, Y.; Vidic, R. D. Consideration of Potential Technologies for Ammonia Removal and Recovery from Produced Water. *Environmental Science & Technology* **2022**, 56 (6), 3305–3308. <https://doi.org/10.1021/acs.est.1c08517>.
- (28) Radjenovic, J.; Sedlak, D. L. Challenges and Opportunities for Electrochemical Processes as Next-Generation Technologies for the Treatment of Contaminated Water. *Environmental Science and Technology* **2015**, 49 (19), 11292–11302. <https://doi.org/10.1021/acs.est.5b02414>.
- (29) Kim, J. F. Recent Progress on Improving the Sustainability of Membrane Fabrication. *Journal of Membrane Science and Research* **2020**, 6 (3), 241–250. <https://doi.org/10.22079/JMSR.2019.106501.1260>.

2



Exploiting Donnan Dialysis to Enhance Ammonia Recovery in an Electrochemical System



This Chapter has been published as:

Rodrigues, M., Sleutels, T., Kuntke, P., Hoekstra, D., ter Heijne, A., Buisman, C.J.N., Hamelers, H.V.M., 2020. Exploiting Donnan Dialysis to enhance ammonia recovery in an electrochemical system. *Chem. Eng. J.* 395, 125143. <https://doi.org/10.1016/j.cej.2020.125143>

Abstract

A hydrogen recycling electrochemical system (HRES) can be used for energy efficient removal of TAN (Total ammonia nitrogen, ammonium and ammonia) from wastewater. When a current is applied, a concentration gradient of cations builds up between catholyte and feed solution. When no current is applied, cations (Na^+ and K^+) diffuse back to the feed solution from the catholyte as a result of the concentration difference. These cations will be exchanged for other cations (NH_4^+ and H^+) to maintain electroneutrality: a phenomenon known as Donnan Dialysis. In this study, Donnan Dialysis was explored as a strategy to enhance the TAN removal efficiency in an HRES. In continuous operation, Donnan Dialysis did not clearly affect TAN removal efficiency. In batch operation, Donnan Dialysis resulted in (10 ± 2) % higher removal efficiency compared to operation without Donnan Dialysis. By analyzing transport numbers of the different cations, we show that in batch mode, Donnan Dialysis indeed exchanges mostly NH_4^+ with Na^+ and K^+ . In continuous mode, however, more protons were transported from anode to cathode. Batch operation with Donnan Dialysis achieved similar removal to continuous operation but consumed less energy (between $7.8 \text{ kJ g}_\text{N}^{-1}$ and $10.1 \text{ kJ g}_\text{N}^{-1}$) than continuous operation. Donnan Dialysis can be a good strategy to enhance TAN recovery in batch operation mode since additional ammonium was removed at a lower energy input.

Introduction

Recovery and re-use of ammonia from aqueous waste streams is gaining more and more attention, both for environmental and economic reasons ¹. The conversion of N_2 to synthetic fertilizer through the energy-intensive Haber–Bosch process is responsible for 1% of the primary global energy consumption. Just in Europe, the removal of the nitrogen compounds from water streams costs up to 320 billion euros per year ². Besides these conventional processes, several ammonia/ammonium recovery methods exist and have been studied at different scales, including NH_3 -stripping, struvite precipitation, and use of zeolites. However, they do require high energy and/or chemicals input ³.

Electrochemical recovery of total ammonia nitrogen (TAN; i.e. NH_4^+ and NH_3) from concentrated streams like urine is an interesting option, considering that TAN can be recovered using less energy compared to other recovery technologies ⁴. The TAN recovered from the electrochemical process is directly suitable for re-use because it is in its reactive form ^{5–7}.

Electrochemical TAN removal relies on an electrical current to drive the positively charged ammonium ion through a cation selective membrane ^{8,9}. Water can be oxidized at the anode to produce oxygen and reduced at the cathode to produce hydrogen gas. Electrodialysis systems have been shown to recover ammonia from wastewater at high energy input ^{4,8,10,11}. Recently, it was shown that the energy input for TAN removal can be reduced when the produced hydrogen gas at the cathode is recycled to the anode to be oxidized again ¹². This hydrogen recycling electrochemical system (HRES) achieved a TAN removal efficiency of 73% while consuming 26 kJ g_N^{-1} , when operating at 20 A m^{-2} . These results were a considerable improvement compared to a previous electrochemical system without H_2 recycling treating digestate achieving 58% TAN removal and consuming 60.1 kJ g_N^{-1} , when operated at the same current density ⁸. Rodriguez Arredondo et al., 2017 achieved a TAN removal efficiency of 63% in an electrochemical system using synthetic urine as influent. This system was operated at 50 A m^{-2} and used 49 kJ g_N^{-1} ¹³.

A successful HRES design provides high TAN removal at low energy input and is dependent on several parameters, the main ones being: the ratio between applied current density and the TAN loading (L_N , load ratio), the catholyte pH and the internal resistance of the system ⁷.

One major challenge in achieving a high TAN removal efficiency is reducing the co-transport of cations other than ammonium (e.g., Na^+ , K^+ , Ca^{2+} , Mg^{2+}) towards the cathode (as a result of the applied current). Most of these cations are present in urine at high concentrations ^{14,15}. The flux of ions through a cation exchange membrane (CEM) can be described by two driving forces, an electric field and a concentration gradient in the membrane. The Nernst-Planck equation describes these two forces:

$$J_i = D_i \left(\frac{\partial c_i}{\partial x} + \frac{z_i F}{RT} c_i \frac{\partial \phi}{\partial x} \right)$$

Where J_i is the flux of the ion ($\text{mol m}^{-2} \text{s}^{-1}$), D_i is the diffusion co-efficient of the ion ($\text{m}^2 \text{s}^{-1}$), c_i is the concentration of ion (mol m^{-3}), x is the position inside the membrane (m), z_i is the valence of the ion, F is the Faraday constant (C mol^{-1}), R is the universal gas constant ($\text{J K}^{-1} \text{mol}^{-1}$), T is the temperature (K), and ϕ is the electric field potential (V). In general, we assume for simplification that: (i) CEM behaves as an ideal membrane and no counter ions (anions) are being transported, (ii) electron neutrality is maintained, (iii) the diffusion coefficients of the main cations are almost identical, and (iv) hydroxide ions concentrations are negligible (pH range 4 - 10). Therefore, when operating an HRES, the concentration of cations in the catholyte will initially increase, until a stationary equilibrium is reached. At equilibrium conditions, only ammonium and protons are effectively transported through the CEM ¹⁶. The accumulation of cations other than ammonium in the catholyte leads to an additional energy loss, due to the formation of a concentration gradient induced membrane potential ¹⁷. Therefore, to maintain the same TAN removal more energy is required to force the ammonium transport against the concentration gradient, increasing the cost of operation.

In the absence of an applied electrical potential, the cations accumulated in the cathode compartment will diffuse back towards the anode (feed) compartment as a result of the concentration difference. For reasons of electro neutrality, this can only happen when either anions also diffuse from cathode to anode, or when other cations diffuse from anode to cathode. Based on the above mentioned assumption the flux of ammonium $J_{\text{NH}_4^+}$ can be described as following:

$$J_{\text{NH}_4^+} = - \sum_{\text{CEM}} z_i J_i$$

This exchange of ions of the same charge through a selective membrane is known as Donnan Dialysis. As an example, Donnan Dialysis has been explored in desalination processes Dialysis via DC electro Dialysis ¹⁸, in the removal of metal ions such as Cu^{+2}

from refinery wastewater or to remove divalent cations present in the influent of reverse electrodialysis^{19,20}. Donnan Dialysis has been previously observed for current driven ammonium transport in Microbial Fuel cell (MFC)²¹. It was shown that the diffusion (j_{dif}) of potassium from cathode to anode increased the expected transport of ammonium from anode to cathode. Donnan Dialysis has not yet been investigated as a strategy to enhance ammonium recovery²¹.

The combination of HRES and Donnan Dialysis can increase the recovery efficiency for ammonium by (i) improving the TAN removal efficiency, as the diffusion of cations from cathode to anode can be used to transport additional TAN, (ii) reducing energy consumption, since the Donnan Dialysis operates without electrical energy input.

In this work, we study how Donnan Dialysis can be exploited to increase the removal efficiency of TAN from synthetic urine using an HRES. We show how TAN transport is influenced by Donnan Dialysis in batch and continuous operation of the system.

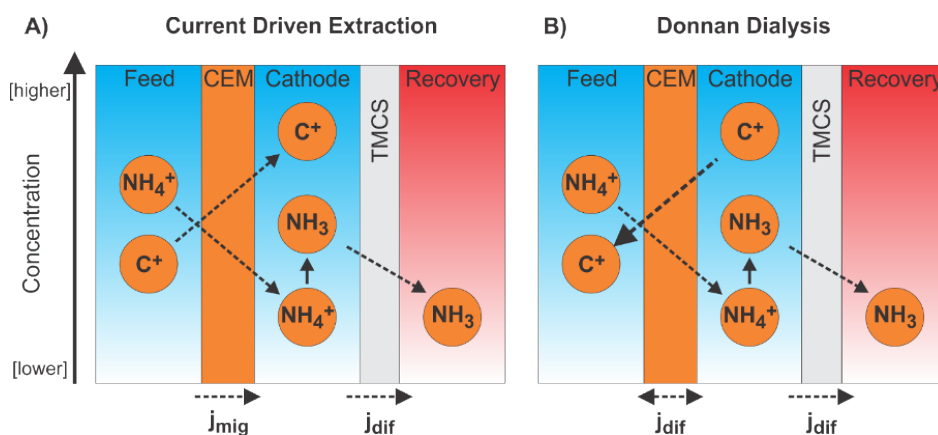


Figure 1. Donnan Dialysis principle for the removal of ammonium. (A) Under the influence of the applied current (j_{mig}), ammonium and other cations (i.e. K^+ and Na^+ ; here represented as C^+) are transported over the cation exchange membrane (CEM) to the cathode. Since ammonium is continuously removed from the cathode solution, only a concentration gradient of C^+ builds up across the CEM. (B) When the current is switched off (j_{dif}), this concentration gradient can be used to extract the remaining ammonium from the feed compartment. C^+ diffuse to the feed and because of electroneutrality, ammonium is forced to diffuse towards the cathode compartment.

Materials and methods

System design

The HRES cell, or electrodialysis cell, consisted of two PMMA (poly methyl methacrylate) panels (21 cm x 21 cm) as frame, with three compartments in between: (i) anode, (ii) feed, and (iii) cathode. The inner dimensions of the anode and the cathode compartments were 10 cm x 10 cm x 0.2 cm. Both compartments were separated from the feed compartment by a cation exchange membrane (CEM; 15 cm x 15 cm Nafion 117, Ion Power GmbH, Germany) with a projected surface of 100 cm². The CEM between feed and anode was coated on one side with a 10 cm x 10 cm of Platinum - Vulcan (carbon) catalyst (0.5 mg Pt cm⁻²), which was connected through a current collector (Pt coated titanium mesh electrode (9.8 cm x 9.8 cm, 5 mg Pt cm⁻² Magneto Special Anodes BV, The Netherlands)), with the electrical circuit. This combination of the CEM and Pt/C catalyst formed a gas diffusion electrode. At this anode, hydrogen was oxidized to electrons and protons. A Pt coated titanium mesh electrode (9.8 cm x 9.8 cm, 5 mg Pt cm⁻² Magneto Special Anodes BV, The Netherlands) was used as a cathode for water reduction to hydrogen gas.

The total volume of the feed and catholyte loops were 1L and 0.5L, respectively. A peristaltic pump was used to circulate the feed and catholyte at 80 ml min⁻¹. The catholyte was recirculated over a gas-permeable hydrophobic membrane (Trans Membrane ChemiSorption, TMCS) module where the ammonia was extracted from the catholyte into a 1 M sulfuric acid solution. The TMCS consisted of a custom-made polypropylene (PP) housing and commercially available membranes (1.5m, 0.2μm pore size, V8/v Type TP, MICRODYN-NADIR GmbH, Wiesbaden, Germany). The initial solution was 2L sulfuric acid (1M) and it was replaced regularly before saturation occurred, to avoid limitations in the extraction of ammonium from the catholyte solution.

For continuous operation, a separate cell was used for the Donnan Dialysis process. This Donnan Dialysis cell consisted of two PMMA (poly methyl methacrylate) panels (21 cm x 21 cm) as frame, including two compartments for: (i) feed and (ii) catholyte. The feed and cathode compartment were separated by a cation exchange membrane (CEM; 15 cm x 15 cm Nafion 117, Ion Power GmbH, Germany) with a projected surface of 100 cm² and dimensions of 10 cm x 10 cm x 0.2 cm.

Experimental strategy

The experiments were performed in continuous and batch mode of operation. The electro dialysis cell was always operated at constant applied current density, 20 A m⁻². The TAN loading to feed compartment was previously optimized in relation to the applied current resulting using the load ratio model ^{7,13}. For a L_N lower than 1, the applied current is

lower than the TAN loaded to the system, meaning that TAN removal over the CEM is limited by the available current, and a limited removal efficiency. A L_N equal to 1 means the current is equal to the TAN loading, meaning that in theory, 100% of TAN can be removed. However, it was previously determined both experimentally and theoretically that a L_N of approximately 1.3 is ideal to achieve high removal efficiency¹³. For higher L_N values, the TAN removal efficiency only slightly increases, as the energy input increases drastically. In the experiments presented, three different load ratios were tested for both modes of operation to characterize the system under ideal and close to the optimum conditions, an excess ($L_N = 0.8$), a sufficient ($L_N = 1$) and an insufficient ($L_N = 1.3$) TAN loading with respect to the applied current density of 20 A m^{-2} .

Continuous experiments

The continuous Donnan Dialysis experiments were performed in the system illustrated in Figure 2. Fresh influent was fed continuously to the feed compartment. Both feed and catholyte solutions were replaced with new synthetic urine at the start of each experiment. The system was operated for 3 to 4 days to reach steady-state (constant TAN removal, cathode pH and cell voltage). The average and standard deviation presented here were from the 5 days during which the system was in steady-state. The catholyte was recirculated in the electro dialysis cell, to the Donnan Dialysis and TMCS module as presented in Figure 2. When operating continuously without the Donnan Dialysis cell, the catholyte was recirculated over the electro dialysis cell and the TMCS module only.

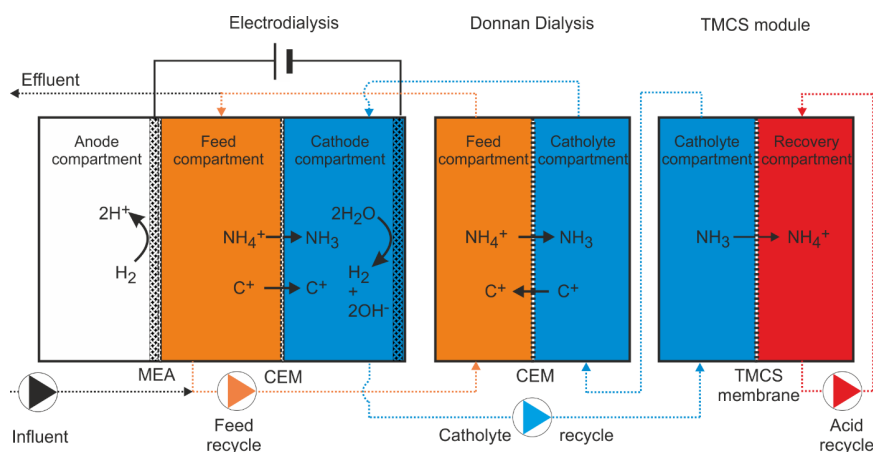


Figure 2. Continuous setup including the HRES, the Donnan Dialysis cell and the TMCS module. Ammonium was continuously extracted from the feed stream in the HRES via electro dialysis, due to the applied current. Additionally, ammonium was removed in the Donnan Dialysis unit through exchange with C^+ . In continuous operation the Donnan Dialysis unit was placed after the TMCS module. First ammonium was extracted from the feed stream through the current and recovered from the catholyte compartment via the TMCS module. Afterwards, remaining ammonium in the feed was extracted through Donnan Dialysis.

Batch experiments

The batch experiments consisted of a 24 hours period where current was applied (Electrodialysis), followed by a 72 hours period where no current was applied (Donnan Dialysis); in the same cell (Figure 3). The batch experiments were performed with a predefined amount of TAN (volume of synthetic wastewater) in the feed compartment. The desired load ratio was obtained by using a certain volume of synthetic urine and at a current density of 20 A m^{-2} during the first 24 hours.

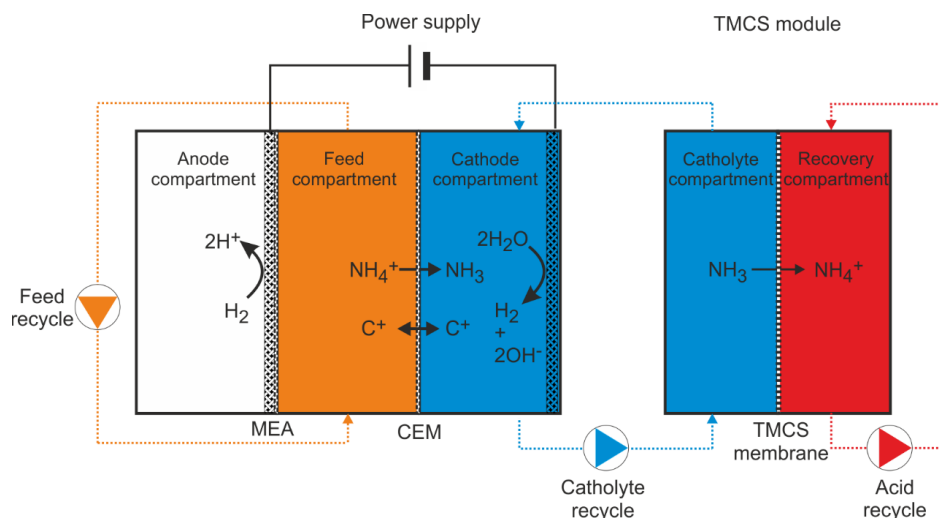


Figure 3. Batch setup including the HRES and the TMCS module. During the first 24 hours, current was applied to the HRES and cation including ammonium were extracted from the feed compartment via electrodialysis. After 24 hours, current was no longer supplied and the HRES acted as Donnan Dialysis cell. Cations (Na^+ and K^+) in the cathode compartment diffused from cathode to the feed compartment and an equal amount of ammonium ions from feed to cathode compartment. The TMCS module was used to continuously extract ammonia from the cathode compartment.

Feed

The synthetic urine consisted of $13.7 \text{ g L}^{-1} (\text{NH}_4)_2\text{CO}_3$, $4.45 \text{ g L}^{-1} \text{ NaCl}$, $1.04 \text{ g L}^{-1} \text{ K}_2\text{SO}_4$ and $1.9 \text{ g L}^{-1} \text{ KCl}$. It had a conductivity of 28.8 mS cm^{-1} and a pH of 9.1. This composition was previously described in Kuntke et al., 2018 and it has similar concentrations of TAN and other cations to urine after a phosphate recovery step. Only monovalent cations were added as it allows to simplify the study of ammonium transport.^{22,23} For continuous operation, the synthetic urine was supplied to the feed recycle vessel by a peristaltic pump (Masterflex L/S, Metrohm Applikon BV, Schiedam, The Netherlands) at a rate of 0.39 mL min^{-1} , 0.51 mL min^{-1} and 0.63 mL min^{-1} corresponding to load ratio of 1.3, 1.0 and 0.8 respectively. During batch experiments, the feed compartment contained 0.93 L, 0.74 L, and 0.62 L of synthetic

urine corresponding to a load ratio of 0.8, 1.0 and 1.3, respectively. The acid solution in the TMCS consisted of 1 M H_2SO_4 with a total volume of 2 L.

Measurements

The following parameters were recorded every minute: the current and cell voltage applied to the electrodialysis cell, the pH and conductivity of feed and catholyte, and the potentials of the anode and cathode. The data was stored in a Memograph M RSG40 datalogger (Endress+Hauser BV, Naarden, The Netherlands). Ag/AgCl reference electrodes (+0.2V vs NHE, QM711X, QiS-Prosence BV, Oosterhout, The Netherlands) were placed in the catholyte and the feed compartment. The pH was measured using an Orbisint CPS112D sensors connected to a Liquiline CM444 transmitter (Endress+Hauser BV). The conductivity of the feed compartment and the catholyte compartment was measured using QC205X EC electrodes and P915-85 – Controller (QiS-Prosence BV, Oosterhout, The Netherlands).

Chemical analysis

For the continuous experiment, samples were taken daily from influent and effluent stream of the feed compartment and from the catholyte. For the batch experiment, samples were taken every 24 hours. All samples were analyzed in duplicate for cations (Na^+ , K^+ , NH_4^+) and anions (SO_4^{2-} , Cl^- , NO_3^- , NO_2^-) with a Metrohm Compact IC Flex 930 with a cation column (Metrosep C 4-150/4.0) and a Metrohm Compact IC 761 with an anion column (Metrosep A Supp 5- 150/4.0) each equipped with a conductivity detector (Metrohm Nederland BV, Schiedam, The Netherlands).

Calculations

All calculations (L_N , removal/recovery, energy use, ion transport number) were based on the methodology reported earlier ¹². L_N was calculated for continuous (a) and for batch operation mode (b).

$$L_{N,c} = \frac{jA}{[NH_4^+]QF} \quad (\text{Equation 1a})$$

$$L_{N,b} = \frac{jAt}{[NH_4^+]VF} \quad (\text{Equation 1b})$$

Where j is the current density ($A\ m^{-2}$), t is the time (s), A is the area of the cell (m^2), $[NH_4^+]$ is the TAN concentration ($mol\ m^{-3}$), V is the volume of the feed (m^3), Q is the inflow rate ($m^3\ s^{-1}$) and F is the Faraday constant ($96485\ C\ mol^{-1}$).

The TAN removal efficiency was calculated as the difference between the initial concentration ($C_{0\text{TAN}}$; mol L⁻¹) and the final concentration of ammonium ($C_{x\text{TAN}}$; mol L⁻¹) related to the initial concentration during the time intervals (0, 24, 48, 72, 96 h)

$$\text{Removal}_{\text{NH}_4} = \frac{C_{0\text{TAN}} - C_{x\text{TAN}}}{C_{0\text{TAN}}} \quad (\text{Equation 2})$$

The energy required for TAN recovery was calculated based on the average cell voltage (E, V), the applied current density (J, A m⁻²), the time interval (t, h), the amount to TAN removed (m_{TAN} , g_N) and the CEM surface area (A, m²).

$$P_{\text{TAN}} = \frac{EJt}{m_{\text{NH}_4A}} \quad (\text{Equation 3})$$

The transport number was calculated based on the difference between the initial ion concentration of the influent and effluent (feed compartment for batch experiments) related to the produced current. The transport number (t_i) was calculated for all ions in solution.

$$t_i = \frac{\Delta C_i z_i F Q A t}{J t} \quad (\text{Equation 4a})$$

$$t_i = \frac{\Delta C_i z_i F V A}{J t} \quad (\text{Equation 4b})$$

where ΔC_i is the difference of concentration between two time points for component i (mol L⁻¹), z_i is the net charge of that cation (-).

Results and discussion

The effect of Donnan Dialysis on the ammonium removal efficiency was studied in continuous and batch mode at different load ratios. For both operation modes, we compared the HRES performance with and without Donnan Dialysis.

Donnan Dialysis led to an increase in TAN removal efficiency only for batch operation.

Figure 4 shows the removal efficiency for TAN in the continuous system with and without Donnan Dialysis at different load ratios. The TAN removal efficiency without Donnan Dialysis was 71% for a load ratio of 0.8, 80% for a load ratio of 1, and 85% for a load ratio of 1.3. Unexpectedly, the TAN removal efficiency with Donnan Dialysis was similar: 68%, 83% and 87%. This increase in TAN removal efficiency with an increase in load ratio is in accordance with previous studies 13.

To understand why Donnan Dialysis did not clearly enhance TAN removal efficiency in the continuous system, batch experiments were performed. In these batch experiments, the Donnan Dialysis process can be distinguished more clearly since it does not occur at the same time as current driven TAN transport.

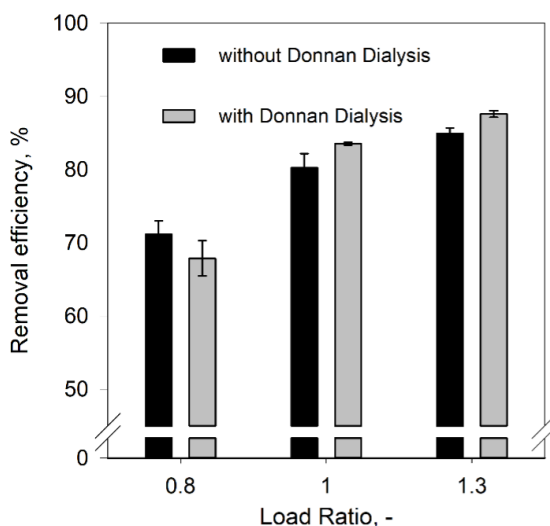


Figure 4. Average removal efficiency obtained during 5 days of continuous operation. The removal was determined with and without Donnan Dialysis at load ratios of 0.8, 1 and 1.3. The total removal was similar with and without Donnan dialysis. Moreover, the relation of removal with the load ratio was confirmed.

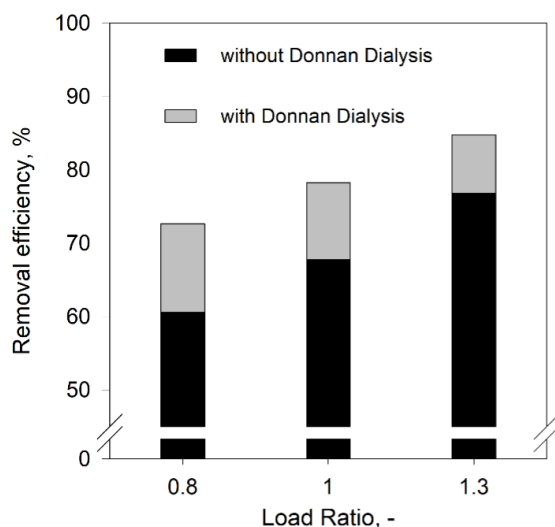


Figure 5. TAN removal efficiency obtained during batch operation. The TAN removal was determined with (w/) and without (w/o) Donnan Dialysis. Donnan dialysis increased the total removal about 10%. The effect of load ratio was also observed as the removal efficiency increased at the higher Load Ratio.

Figure 5 shows the removal efficiency obtained after the first 24h (without Donnan Dialysis) and after 72h, with Donnan Dialysis. The removal efficiency without Donnan Dialysis resulted from current driven migration of cations through the CEM to the cathode. During this period, the removal of TAN was 61% for a load ratio of 0.8, 68% for a load ratio of 1 and 77% for a load ratio of 1.3.

In the period with Donnan Dialysis, the TAN removal efficiency increased around 10% (Figure 5) to 73%, 78% and 85%. Overall, the TAN removal efficiencies for the batch experiments with Donnan Dialysis were similar to those in the continuous experiments and values previously reported ¹³.

In batch operation, the Donnan Dialysis cell successfully exchanged sodium and potassium from the catholyte with ammonium from the feed.

To have a closer look at the individual influence of Donnan Dialysis and electrodialysis, the transport number of each ionic species and its contribution to the total charge transport through the CEM were calculated for the batch and continuous experiments (Figure 6). The (ion) transport number describes the fraction of current used to transport the different ions present in solution over the total charge supplied to the system ⁷. The main transported charge was in the form of ammonium, representing over 60% of the charge transport through the CEM. The remainder of the charge was carried by Na⁺, K⁺ and protons/hydronium ions.

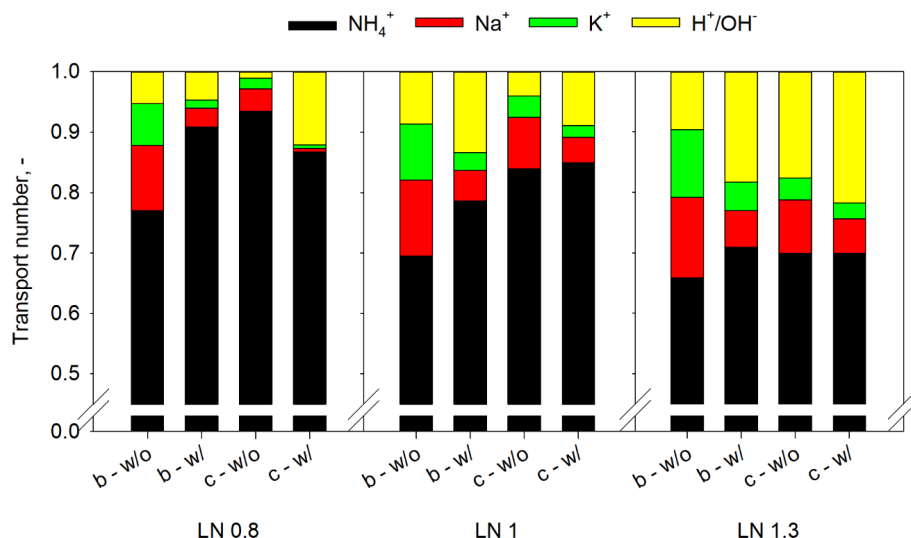


Figure 6. Ion transport numbers calculated per Load Ratio (0.8, 1 and 1.3) for continuous (c -) and batch experiments (b -). The influence of batch and continuous operation as well as the operation with (w/) and without (w/o) Donnan dialysis on the transport number were examined.

For batch operation mode (b -), all load ratios presented the same trend in the transport number. During batch operation mode, a decrease of the transport number of sodium and potassium (b - w/o to b - w/), shows that most of the sodium and potassium returned to the feed due to Donnan Dialysis. The sodium and potassium ions were successfully exchanged with ammonium ions from the feed, as observed by an increase of the ammonium transport number and consequently an additional 10% TAN removal, in b - w/. Moreover, the transport number of ammonium in batch with Donnan Dialysis and continuous without Donnan Dialysis were similar for each Load Ratio. Hence, the TAN removal efficiency achieved was similar.

When operating continuously with Donnan Dialysis, for Load Ratio 0.8, the transport number of sodium, potassium and ammonium ions were lower compared to the situation without Donnan Dialysis. Hence, the exchange of sodium and potassium ions from the catholyte occurred mostly with protons from the feed. Additionally, the exchange of sodium and potassium with protons resulted in catholyte pH of 9.3 that led to an inefficient TAN recovery. A lower cathode pH decreases the amount of nitrogen present as ammonia (NH_3), which leads to a lower TAN transport over the TMCS. As reported earlier⁷, the pH influences the TAN stripping efficiency from the catholyte into the acid. At a pH of 9.24 (pKa for ammonium/ammonia), the TAN in

solution is 50% ammonia (NH_3) and 50% ammonium (NH_4^+). In the TMCS module, the ammonia (NH_3) concentration gradient across the gas permeable membrane drives the transport of ammonia. At lower pH, the concentration of ammonia is lower, hence the transport of ammonia to the acid is lower. Whereas, for Load Ratio 1 and 1.3 in continuous operation with Donnan Dialysis (c – w/) the ammonium transport number was equal to operation without Donnan Dialysis. The exchange of Na^+ and K^+ from catholyte also occurred mostly with protons from the feed, but this did not impair the ammonia extraction over the TMCS since the pH of the catholyte was sufficiently high (LN 1: pH 10.2 and LN1.3: pH 10.1). Donnan dialysis is not selective for the exchange of a specific ion. The exchange of Na^+ and K^+ from the cathode with ions from the feed will occur based on the concentration of the specific ions in the feed. In continuous operation, protons were exchanged with Na^+ and K^+ , since TAN concentration was mostly removed from the feed. As the same amount of ammonium is transported through the membranes, the Donnan Dialysis did not contribute to increase the overall TAN removal.

The energy input was lower than reported in previous studies.

Ideally, a balance between NH_4^+ removal and energy input should be achieved when operating a (HR)ES⁷. The energy consumption for TAN removal in all Electrochemical Systems is mostly influenced by three factors: cell voltage, applied current density, and the TAN transport. The energy input for batch operation was between $9.3 \text{ kJ g}_\text{N}^{-1}$ and $11.1 \text{ kJ g}_\text{N}^{-1}$, increasing with the load ratio (Table 1). The energy input for continuous operation was between $9.7 \text{ kJ g}_\text{N}^{-1}$ and $14.2 \text{ kJ g}_\text{N}^{-1}$ (Table 1). The energy input was lower for batch operation with Donnan Dialysis compared to without Donnan Dialysis, since additional ammonium was removed from the feed without additional energy input (Figure 6). For continuous operation, there was no clear impact of Donnan Dialysis on the energy consumption. The higher energy input required in continuous compared to batch operation mode was a result of a higher internal resistance (due to ionic and membrane losses) built up during the longer operation with applied current in continuous mode. The higher concentration of positively charged ions in solution means more energy was spent to force ions with the same charge in this direction. The required specific energy input for ammonium removal was lower than Rodriguez Arredondo et al. (2017)¹³ and Kuntke et al.¹². The studied hydrogen recycling electrochemical system (HRES) achieved a TAN removal efficiency of 87% at Load Ratio 1.3 while consuming $13.4 \text{ kJ g}_\text{N}^{-1}$, when operating continuously at 20 A m^{-2} . Rodriguez Arredondo et al., 2017¹³ achieved 83% TAN recovery while consuming $21.5 \text{ kJ g}_\text{N}^{-1}$ at 10 m^{-2} and the same load Ratio. Kuntke et al., 2017¹² achieved 73% TAN recovery with a similar HRES while consuming $26.1 \text{ kJ g}_\text{N}^{-1}$ when operated at the same current density in Load Ratio⁸. Tarpeh et. al., 2018

achieved a 93% efficiency in batch experiments with real urine, which required $30.6 \text{ MJ kg}_\text{N}^{-1}$ ⁴. The “CapAmm cell” from Zhang et al., 2018 exhibited up to 90% ammonia removal and 80% recovery efficiencies. The energy consumption for synthetic urine was $28.1 \text{ MJ kg}_\text{N}^{-1}$ ¹¹.

Donnan Dialysis is most suitable to enhance TAN recovery during batch operation, as it increases the removal efficiency and decreases the energy input of the process. Moreover, by operating an HRES system in batch mode, a higher removal can be achieved without additional membrane surface area and the need of a new cell.

Table 1. Energy input per gN removed for batch and continuous operation.

LN	Continuous		Batch	
	w/o Donnan (kJ gN ⁻¹)	w/ Donnan (kJ gN ⁻¹)	w/o Donnan (kJ gN ⁻¹)	w/ Donnan (kJ gN ⁻¹)
0.8	9.7	10.1	9.3	7.8
1	11.5	11.7	10.3	9.0
1.3	13.4	14.2	11.1	10.1

Conclusion

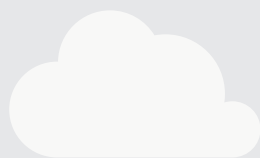
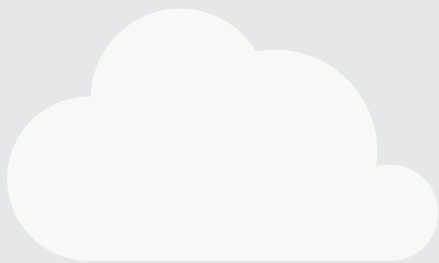
In continuous operation, the benefits of including a dedicated Donnan Dialysis cell on the overall ammonium recovery were limited. Donnan Dialysis can be exploited to enhance TAN recovery in batch operation. It increased the transport of ammonium from feed to cathode and consequently the TAN removal. Additionally, it resulted in lower energy consumption for TAN removal.

References

- (1) Miller, S. A.; Landis, A. E.; Theis, T. L. Environmental Trade-Offs of Biobased Production. *Environmental Science and Technology* **2007**, 41 (15), 5176–5182. <https://doi.org/10.1021/es072581z>.
- (2) Sutton, M. A.; Oenema, O.; Erisman, J. W.; Leip, A.; van Grinsven, H.; Winiwarter, W. Too Much of a Good Thing. *Nature* **2011**, 472 (7342), 159–161. <https://doi.org/10.1038/472159a>.
- (3) Maurer, M.; Pronk, W.; Larsen, T. A. Treatment Processes for Source-Separated Urine. *Water Research* **2006**, 40 (17), 3151–3166. <https://doi.org/10.1016/j.watres.2006.07.012>.
- (4) Tarpeh, W. A.; Barazesh, J. M.; Cath, T. Y.; Nelson, K. L. Electrochemical Stripping to Recover Nitrogen from Source-Separated Urine. *Environmental Science and Technology* **2018**, 52 (3), 1453–1460. <https://doi.org/10.1021/acs.est.7b05488>.
- (5) Ledezma, P.; Kuntke, P.; Buisman, C. J. N.; Keller, J.; Freguia, S. Source-Separated Urine Opens Golden Opportunities for Microbial Electrochemical Technologies. *Trends in Biotechnology*. April 2015, pp 214–220. <https://doi.org/10.1016/j.tibtech.2015.01.007>.
- (6) Rodríguez Arredondo, M.; Kuntke, P.; Jeremiasse, A. W.; Sleutels, T. H. J. a.; Buisman, C. J. N.; ter Heijne, A. Bioelectrochemical Systems for Nitrogen Removal and Recovery from Wastewater. *Environ. Sci.: Water Res. Technol.* **2015**, 1 (1), 22–33. <https://doi.org/10.1039/C4EW0066H>.
- (7) Kuntke, P.; Sleutels, T. H. J. A.; Rodríguez Arredondo, M.; Georg, S.; Barbosa, S. G.; Heijne, A. (Bio) *Electrochemical Ammonia Recovery: Progress and Perspectives*; 2018; Vol. 2. <https://doi.org/https://doi.org/10.1007/s00253-018-8888-6>.
- (8) Desloover, J.; Woldeyohannis, A. A.; Verstraete, W.; Abate Woldeyohannis, A.; Verstraete, W.; Boon, N.; Rabaey, K. Electrochemical Resource Recovery from Digestate to Prevent Ammonia Toxicity during Anaerobic Digestion. *Environmental Science & Technology* **2012**, 46 (21), 12209–12216. <https://doi.org/10.1021/es3028154>.
- (9) Luther, A. K.; Desloover, J.; Fennell, D. E.; Rabaey, K. Electrochemically Driven Extraction and Recovery of Ammonia from Human Urine. *Water Research* **2015**, 87, 367–377. <https://doi.org/10.1016/j.watres.2015.09.041>.
- (10) Rodríguez Arredondo, M.; Kuntke, P.; ter Heijne, A.; Hamelers, H.; Buisman, C. Load Ratio Determines the Ammonia Recovery and Energy Input of an Electrochemical System. *Water Research* **2017**, 111 (3), 330–337. <https://doi.org/10.1016/j.watres.2016.12.051>.
- (11) Zhang, C.; Ma, J.; Song, J.; He, C.; Waite, T. D. Continuous Ammonia Recovery from Wastewaters Using an Integrated Capacitive Flow Electrode Membrane Stripping System. *Environmental Science and Technology* **2018**, 52 (24), 14275–14285. <https://doi.org/10.1021/acs.est.8b02743>.
- (12) Kuntke, P.; Rodríguez Arredondo, M.; Widyakristi, L.; Ter Heijne, A.; Sleutels, T. H. J. A. J. A.; Hamelers, H. V. M. M.; Buisman, C. J. N. N. Hydrogen Gas Recycling for Energy Efficient Ammonia Recovery in Electrochemical Systems. *Environmental Science and Technology* **2017**, 51 (5), 3110–3116. <https://doi.org/10.1021/acs.est.6b06097>.
- (13) Rodríguez Arredondo, M.; Kuntke, P.; ter Heijne, A.; Hamelers, H. V. M.; Buisman, C. J. N. Load Ratio Determines the Ammonia Recovery and Energy Input of an Electrochemical System. *Water Research* **2017**, 111, 330–337. <https://doi.org/10.1016/j.watres.2016.12.051>.
- (14) Sleutels, T. H. J. A.; Hamelers, H. V. M.; Rozendal, R. A.; Buisman, C. J. N. Ion Transport Resistance in Microbial Electrolysis Cells with Anion and Cation Exchange Membranes. *International Journal of Hydrogen Energy* **2009**, 34 (9), 3612–3620. <https://doi.org/10.1016/j.ijhydene.2009.03.004>.
- (15) Rozendal, R. A.; Hamelers, H. V. M.; Buisman, C. J. N. Effects of Membrane Cation Transport on PH and Microbial Fuel Cell Performance. *Environmental Science and Technology* **2006**, 40 (17), 5206–5211. <https://doi.org/10.1021/es060387r>.

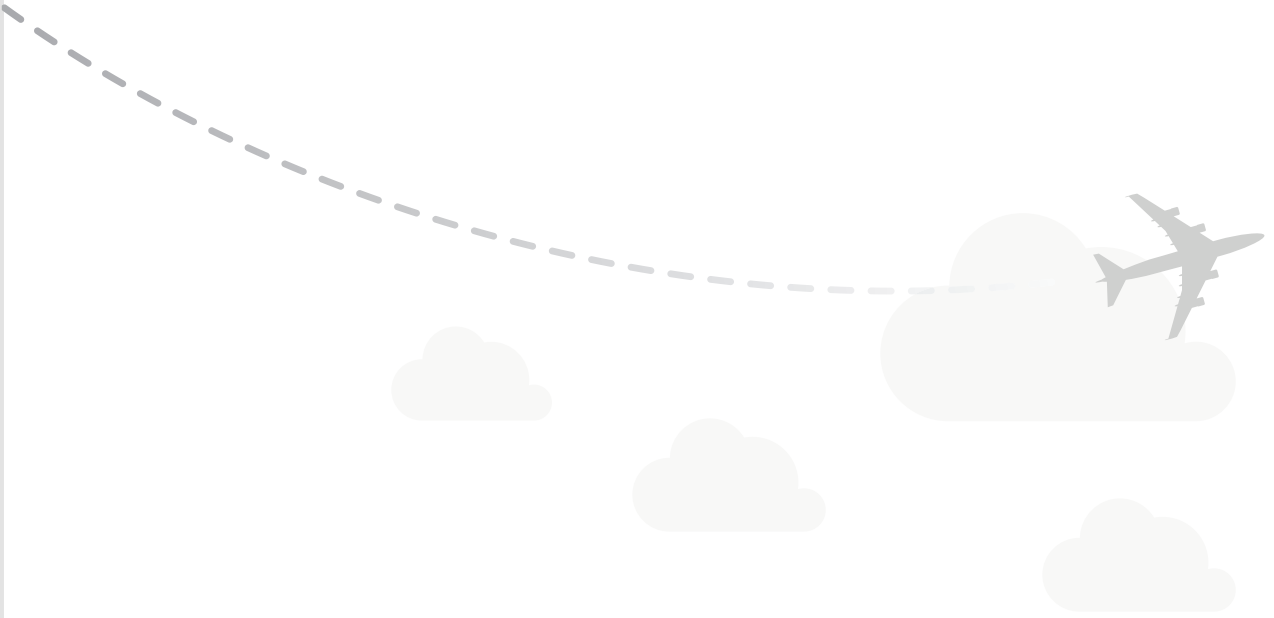
- (16) Sleutels, T. H. J. A.; Heijne, A. ter; Buisman, C. J. N.; Hamelers, H. V. M. Steady-State Performance and Chemical Efficiency of Microbial Electrolysis Cells. *International Journal of Hydrogen Energy* **2013**, *38* (18), 7201–7208. <https://doi.org/10.1016/j.ijhydene.2013.04.067>.
- (17) Sleutels, T. H. J. A.; ter Heijne, A.; Kuntke, P.; Buisman, C. J. N.; Hamelers, H. V. M. Membrane Selectivity Determines Energetic Losses for Ion Transport in Bioelectrochemical Systems. *ChemistrySelect* **2017**, *2* (12), 3462–3470. <https://doi.org/10.1002/slct.201700064>.
- (18) Rijnaarts, T.; Shenkute, N. T.; Wood, J. A.; De Vos, W. M.; Nijmeijer, K. Divalent Cation Removal by Donnan Dialysis for Improved Reverse Electrodialysis. *ACS Sustainable Chemistry and Engineering* **2018**, *6* (5), 7035–7041. <https://doi.org/10.1021/acssuschemeng.8b00879>.
- (19) Cox, J. A.; Dinunzio, J. E. Donnan Dialysis Enrichment of Cations. *Analytical Chemistry* **1977**, *49* (8), 1272–1275. <https://doi.org/10.1021/ac50016a056>.
- (20) Sarkar, S.; Sengupta, A. K.; Prakash, P. The Donnan Membrane Principle: Opportunities for Sustainable Engineered Processes and Materials. *Environmental Science and Technology*. February 2010, pp 1161–1166. <https://doi.org/10.1021/es9024029>.
- (21) Kuntke, P.; Geleji, M.; Bruning, H.; Zeeman, G.; Hamelers, H. V. M.; Buisman, C. J. N. Effects of Ammonium Concentration and Charge Exchange on Ammonium Recovery from High Strength Wastewater Using a Microbial Fuel Cell. *Bioresource Technology* **2011**, *102* (6), 4376–4382. <https://doi.org/10.1016/j.biortech.2010.12.085>.
- (22) Maurer, M.; Schwegler, P.; Larsen, T. A. Nutrients in Urine: Energetic Aspects of Removal and Recovery. *Water Science and Technology* **2003**, *48* (1), 37–46. <https://doi.org/10.1017/S000748530002229X>.
- (23) Kuntke, P.; Rodrigues, M.; Sleutels, T.; Saakes, M.; Hamelers, H. V. M.; Buisman, C. J. N. Energy-Efficient Ammonia Recovery in an Up-Scaled Hydrogen Gas Recycling Electrochemical System. *ACS Sustainable Chemistry & Engineering* **2018**, *acssuschemeng.8b00457*. <https://doi.org/10.1021/acssuschemeng.8b00457>.

3



Chapter 3

Donnan Dialysis for scaling mitigation during electrochemical ammonium recovery from complex wastewater



This Chapter has been published as:

Rodrigues, M., Paradkar, A., Sleutels, T., Heijne, A., Buisman, C.J.N., Hamelers, H.V.M., Kuntke, P., 2021. Donnan Dialysis for scaling mitigation from during complex electrochemical wastewater ammonium recovery. *Water Res.* 117260. <https://doi.org/10.1016/j.watres.2021.117260>

Abstract

Inorganic scaling is often an obstacle for implementing electrodialysis systems in general and for nutrient recovery from wastewater specifically. In this work, Donnan dialysis was explored, to prevent scaling and to prolong operation of an electrochemical system for TAN (total ammonia nitrogen) recovery. An electrochemical system was operated with and without an additional Donnan dialysis cell, while being supplied with synthetic influent and real digested black water. For the same Load Ratio while treating digested black water (nitrogen load vs applied current), the system operated for a period three times longer when combined with a Donnan cell. Furthermore, the amount of nitrogen recovered was higher. System performance was evaluated in terms of both TAN recovery and energy efficiency, at different Load Ratios. At a Load Ratio 1.3 and current density of 10 A m^{-2} , a TAN recovery of 83% was achieved while consuming $10.85 \text{ kWh g}_\text{N}^{-1}$.

Introduction

Towards closing the resources cycle for a circular economy, our considered “waste” water has become a source of nutrients and energy ^{1–6}. Amongst all the nutrients present in wastewater, phosphorus and nitrogen are of the utmost importance as they play a vital role in plant growth. As phosphorus is a scarce nutrient, considerable efforts were taken in the last two decades to recover it from our wastewater ^{7–9}. Nitrogen (N_2), however, amounts to 78% of all gases present in the atmosphere and it can be artificially fixed by the Haber-Bosch process into reactive nitrogen forms (e.g. NH_3 and NH_4^+) to be used as fertilizer ^{7,10}. In order to decrease its environmental effect, such as eutrophication, nitrogen has been removed from wastewater via nitrification-denitrification or Anammox at wastewater treatment plants (WWTP) ^{11–14}. These aforementioned nitrogen removal processes are energy intensive and contribute N_2O emissions to the atmosphere. In addition, up to 2% of the energy produced worldwide is consumed by the Haber-Bosch process ^{15–17}.

Source separation of wastewater has been investigated as a promising concept to allow for energy efficient wastewater treatment and nutrient recovery ^{18,19}. Phosphorus and nitrogen were recovered from source separated streams such as black water (combined feces and urine) or urine ^{20–22}. Black water is responsible for up to 70% of chemical oxygen demand (COD), 80% phosphorous and 90% nitrogen found in conventional wastewater ^{23,24}.

Phosphate recovery was successfully described by forming struvite ²⁵ or calcium phosphate granules ^{26,27}. Nonetheless, after phosphate recovery in these processes, almost all the ammonium remains in solution ^{2,26}. An electrochemical system (ES) has been proposed to recover the remaining ammonia and ammonium (total ammonia nitrogen, TAN), as it does not require chemical dosing and requires less energy than NH_3 stripping, chemical precipitation or adsorption ^{10,28–30}. However, digested black water or urine, although rich in nitrogen, also contain other several ions (incl. Ca^{2+} , Mg^{2+} , K^+ , Na^+ , CO_3^{2-} , Cl^- , SO_4^{2-} , PO_4^{3-}) ^{31–34}. The presence of bivalent ions was previously reported to interfere with electrodialysis process and therefore nutrient recovery, as calcium and magnesium ions are more susceptible to the electric field and CEMs are more selective for divalent ions ^{35–37}. While some studies consider the concentration of calcium and magnesium negligible due to upstream precipitation such as struvite ^{20,38}, it has been shown that under alkaline conditions low concentrations (0.02 M Ca^{2+}) are sufficient to scale ion exchange membranes ^{33,39–41}. Moreover, the presence of Mg^{2+} facilitates the formation of calcium carbonate, even at very low concentrations of both ions and slightly above pH neutrality ^{42,43}. The

cation exchanges membranes (CEM) used in an ES for TAN recovery are not species selective and transport all cations, which accumulate in the concentrate/cathode solution. The alkaline pH in the concentrate results in the formation of inorganic scaling on the CEM (e.g. precipitation of insoluble salts such as calcite, gypsum, struvite etc.)³⁸.

When scaling forms on the surface of ion exchange membranes, the stack electrical resistance increases, leading to an increase in energy input^{41,44}. Some solutions were proposed to address this problem, such as filtration, coagulation and flocculation, the use of anti-scalants, and chemical cleaning of the membranes by in situ use of acidic or alkaline chemicals.^{38,45,46} Despite having several options, all imply additional cost and/or operational interruption in order to regenerate or even replace the scaled membranes^{38,45}. The implementation of electrochemical systems for nutrient recovery applications are thus limited as so far no satisfactory solution has been identified^{38,45}.

During electrodialysis ammonium and other cations are transported toward the cathode and accumulate in a concentrated solution. While ammonia can be extracted through a gas permeable membrane, cations like sodium or potassium will continuously accumulate in this concentrated solution when current is constantly supplied. Donnan dialysis (DD) has been previously described to promote the exchange of ammonium in the feed with other cations (such as Na^+ and K^+) accumulated on the concentrate side^{35,47,48}. During Donnan dialysis, no current is applied and the ions move due to an electrochemical potential difference, generated by a concentration gradient formed between the feed and the concentrate during electrodialysis^{48–50}. Hence, also bivalent cations accumulated in a concentrate solution can exchange with monovalent cations from the feed solution⁴⁸. In reverse electrodialysis, Rijnaarts et al., 2019 used Donnan dialysis as a pre-treatment step to remove SO_4^{2-} from feedwater and were able to achieve 76% reduction of the bivalent ion content, limiting the occurrence of scaling³⁵. The purpose of this research was to assess whether Donnan dialysis can be used as pre-treatment for scaling mitigation when a complex ammonia rich influent is supplied to an ES without further energy consumption and need for chemical addition.

Materials and methods

Experimental Setup

The TAN recovery system consisted of previously described electrodialysis (ED) cell and a transmembrane chemisorption (TMCS) module, which is presented in full detail in the supplementary information Appendix A – A.1. Experimental Setup^{48,51}. An additional cell was introduced in the system for Donnan dialysis, presented in Figure 1.

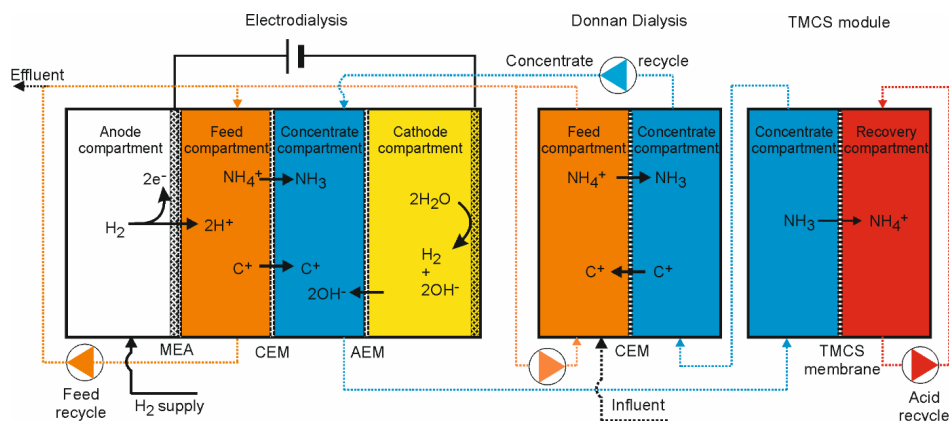


Figure 1: Electrochemical system with hydrogen gas recycling for TAN recovery including DD cell. Oxidation of hydrogen occurs at the anode of the electrodialysis cell, where protons are generated and transferred over a membrane electrode assembly (MEA) to the feed compartment. These protons acidify the influent to form ammonium (NH_4^+). The NH_4^+ can then be transported over a cation exchange membrane (CEM) to a concentrate solution. Other cations (represented here as C^+) are also transported as the CEM is not species selective. Simultaneously, the OH^- ions formed at the cathode, are transported via an anion exchange membrane (AEM) to the concentrate solution increasing the pH. Later, the ammonia formed at the concentrated is recovered through a Transmembrane Chemisorption (TMCS) unit, which consists of a gas permeable hydrophobic membrane. Once the ammonia is transferred over the TMCS, the concentrated solution is supplied to the DD cell. Here, the previously accumulated cations such as sodium or magnesium, return to the feed compartment due to a concentration gradient. The influent was first supplied to the feed compartment of the DD cell to achieve a higher concentration gradient and exchange the cations from the concentrate side with ammonium from the feed side. This configuration allows the hydrogen gas formed at the cathode compartment to be later recycled to the anode compartment, conserving energy.

The electrodialysis cell included a feed and a concentrated compartment (1.2 cm thickness each) and separated by a cation exchange membrane (Fumasep FKB-PK-130, FUMATECH BWT GmbH, Bietigheim-Bissingen, Germany). The anode and cathode compartment included a platinum (Pt) coated titanium mesh electrode measuring (9.8cm x 9.8cm, 5mg Pt cm^{-2} Magneto Special Anodes BV, The Netherlands) in a 0.2cm x 10cm x 10cm compartment. The ion exchange membranes had a projected surface area of 100cm². The anode was separated from

feed compartment by a Membrane Electrode Assembly (MEA). The concentrate compartment was separated from cathode compartment by an anion exchange membrane (fumasep FAB-PK-130, FUMATECH BWT GmbH, Bietigheim-Bissingen, Germany).

The DD cell consisted of feed and concentrate compartments, made of poly methyl methacrylate. Each compartment had a size of 21cm x 21cm x 2.5cm and a machined flow field of 10cm x 10cm x 0.2cm. Feed and concentrate compartments were separated by a 15cm x 15cm CEM Fumasep FKB-PK-130 (FUMATECH BWT GmbH). During DD, the influent was first supplied to the feed compartment of the DD cell.

In order to supply influent and recirculate feed, concentrate, cathode and acid solutions, four Masterflex peristaltic pumps (Masterflex L/S, Metrohm Applikon BV, Schiedam, The Netherlands) were used. The recirculation flow rate for feed, concentrate, cathode and acid was 160 mL min⁻¹.

The influent flow is presented in Table 1, according to the used Load Ratio.

Experimental Strategy

The system was supplied with the effluent of a lab scale Upflow Anaerobic Sludge Blanket digestion reactor (UASB reactor) (Wetsus, European Centre of Excellence for Sustainable Water Technology, Leeuwarden, The Netherlands) used for phosphate recovery as calcium granules as described in Cunha et al., 2018⁵². The addition of calcium to the reactor results in the production of calcium phosphate granules, while removing 89% of the phosphate⁵². Furthermore, > 80% of the total COD is removed and around 0.5 g COD-CH₄ g⁻¹ COD_{Total}-BW was produced^{26,52}. The effluent (digested black water) consisted mainly of NH₄⁺ (1 g L⁻¹), Cl⁻ (0.463 g L⁻¹), Na⁺ (0.290 g L⁻¹), K⁺ (0.230 g L⁻¹), Ca²⁺ (0.046 g L⁻¹), Mg²⁺ (0.024 g L⁻¹), PO₄³⁻ (0.051 g L⁻¹), SO₄²⁻ (0.038 g L⁻¹), and COD (0.419 g L⁻¹). Therefore, it consists of a complex ionic and organic matrix suitable to study nutrient recovery from a complex wastewater stream.

Although, solids were retained in the UASB reactor, the effluent of the UASB passed through a 10-micron filter before being supplied to the ES with (w/) and without (w/o) DD.

The system was also operated with synthetic influent (to compare the transport over the membrane). Synthetic influent mimicked the digested black water collected after the UASB reactor without bivalent cations and an organic carbon source. The synthetic black water consisted of 2.75 g L⁻¹ (NH₄)₂CO₃, 0.08 g L⁻¹ K₂SO₄, 0.47 g L⁻¹ KCl, 0.31 g L⁻¹ NaCl, and 0.5 g L⁻¹ Na₂CO₃.

Table 1: Experiments performed using an electrodialysis cell with or without the DD cell at different Load Ratio.

Setup	Influent	Load ratio	Inflow (ml min ⁻¹)	HRT (h)	Volume (L day ⁻¹)
ED	Synthetic Influent	1	1.63	4.1	2.4
	Black Water	1	1.63	4.1	2.4
ED + DD	Synthetic Influent	1	1.63	4.1(ED) 1 (DD)	2.4
		0.5	3.97	1.7 (ED) 0.4 (DD)	4.7
	Black Water	1	1.63	4.1 (ED) 1 (DD)	2.4
		1.3	1.2	5.6 (ED) 1.4 (DD)	1.7
		1.5	0.96	6.9 (ED) 1.7 (DD)	1.4

Table 1 includes all sets of experiments performed and studied for this research. The experiments were carried out at a constant current density of 10 A m⁻². Choosing 10 A m⁻² allowed to operate the ES system continuously for a longer period considering the effluent flow rate (L d⁻¹) of the UASB reactor.

Calculations

The calculations were based on earlier work and explained in detail in the Supporting Information, Appendix A – A.2. Calculations.

Load Ratio

Load Ratio (L_N) is the ratio of applied current density to the TAN loading. The Load Ratio determines to a large extent the performance of the ES system (removal, energy consumption, Coulombic efficiency) ³⁴. A Load Ratio of one means the amount of current applied to the system is equal to the total charge supplied as TAN. When $L_N < 1$ more TAN is present than the electrons supplied to the cell, conversely when $L_N > 1$ the system is supplied with an excess of current. Load Ratio can be determined using the following formula:

$$L_N = \frac{j \times A_m}{C_{TAN,influent} \times Q_{influent} \times F}$$

Where, j is the current density (A m⁻²), C_{TAN} is the concentration of TAN (mol L⁻¹) in the influent, Q is the influent flow rate (L s⁻¹), F is the Faraday constant (C mol⁻¹) and A_m is the surface area of CEM (m²).

Chemical Analysis

Samples were collected daily from influent and effluent of the DD cell, effluent of the electrodialysis cell, concentrate, cathode, and acid. The samples were analyzed for cations (NH_4^+ , Na^+ , K^+ , Ca^{2+} , Mg^{2+}) and anions (NO_3^- , NO_2^- , Cl^- , SO_4^{2-} , PO_4^{3-}) using a Metrohm Compact IC Flex 930 with a cation column (Metrosep C 4-150/4.0) and a Metrohm Compact IC 761 with an anion column (Metrosep A Supp 5-150/4.0) respectively. The samples were also analyzed for organic carbon, inorganic carbon, non-purgeable organic carbon and total carbon using a TOC analyzer (TOC-L CPH, Shimadzu BENELUX, 's-Hertogenbosch, The Netherlands). When supplying the ES with black water all samples were also analyzed for metals, using inductively coupled plasma optical emission spectrometry (ICP-OES), and for chemical oxygen demand (COD), using a cuvette test kit LCK 414 and a spectrophotometer DR3900 (HACH NEDERLAND, Tiel, The Netherlands).

Results

Donnan dialysis slows CEM scaling allowing longer operation.

The ES was operated at a Load ratio one at 10 A m^{-2} with and without the DD cell using digested black water as influent. Figure 2 shows the measured cell voltage and the potential losses in the cell including MEA overpotential (η_{MEA}) and cathode overpotential (η_{cathode}), ionic losses (E_{ion}), pH losses (E_{pH}) and the membranes potential (E_{membrane}) of the ED cell at three distinct regions. The potential losses were calculated as explained in the Supporting Information, Appendix A – A.2. Calculations.

After 12 hours the measured voltage spiked to more than 5V and the operation was therefore interrupted, when operating the system with digested black water without a DD cell (Figure 2). This cell voltage of 5V can be associated with pH change in the concentrate compartment and scaling formation. When operating the system with Donnan dialysis at the same conditions, scaling was delayed by almost 30h, meaning the period of continuous operation was extended by more than three times that without Donnan. The potential losses showed an increase of the membrane resistance (E_{membrane}) over time, Figure 2. By SEM EDS analysis of the CEM, it was clear that the membrane was scaled with calcium salts (SI, Appendix B -Figure A.1). Some of the calcium present in the UASB reactor effluent (influent of ES) precipitated in the form of calcium carbonate (CaCO_3) on the CEM. While operating with synthetic influent, the ES performed at a constant voltage of approximately 3V both with and without Donnan dialysis.

When supplied with digested black water, it was not possible to operate the ES system for more than 12 hours, at the same Load Ratio and current density again due to scaling on the CEM. As the membrane scales, the effective area of the membrane where the ions can be exchanged is therefore reduced⁴³. This limits the overall ion transport and in-turn affects the TAN recovery. Nevertheless, within this 12h stable period of operation, 79% TAN recovery was achieved. A DD cell was introduced to overcome the scaling of the CEM; at the same Load Ratio, $L_N=1$, and at 10 A m^{-2} , the TAN recovery was 82% when using synthetic influent. This experiment was carried out over 5 days. When using digested black water, the TAN recovery was 75.5% over 36 hours. Without DD, 1.2 g ammonium were supplied, 0.9 g were recovered in the acid, and 0.3 g were found in the effluent. With DD, 2.8 g ammonium were supplied, 2.1 g were recovered in the acid, and 0.7 g were found in the effluent. The TAN recovery efficiency was affected by operating with real wastewater and by operating the ED combined with DD. Nevertheless, as the system operated during a three times longer period with Donnan, although the TAN recovery was reduced, more total influent was treated and consequently more nitrogen was recovered.

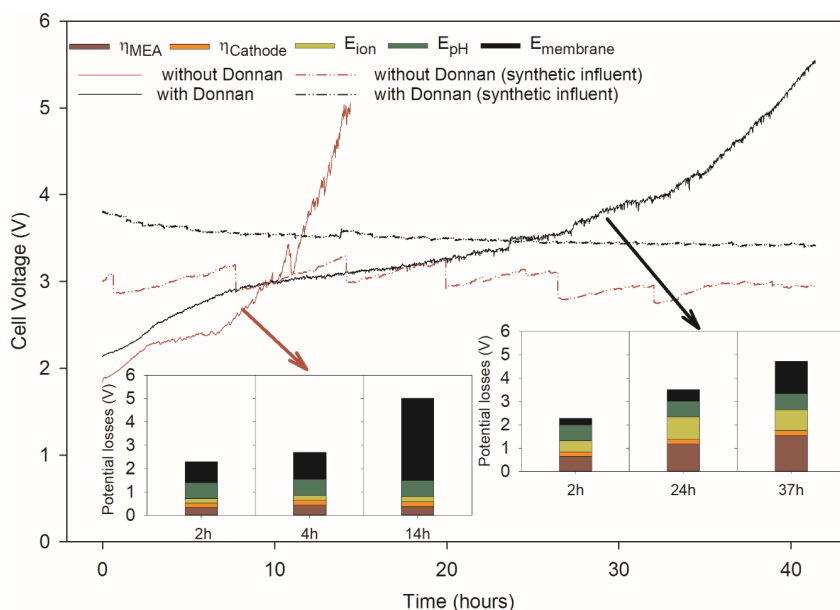


Figure 2: Electrodesialysis cell voltage (V) with and without Donnan dialysis over time at $L_N=1$ and 10 A m^{-2} . The ED cell voltage is the result of electrode overpotential (η_{MEA} and η_{cathode}), ionic losses (E_{ion}), pH losses (E_{pH}) and membrane potential (E_{membrane}). The potential losses were calculated after 2, 4 and 14h for the ES while operating without Donnan dialysis. With Donnan dialysis, the potential losses were calculated after 2, 24 and 37h. Three regions were distinguished during the operation period: 1) an initial increase until stable state, 2) stable operation and 3) voltage ramp up as the scale blocks the CEM.

Furthermore, the energy consumption was nearly constant, independent of Donnan dialysis and the influent composition. Operating the system consumed around 27 kJ g_N^{-1} (SI, Figure A.2). The energy consumption can be explained when we look at the potential losses (SI, Figure A.2). Ionic losses occur due to the transport of ions and are thus, dependent on the conductivity of the solution. The conductivity of the digested black water was 6.5 mS cm^{-1} on average resulting in higher potential losses compared to influents such as urine (around 29 mS cm^{-1}) or reject water (around 12 mS cm^{-1}), as previously shown^{48,53–55}. The fluctuation of MEA overpotential was not expected. The MEA overpotential is the difference between the measured anode potential and the theoretical anode potential. If the contact between H_2 gas and gas diffusion electrode is not efficient, then the MEA overpotential can increase⁵⁶. Also, scaling and biofouling of the cation exchange membrane in the MEA can also cause an increase of the MEA overpotential^{37,57}. However, we observed that the MEA overpotential was independent of the influent supplied to the system (SI, Figure A.2). Thus, we suspect that the MEA could have suffered some unexpected damage (not further identified) leading to a fluctuation in the potential loss.

The performance was enhanced and the operation window was expanded by operating at higher Load ratio.

We evaluated the ES performance with DD cell regarding TAN recovery efficiency and energy consumption for different nitrogen loading at constant current (Load Ratio) (Figure 3).

Figure 3 shows that the overall TAN recovery and energy consumption of the ES combined with Donnan dialysis increased with Load Ratio. This phenomenon is in accordance with the Load Ratio model previously established for electrochemical systems for TAN recovery.³⁴ At Load ratio 1.3, TAN recovery of 83% was achieved, whereas for Load Ratio 1.5, the TAN recovery was 85%. As no significant improvement was observed for Load Ratio 1.5, no higher Load Ratio were tested. The presented energy consumption is the average for each experiment operated with ES including DD cell using filtered digested black water at Load Ratios 0.5, 1, 1.3 and 1.5. The average does not consider the last day of each experiment as the voltage ramped up and consequently the operation was interrupted (SI, Figure A.3). During stable operation the electro dialysis with Donnan dialysis treated in total 2.4 L for Load Ratio 0.5, 3.5 L for Load ratio 1, 5.2 L for Load Ratio 1.3, and 4.8 L for Load Ratio 1.5. The combined system consumed between 6.9 kWh g_N⁻¹ for Load Ratio 0.5 and 13.1 kWh g_N⁻¹ for Load ratio 1.5. The ES operated without the DD cell consumed around 7.5 kWh g_N⁻¹ during the 12h of operation at Load ratio one.

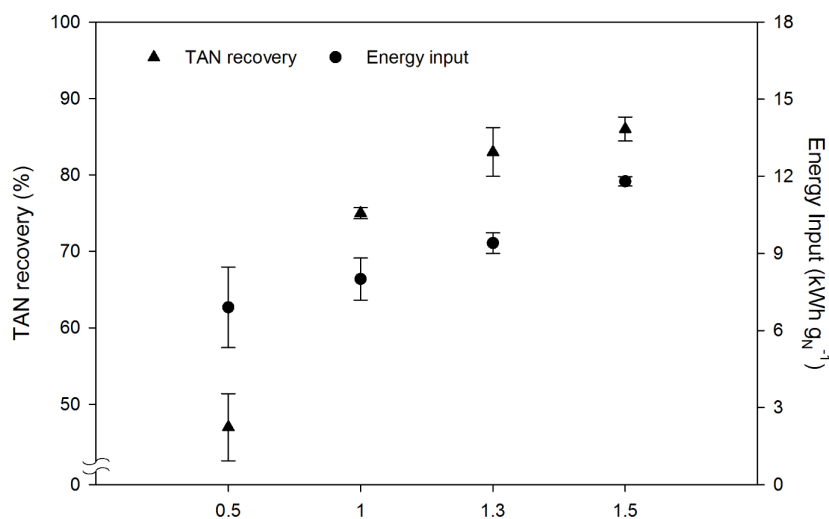


Figure 3: TAN Recovery and Energy Input of the ES treating digested black water with Donnan dialysis at different Load Ratio. TAN recovery and energy consumption increased with Load Ratio. The combined system achieved up to 85% TAN recovery.

Donnan dialysis enables ammonia recovery from a complex wastewater including calcium ions, by regulating the pH at 9.7.

Figure 4 represents the average charge species transported over the CEM on the electrodialysis cell (A) and over the CEM in the DD cell (B) for different Load Ratio and a current density of 10 A m^{-2} .

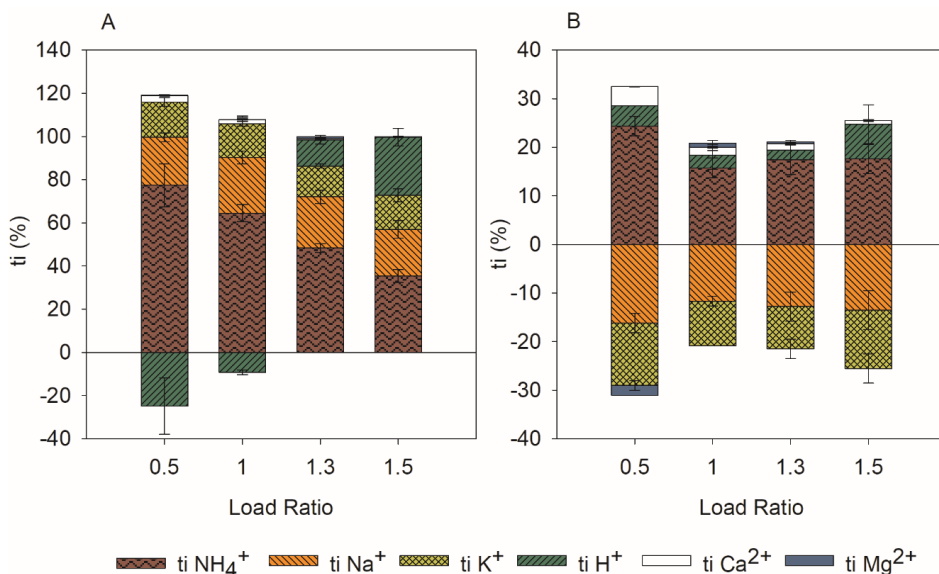


Figure 4: A) Transported charge over the CEM in the electrodialysis cell system. B) Exchanged charge over the CEM in the DD cell. The measured transported species were NH_4^+ , Na^+ , K^+ , Ca^{2+} , Mg^{2+} , and H^+ .

Figure 4 shows the average ion transport before the experiments were interrupted due to the extreme cell voltage increase. The average transport for each ion was calculated up to the point that scaling was detected. Scaling affects the ion flux as previously demonstrated by Asraf-Snir et al., 2018 and can be detected by the voltage increase⁴⁴. Overall, ammonium is the dominant charge carrier (highest t_i), followed by sodium and potassium, shown in Figure 4A. The ionic composition of the influent and the Load Ratio affect the transport of charged species over the CEM in the electrodialysis cell. The relative ammonium transport decreased with increasing Load Ratio, while the proton transport increased accordingly. Sodium (0.23 ± 0.02) and potassium (0.16 ± 0.01) transport remain constant, probably due to ion exchange during the Donnan dialysis pre-treatment.

Once a gradient is formed between feed and concentrate, potassium (K^+) and sodium (Na^+) are exchanged with ammonium (NH_4^+) and protons (H^+) in the DD cell (Figure 4 B). For Load Ratio higher than one, calcium (Ca^{2+}) and magnesium

(Mg^{2+}) are both transported to the concentrate compartment through the Donnan and electrodialysis CEMs. Magnesium was only returned to the feed at Load Ratio 0.5. Moreover, calcium and magnesium only represented less than 5% of the charge exchange. The desired transport of calcium ions to the feed did not occur.

In this study, up to 4 mmol (150mg) of calcium was removed from the supplied influent by DD+ED. Calcite (CaCO_3) precipitation occurs even at very low concentrations and pH just slightly above neutral conditions⁵⁸. This precipitation can occur simultaneously on the surface and at the pores of the membrane. With a continuous electric field transporting cations through the CEM, a high enough concentration at the membrane solution interface induced precipitation^{43,59}, causing the obstruction of the membrane pores and possibly membrane dehydration. In our system magnesium was also removed to a certain extent, and while the analyzed membranes did not show any magnesium salt precipitates, its contribution on facilitating calcium precipitation was previously demonstrated.

The considerable increase of membrane resistance (SI, Figure A.3), which is related to the increase of membrane potential, is the result of scaling formation at the cation exchange membrane. Here, CEMs become more resistant to ion transport, and as a result water splitting at the surface of the membrane is enhanced^{44,45}. The high membrane potential coincides with an increase in the pH of the concentrate.

Figure 5 is the average pH measured over each 12 hours in feed and concentrate solutions for different Load Ratios.

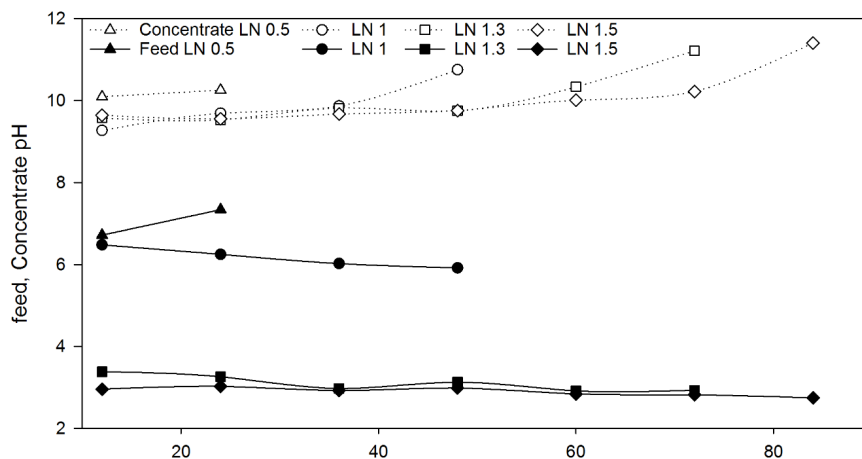


Figure 5. Average pH measured in the feed (solid fill) and concentrate (empty fill) solutions over time for different Load Ratio (LN).

Figure 5 also shows that the average pH of the concentrate is approximately 10 during the first 12 hours. For Load Ratio 1.3 and 1.5, the pH of the concentrate was stable for almost five to six days at pH 9.7 with Donnan dialysis; conversely, when operating without Donnan dialysis, the pH rapidly reached 11.6. A comparison of Figure 5 with Figure A.3 (SI) reveals that the membrane loss increases sharply when the concentrate pH reached 12. Donnan dialysis thus acts, to a certain extent, as a pH regulator, an effect that is enhanced with increased Load Ratio. The transport of protons for high Load Ratio in the electrodialysis cell, combined with the protons exchanged in DD cell, decreased the pH of the concentrate (Figure 5). Although the pH was lower, the concentration of calcium on the concentrate side increased with time reaching a saturation point. Earlier experiments have shown that calcium carbonate precipitates at a pH as low as 8.6^{60,61}. After scaling precipitation, the CEM was restored with an acid cleaning. In the experiments presented here, Donnan dialysis extended the operation period and therefore reduced the chemical need as the frequency of cleaning is reduced. Although Donnan dialysis extended the operation period and therefore reduced the chemical need, it can still be combined with a in situ cleaning to guarantee the long term operation of the ES operation.

Thompson-Brewster et al., 2017 predicted the major scaling site occurring in electrochemical recovery of ammonium to be in the double layer on the concentrate side of the CEM. The model described how two different pre-treatments can reduce the occurrence of scaling (such as struvite)³⁸. In our study, the predominant anion responsible for scaling was carbonate unlike previous studies that observed phosphate or sulphate precipitation^{38,44}. As the CEM blocks anions, we believe CO₂ formed in acidic conditions is transported by diffusion through the CEM and forms carbonate under alkaline conditions in the concentrate solution^{62–64}.

As previous work has shown, the membrane structure and influent composition must be considered when designing an electrodialysis cell for nutrient recovery^{41,44,59}. Bivalent ions are present in several (source separated) wastewater streams such as black water and urine.^{38,65} Pre-treatments that simultaneously minimize the application of chemicals, maintain the overall energy demand, and limit additional capital investments should be further investigated to prevent scaling and consequently improve the system performance^{44,66}. By combining electrodialysis and Donnan dialysis, we extended the operation of an electrochemical system supplied with a complex wastewater from 12 hour to 36 hours at the same nitrogen load vs applied current. The period of operation was further extended from 36 hours up to 96 hours by increasing the Load Ratio from 1 to 1.5. Moreover, the combined system was able to effectively remove the ammonium present in the influent (to less than 100 mg L⁻¹ in the effluent).

Future research should include the performance of the system at higher current densities and the use of other more concentrated streams such as manure.

Conclusion

Donnan dialysis delayed the scaling effect on cation exchange membranes, allowing the operation of an electrodialysis system for a longer period without interruption for cleaning. At the same Load ratio and current density, the combined system operated for 24 hours more than a stand-alone electrochemical system, before the cell voltage increased significantly. Here, Donnan dialysis acted as a pH regulator of the concentrate solution and consequently delayed calcite (CaCO_3) precipitation. By increasing the current compared to the TAN loading (Load ratio), the operation window was further extended up to 96 hours and consequently increasing the treatment capacity, while maintaining a high TAN recovery of 83% and consuming $10.9 \text{ kWh g}_\text{N}^{-1}$.

References

- (1) Gao, M.; Zhang, L.; Florentino, A. P.; Liu, Y. Performance of Anaerobic Treatment of Blackwater Collected from Different Toilet Flushing Systems: Can We Achieve Both Energy Recovery and Water Conservation? *Journal of Hazardous Materials* **2019**, 365, 44–52. <https://doi.org/10.1016/j.jhazmat.2018.10.055>.
- (2) Moges, M. E.; Todt, D.; Heistad, A. Treatment of Source-Separated Blackwater: A Decentralized Strategy for Nutrient Recovery towards a Circular Economy. *Water (Switzerland)* **2018**, 10 (4). <https://doi.org/10.3390/w10040463>.
- (3) Maurer, M.; Schwegler, P.; Larsen, T. A. Nutrients in Urine: Energetic Aspects of Removal and Recovery. *Water Science and Technology* **2003**, 48 (1), 37–46. <https://doi.org/10.1017/S000748530002229X>.
- (4) Galloway, J. N.; Townsend, A. R.; Erisman, J. W.; Bekunda, M.; Cai, Z.; Freney, J. R.; Martinelli, L. A.; Seitzinger, S. P.; Sutton, M. A. Transformation of the Nitrogen Cycle : *Science (1979)* **2008**, 320 (May), 889–892. <https://doi.org/10.1126/science.1136674>.
- (5) Theregowda, R. B.; González-Mejía, A. M.; Ma, X.; Garland, J. Nutrient Recovery from Municipal Wastewater for Sustainable Food Production Systems: An Alternative to Traditional Fertilizers. *Environmental Engineering Science* **2019**, 36 (7), 833–842. <https://doi.org/10.1089/ees.2019.0053>.
- (6) Cordell, D.; Rosemarin, A.; Schröder, J. J.; Smit, A. L. Towards Global Phosphorus Security: A Systems Framework for Phosphorus Recovery and Reuse Options. *Chemosphere* **2011**, 84 (6), 747–758. <https://doi.org/10.1016/j.chemosphere.2011.02.032>.
- (7) Cordell, D.; Drangert, J. O.; White, S. The Story of Phosphorus: Global Food Security and Food for Thought. *Global Environmental Change* **2009**, 19 (2), 292–305. <https://doi.org/10.1016/j.gloenvcha.2008.10.009>.
- (8) Wilfert, P.; Kumar, P. S.; Korving, L.; Witkamp, G. J.; van Loosdrecht, M. C. M. *The Relevance of Phosphorus and Iron Chemistry to the Recovery of Phosphorus from Wastewater: A Review*; 2015; Vol. 49. <https://doi.org/10.1021/acs.est.5b00150>.
- (9) Egle, L.; Rechberger, H.; Krampe, J.; Zessner, M. Phosphorus Recovery from Municipal Wastewater: An Integrated Comparative Technological, Environmental and Economic Assessment of P Recovery Technologies. *Science of the Total Environment*. 2016, pp 522–542. <https://doi.org/10.1016/j.scitotenv.2016.07.019>.
- (10) Kuntke, P.; Sleutels, T. H. J. A.; Rodríguez Arredondo, M.; Georg, S.; Barbosa, S. G.; ter Heijne, A.; Hamelers, H. V. M.; Buisman, C. J. N. (Bio)Electrochemical Ammonia Recovery: Progress and Perspectives. *Applied Microbiology and Biotechnology* **2018**, 102 (9), 3865–3878. <https://doi.org/10.1007/s00253-018-8888-6>.
- (11) Ahn, Y. H. Sustainable Nitrogen Elimination Biotechnologies: A Review. *Process Biochemistry* **2006**, 41 (8), 1709–1721. <https://doi.org/10.1016/j.procbio.2006.03.033>.
- (12) Rodríguez Arredondo, M.; Kuntke, P.; ter Heijne, A.; Hamelers, H. V. M.; Buisman, C. J. N. Load Ratio Determines the Ammonia Recovery and Energy Input of an Electrochemical System. *Water Research* **2017**, 111 (3), 330–337. <https://doi.org/10.1016/j.watres.2016.12.051>.
- (13) Rodríguez Arredondo, M.; Kuntke, P.; Jeremiasse, A. W.; Sleutels, T. H. J. A.; Buisman, C. J. N.; ter Heijne, A. Bioelectrochemical Systems for Nitrogen Removal and Recovery from Wastewater. *Environ. Sci.: Water Res. Technol.* **2015**, 1 (1), 22–33. <https://doi.org/10.1039/C4EW00066H>.
- (14) Giddey, S.; Badwal, S. P. S.; Kulkarni, A. Review of Electrochemical Ammonia Production Technologies and Materials. *International Journal of Hydrogen Energy*. Elsevier Ltd 2013, pp 14576–14594. <https://doi.org/10.1016/j.ijhydene.2013.09.054>.
- (15) Shipman, M. A.; Symes, M. D. Recent Progress towards the Electrosynthesis of Ammonia from Sustainable Resources. *Catalysis Today* **2017**, 286, 57–68. <https://doi.org/10.1016/j.cattod.2016.05.008>.

- (16) Kuntke, P.; Rodríguez Arredondo, M.; Widyakristi, L.; Ter Heijne, A.; Sleutels, T. H. J. A. J. A. H. J. A. J. A.; Hamelers, H. V. M. M. V. M. M.; Buisman, C. J. N. N. J. N. N. Hydrogen Gas Recycling for Energy Efficient Ammonia Recovery in Electrochemical Systems. *Environmental Science and Technology* **2017**, 51 (5), 3110–3116. <https://doi.org/10.1021/acs.est.6b06097>.
- (17) Kuntke, P.; Rodrigues, M.; Sleutels, T.; Saakes, M.; Hamelers, H. V. M.; Buisman, C. J. N. Energy-Efficient Ammonia Recovery in an Up-Scaled Hydrogen Gas Recycling Electrochemical System. *ACS Sustainable Chemistry & Engineering* **2018**, 6 (6), acssuschemeng.8b00457. <https://doi.org/10.1021/acssuschemeng.8b00457>.
- (18) Zeeman, G.; Kujawa-Roeleveld, K. Resource Recovery from Source Separated Domestic Waste(Water) Streams; Full Scale Results. *Water Science and Technology* **2011**, 64 (10), 1987–1992. <https://doi.org/10.2166/wst.2011.562>.
- (19) Larsen, T. A.; Udert, K. M.; Lienert, J. *Source Separation and Decentralization for Wastewater Management*; 2015. <https://doi.org/10.2166/9781780401072>.
- (20) Tarpeh, W. A.; Barazesh, J. M.; Cath, T. Y.; Nelson, K. L. Electrochemical Stripping to Recover Nitrogen from Source-Separated Urine. *Environmental Science and Technology* **2018**, 52 (3), 1453–1460. <https://doi.org/10.1021/acs.est.7b05488>.
- (21) Ledezma, P.; Kuntke, P.; Buisman, C. J. N.; Keller, J.; Freguia, S. Source-Separated Urine Opens Golden Opportunities for Microbial Electrochemical Technologies. *Trends in Biotechnology*. April 2015, pp 214–220. <https://doi.org/10.1016/j.tibtech.2015.01.007>.
- (22) Kuntke, P.; Rodrigues, M.; Sleutels, T.; Saakes, M.; Hamelers, H. V. M.; Buisman, C. J. N. Energy-Efficient Ammonia Recovery in an Up-Scaled Hydrogen Gas Recycling Electrochemical System. *ACS Sustainable Chemistry & Engineering* **2018**, acssuschemeng.8b00457. <https://doi.org/10.1021/acssuschemeng.8b00457>.
- (23) de Graaff, M. S.; Temmink, H.; Zeeman, G.; Buisman, C. J. N. Anaerobic Treatment of Concentrated Black Water in a UASB Reactor at a Short HRT. *Water (Basel)* **2010**, 2 (1), 101–119. <https://doi.org/10.3390/w2010101>.
- (24) Vlaeminck, S. E.; Terada, A.; Smets, B. F.; van der Linden, D.; Boon, N.; Verstraete, W.; Carballa, M. Nitrogen Removal from Digested Black Water by One-Stage Partial Nitrification and Anammox. *Environmental Science and Technology* **2009**, 43 (13), 5035–5041. <https://doi.org/10.1021/es803284y>.
- (25) Zamora, P.; Georgieva, T.; Salcedo, I.; Elzinga, N.; Kuntke, P.; Buisman, C. J. N. Long-Term Operation of a Pilot-Scale Reactor for Phosphorus Recovery as Struvite from Source-Separated Urine. *Journal of Chemical Technology and Biotechnology* **2017**, 92 (5), 1035–1045. <https://doi.org/10.1002/jctb.5079>.
- (26) Cunha, J. R.; Schott, C.; van der Weijden, R. D.; Leal, L. H.; Zeeman, G.; Buisman, C. J. N. Recovery of Calcium Phosphate Granules from Black Water Using a Hybrid Upflow Anaerobic Sludge Bed and Gas-Lift Reactor. *Environmental Research* **2019**, 178 (March), 108671. <https://doi.org/10.1016/j.envres.2019.108671>.
- (27) Lei, Y.; Du, M.; Kuntke, P.; Saakes, M.; Van Der Weijden, R.; Buisman, C. J. N. Energy Efficient Phosphorus Recovery by Microbial Electrolysis Cell Induced Calcium Phosphate Precipitation. *ACS Sustainable Chemistry and Engineering* **2019**, 7 (9), 8860–8867. <https://doi.org/10.1021/acssuschemeng.9b00867>.
- (28) Lei, X.; Sugiura, N.; Feng, C.; Maekawa, T. Pretreatment of Anaerobic Digestion Effluent with Ammonia Stripping and Biogas Purification. *Journal of Hazardous Materials* **2007**, 145 (3), 391–397. <https://doi.org/10.1016/j.jhazmat.2006.11.027>.
- (29) Wasielewski, S.; Morandi, C. G.; Minke, R.; Steinmetz, H. Ammonium Recovery by Ion Exchange from Effluents of Anaerobic Blackwater Co-Digestion and Struvite Precipitation Reactors. **2016**.
- (30) Rodríguez Arredondo, M.; Kuntke, P.; Jeremiasse, A. W.; Sleutels, T. H. J. A.; Buisman, C. J. N.; ter Heijne, A. Bioelectrochemical Systems for Nitrogen Removal and Recovery from Wastewater. *Environ. Sci.: Water Res. Technol.* **2015**, 1 (1), 22–33. <https://doi.org/10.1039/C4EW00066H>.

- (31) Casademont, C.; Farias, M. A.; Pourcelly, G.; Bazinet, L. Impact of Electrodialytic Parameters on Cation Migration Kinetics and Fouling Nature of Ion-Exchange Membranes during Treatment of Solutions with Different Magnesium/Calcium Ratios. *Journal of Membrane Science* **2008**, *325* (2), 570–579. <https://doi.org/10.1016/j.memsci.2008.08.023>.
- (32) Choi, M. J.; Chae, K. J.; Ajayi, F. F.; Kim, K. Y.; Yu, H. W.; Kim, C. won; Kim, I. S. Effects of Biofouling on Ion Transport through Cation Exchange Membranes and Microbial Fuel Cell Performance. *Bioresource Technology* **2011**, *102* (1), 298–303. <https://doi.org/10.1016/j.biortech.2010.06.129>.
- (33) Luther, A. K.; Desloover, J.; Fennell, D. E.; Rabaey, K. Electrochemically Driven Extraction and Recovery of Ammonia from Human Urine. *Water Research* **2015**, *87*, 367–377. <https://doi.org/10.1016/j.watres.2015.09.041>.
- (34) Rodríguez Arredondo, M.; Kuntke, P.; ter Heijne, A.; Hamelers, H. V. M.; Buisman, C. J. N. Load Ratio Determines the Ammonia Recovery and Energy Input of an Electrochemical System. *Water Research* **2017**, *111* (3), 330–337. <https://doi.org/10.1016/j.watres.2016.12.051>.
- (35) Rijnaarts, T.; Shenkute, N. T.; Wood, J. A.; De Vos, W. M.; Nijmeijer, K. Divalent Cation Removal by Donnan Dialysis for Improved Reverse Electrodialysis. *ACS Sustainable Chemistry and Engineering* **2018**, *6* (5), 7035–7041. <https://doi.org/10.1021/acssuschemeng.8b00879>.
- (36) Yang, Y.; Gao, X.; Fan, A.; Fu, L.; Gao, C. An Innovative Beneficial Reuse of Seawater Concentrate Using Bipolar Membrane Electrodialysis. *Journal of Membrane Science* **2014**, *449*, 119–126. <https://doi.org/10.1016/j.memsci.2013.07.066>.
- (37) Ping, Q.; Cohen, B.; Dosoretz, C.; He, Z. Long-Term Investigation of Fouling of Cation and Anion Exchange Membranes in Microbial Desalination Cells. *Desalination* **2013**, *325*, 48–55. <https://doi.org/10.1016/j.desal.2013.06.025>.
- (38) Thompson Brewster, E.; Ward, A. J.; Mehta, C. M.; Radjenovic, J.; Batstone, D. J. Predicting Scale Formation during Electrodialytic Nutrient Recovery. *Water Research* **2017**, *110*, 202–210. <https://doi.org/10.1016/j.watres.2016.11.063>.
- (39) Pan, Y.; Zhu, T.; He, Z. Minimizing Effects of Chloride and Calcium towards Enhanced Nutrient Recovery from Sidestream Centrate in a Decoupled Electrodialysis Driven by Solar Energy. *Journal of Cleaner Production* **2020**, *263*, 121419. <https://doi.org/10.1016/j.jclepro.2020.121419>.
- (40) Shaposhnik, V. A.; Zubets, N. N.; Strygina, I. P.; Mill, B. E. High Demineralization of Drinking Water by Electrodialysis without Scaling on the Membranes. *Desalination* **2002**, *145* (1–3), 329–332. [https://doi.org/10.1016/S0011-9164\(02\)00431-9](https://doi.org/10.1016/S0011-9164(02)00431-9).
- (41) Andreeva, M. A.; Gil, V. v.; Pismenskaya, N. D.; Nikonenko, V. v.; Dammak, L.; Larchet, C.; Grande, D.; Kononenko, N. A. Effect of Homogenization and Hydrophobization of a Cation-Exchange Membrane Surface on Its Scaling in the Presence of Calcium and Magnesium Chlorides during Electrodialysis. *Journal of Membrane Science* **2017**, *540* (April), 183–191. <https://doi.org/10.1016/j.memsci.2017.06.030>.
- (42) Casademont, C.; Pourcelly, G.; Bazinet, L. Effect of Magnesium/Calcium Ratio in Solutions Subjected to Electrodialysis: Characterization of Cation-Exchange Membrane Fouling. *Journal of Colloid and Interface Science* **2007**, *315* (2), 544–554. <https://doi.org/10.1016/j.jcis.2007.06.056>.
- (43) Ayala-Bribiesca, E.; Pourcelly, G.; Bazinet, L. Nature Identification and Morphology Characterization of Cation-Exchange Membrane Fouling during Conventional Electrodialysis. *Journal of Colloid and Interface Science* **2006**, *300* (2), 663–672. <https://doi.org/10.1016/j.jcis.2006.04.035>.
- (44) Asraf-Snir, M.; Gilron, J.; Oren, Y. *Scaling of Cation Exchange Membranes by Gypsum during Donnan Exchange and Electrodialysis*; Elsevier B.V., 2018; Vol. 567. <https://doi.org/10.1016/j.memsci.2018.08.009>.
- (45) Andreeva, M. A.; Gil, V. v.; Pismenskaya, N. D.; Dammak, L.; Kononenko, N. A.; Larchet, C.; Grande, D.; Nikonenko, V. v. Mitigation of Membrane Scaling in Electrodialysis by Electroconvection Enhancement, PH Adjustment and Pulsed Electric Field Application. *Journal of Membrane Science* **2018**, *549* (December 2017), 129–140. <https://doi.org/10.1016/j.memsci.2017.12.005>.

- (46) Tran, A. T. K.; Jullok, N.; Meesschaert, B.; Pinoy, L.; van der Bruggen, B. Pellet Reactor Pretreatment: A Feasible Method to Reduce Scaling in Bipolar Membrane Electrodialysis. *Journal of Colloid and Interface Science* **2013**, 401, 107–115. <https://doi.org/10.1016/j.jcis.2013.03.036>.
- (47) Cox, J. A.; Dinunzio, J. E. Donnan Dialysis Enrichment of Cations. *Analytical Chemistry* **1977**, 49 (8), 1272–1275. <https://doi.org/10.1021/ac50016a056>.
- (48) Rodrigues, M.; Sleutels, T.; Kuntke, P.; Hoekstra, D.; ter Heijne, A.; Buisman, C. J. N.; Hamelers, H. V. M. Exploiting Donnan Dialysis to Enhance Ammonia Recovery in an Electrochemical System. *Chemical Engineering Journal* **2020**, 395 (April), 125143. <https://doi.org/10.1016/j.cej.2020.125143>.
- (49) Chen, C.; Dong, T.; Han, M.; Yao, J.; Han, L. Ammonium Recovery from Wastewater by Donnan Dialysis: A Feasibility Study. *Journal of Cleaner Production* **2020**, 265, 121838. <https://doi.org/10.1016/j.jclepro.2020.121838>.
- (50) Campione, A.; Gurreri, L.; Ciofalo, M.; Micale, G.; Tamburini, A.; Cipollina, A. Electrodialysis for Water Desalination: A Critical Assessment of Recent Developments on Process Fundamentals, Models and Applications. *Desalination* **2018**, 434 (December 2017), 121–160. <https://doi.org/10.1016/j.desal.2017.12.044>.
- (51) Kuntke, P.; Rodríguez Arredondo, M.; Widyakristi, L.; ter Heijne, A.; Sleutels, T. H. J. A.; Hamelers, H. V. M.; Buisman, C. J. N. Hydrogen Gas Recycling for Energy Efficient Ammonia Recovery in Electrochemical Systems. *Environmental Science & Technology* **2017**, 51 (5), 3110–3116. <https://doi.org/10.1021/acs.est.6b06097>.
- (52) Cunha, J. R.; Schott, C.; van der Weijden, R. D.; Leal, L. H.; Zeeman, G.; Buisman, C. J. N. Calcium Addition to Increase the Production of Phosphate Granules in Anaerobic Treatment of Black Water. *Water Research* **2018**, 130, 333–342. <https://doi.org/10.1016/j.watres.2017.12.012>.
- (53) Sleutels, T. H. J. A.; Heijne, A. ter; Buisman, C. J. N.; Hamelers, H. V. M. Steady-State Performance and Chemical Efficiency of Microbial Electrolysis Cells. *International Journal of Hydrogen Energy* **2013**, 38 (18), 7201–7208. <https://doi.org/10.1016/j.ijhydene.2013.04.067>.
- (54) Sleutels, T. H. J. A.; ter Heijne, A.; Kuntke, P.; Buisman, C. J. N.; Hamelers, H. V. M. Membrane Selectivity Determines Energetic Losses for Ion Transport in Bioelectrochemical Systems. *ChemistrySelect* **2017**, 2 (12), 3462–3470. <https://doi.org/10.1002/slct.201700064>.
- (55) Rodrigues, M.; de Mattos, T. T.; Sleutels, T.; ter Heijne, A.; Hamelers, H. V. M.; Buisman, C. J. N.; Kuntke, P. Minimal Bipolar Membrane Cell Configuration for Scaling up Ammonium Recovery. *ACS Sustainable Chemistry and Engineering* **2020**, 8 (47), 17359–17367. <https://doi.org/10.1021/acssuschemeng.0c05043>.
- (56) Post, J. W.; Hamelers, H. V. M.; Buisman, C. J. N. Influence of Multivalent Ions on Power Production from Mixing Salt and Fresh Water with a Reverse Electrodialysis System. *Journal of Membrane Science* **2009**, 330 (1–2), 65–72. <https://doi.org/10.1016/j.memsci.2008.12.042>.
- (57) Choi, M. J.; Chae, K. J.; Ajayi, F. F.; Kim, K. Y.; Yu, H. W.; Kim, C. won; Kim, I. S. Effects of Biofouling on Ion Transport through Cation Exchange Membranes and Microbial Fuel Cell Performance. *Bioresource Technology* **2011**, 102 (1), 298–303. <https://doi.org/10.1016/j.biortech.2010.06.129>.
- (58) Hasson, D.; Sidorenko, G.; Semiat, R. Calcium Carbonate Hardness Removal by a Novel Electrochemical Seeds System. *Desalination* **2010**, 263 (1–3), 285–289. <https://doi.org/10.1016/j.desal.2010.06.036>.
- (59) Belashova, E.; Mikhaylin, S.; Pismenskaya, N.; Nikonenko, V.; Bazinet, L. Impact of Cation-Exchange Membrane Scaling Nature on the Electrochemical Characteristics of Membrane System. *Separation and Purification Technology* **2017**, 189 (May), 441–448. <https://doi.org/10.1016/j.seppur.2017.08.045>.
- (60) Koutsoukos, P. G.; Kontoyannis, C. G. Precipitation of Calcium Carbonate in Aqueous Solutions. *Journal of the Chemical Society, Faraday Transactions 1: Physical Chemistry in Condensed Phases* **1984**, 80 (5), 1181–1192. <https://doi.org/10.1039/F19848001181>.

- (61) Söhnel, O.; Mullin, J. W. Precipitation of Calcium Carbonate. *Journal of Crystal Growth* **1982**, 60 (2), 239–250. [https://doi.org/10.1016/0022-0248\(82\)90095-1](https://doi.org/10.1016/0022-0248(82)90095-1).
- (62) Nikonenko, V.; Lebedev, K.; Manzanares, J. A.; Pourcelly, G. Modelling the Transport of Carbonic Acid Anions through Anion-Exchange Membranes. *Electrochimica Acta* **2003**, 48 (24), 3639–3650. [https://doi.org/10.1016/S0013-4686\(03\)00485-7](https://doi.org/10.1016/S0013-4686(03)00485-7).
- (63) Paz-Garcia, J. M.; Schaetzle, O.; Biesheuvel, P. M.; Hamelers, H. V. M. Energy from CO₂ Using Capacitive Electrodes - Theoretical Outline and Calculation of Open Circuit Voltage. *Journal of Colloid and Interface Science* **2014**, 418, 200–207. <https://doi.org/10.1016/j.jcis.2013.11.081>.
- (64) Legrand, L.; Shu, Q.; Tedesco, M.; Dykstra, J. E.; Hamelers, H. V. M. Role of Ion Exchange Membranes and Capacitive Electrodes in Membrane Capacitive Deionization (MCDI) for CO₂ Capture. *Journal of Colloid and Interface Science* **2020**, 564 (Mcdi), 478–490. <https://doi.org/10.1016/j.jcis.2019.12.039>.
- (65) Shi, L.; Hu, Y.; Xie, S.; Wu, G.; Hu, Z.; Zhan, X. Recovery of Nutrients and Volatile Fatty Acids from Pig Manure Hydrolysate Using Two-Stage Bipolar Membrane Electrodialysis. *Chemical Engineering Journal* **2018**, 334 (August 2017), 134–142. <https://doi.org/10.1016/j.cej.2017.10.010>.
- (66) Zabolotsky, V. I.; Nikonenko, V. v.; Pismenskaya, N. D.; Istoshin, A. G. Electrodialysis Technology for Deep Demineralization of Surface and Ground Water. *Desalination* **1997**, 108 (1–3), 179–181. [https://doi.org/10.1016/S0011-9164\(97\)00025-8](https://doi.org/10.1016/S0011-9164(97)00025-8).

Appendix A – Materials and Methods

A.1. Experimental Setup

The ED cell had four compartments namely, anode, feed, concentrate and cathode. The anode and cathode compartment compartments were poly methyl methacrylate (PMMA) plates, having a size of 21cm x 21cm x 2.5cm and a machined flow field of 10cm x 10cm x 0.2cm. Both compartments included a platinum (Pt) coated titanium mesh electrode measuring 9.8cm x 9.8cm (5mg Pt cm⁻² Magneto Special Anodes BV, The Netherlands) used as a current collector.

The compartments were separated by customized silicon rubber gaskets and different ion exchange membranes. The silicon rubber gaskets were used to make the system leak proof and gastight. The ion exchange membranes had a projected surface area of 100cm², in accordance with the flow field dimensions of different compartments. Nitril spacers (50% open) were used between the serpentine shaped flow fields and the adjacent ion exchange membranes.

Anode was separated from feed compartment by a Membrane Electrode Assembly (MEA). MEA consisted a 15cm x 15cm Nafion N117 cation exchange membrane (CEM) coated with a 10cm x 10cm of Platinum-Vulcan (carbon) Catalyst (0.5mg Pt cm⁻²), having an integrated Gas Diffusion Layer (GDL) and purchased from FuelCellsEtc (Texas, USA). The reactive side of MEA i.e. catalyst with a GDL was facing the anode compartment. Feed and concentrate compartment were separated from each other by, a 15cm x 15cm cation exchange membrane (CEM) fumasep FKB-PK-130 (FUMATECH BWT GmbH, Bietigheim-Bissingen, Germany). Concentrate compartment was separated from cathode compartment by a 15cm x 15cm anion exchange membrane (AEM) fumasep FAB-PK-130 (FUMATECH BWT GmbH, Bietigheim-Bissingen, Germany).

Feed and concentrate compartments were customized polypropylene (PP) plates with each having a size of 21cm x 21cm x 1.2cm and a serpentine shaped flow-field of 10cm x 10cm x 1.2cm, 60% open.

TAN was recovered through a transmembrane chemisorption (TMCS) module, a membrane module consisting of a gas permeable hydrophobic membrane (pore size – 200nm, type – Accurel PP V8/HE, CUT Membrane Technology, GmbH, Germany). The lumen was supplied with concentrate and the shell with acid. Due to the concentration gradient across the membrane, ammonia from the concentrate solution was transported over this gas permeable hydrophobic membrane and was recovered in sulphuric acid (1M H₂SO₄) with a volume of 2 L (batch).

The total liquid volume of the feed, concentrate and cathode compartments including the recirculation vessels was 500 mL, 620 mL and 400 mL, respectively.

H₂ was recycled from cathode to anode in the ED cell and additionally extra hydrogen was supplied for losses (25% of the supplied current). The additional H₂ was produced in an electrolyser operated at a constant current using 0.01 M of H₂SO₄. Nitrogen (N₂) was used as a carrier gas to transport H₂ formed at the cathode to the anode. In order to have an oxygen free environment, a water lock was added to the anode compartment.

Ag/AgCl reference electrodes (+0.2V vs NHE, QMX711X, QiS-Prosence BV, Oosterhout, The Netherlands) were placed in the feed, concentrate and cathode compartments, so as to measure MEA potential (anode), cathode potential, CEM potential and AEM potential. The reference electrodes were connected to a high impedance pre-amplifier (PPM-3C, Bank Elektronik – Intelligent Controls GmbH Pohlheim, Germany). Temperature and pH of the feed, concentrate and cathode was measured using sensors (Orbisint CPS11D) connected to a transmitter (Liquiline CM444, Endress+Hauser BV, Naarden, The Netherlands). Similarly, conductivity of the feed and cathode was measured using electrodes (QC205X EC) and a controller (P915-85, QiS-Prosence BV, Oosterhout, The Netherlands). The system was supplied with a constant current by a Delta power supply (ES 030-5, Delta Elektronika BV, Zierikzee, The Netherlands). The data for pH, temperature, conductivity, cell voltage, anode potential and cathode potential was recorded every minute and stored using a data logger (Memograph M, RSG40, Endress+Hauser, BV).

A.2. Calculations

TAN Recovery Efficiency

It determines the amount of TAN recovered from the total amount of TAN supplied to the system.

$$TAN\ Recovery\ (\%) = \left(\frac{C_{TAN,influent} - C_{TAN,effluent}}{C_{TAN,influent}} \right) \times 100$$

Where, $C_{TAN,effluent}$ is the TAN concentration in the effluent (mol L^{-1}).

TAN Transport Rate

It is the amount of TAN transported over CEM i.e. from feed compartment to the concentrate compartment.

TAN transport rate ($g_N m^{-2} d^{-1}$)

$$= \frac{(C_{TAN,influent} - C_{TAN,effluent}) \times Q_{influent} \times t \times M_N}{A_m}$$

Where, M_N is the molar mass nitrogen ($g\ mol^{-1}$), $M_{NH_4^+}$ is the molar mass of ammonium ($g\ mol^{-1}$) and t is the number of seconds per day, respectively.

Potential Losses

Were calculated as previously described in ⁵¹

1) Cathode Overpotential ($\eta_{cathode}$)

$$\eta_{cathode}(V) = E_{cathode}^0 - E_{cathode}$$

Where, $E_{cathode}$ is the measured cathode potential and $E_{cathode}^0$ is the calculated cathode potential (-1.029V).

2) MEA Overpotential (η_{anode})

$$\eta_{anode}(V) = E_{anode} - E_{anode}^0$$

Where, E_{anode} is the measured anode potential and E_{anode}^0 is the calculated anode potential (-0.201V).

3) E_{pH} is a potential loss due to pH gradient.

$$E_{pH} (V) = \frac{RT}{F} \times (pH_{cathode} - pH_{CEM})$$

Where, R is the gas constant ($J \text{ mol}^{-1} \text{ K}^{-1}$), T is the temperature (K), F is the Faraday constant ($C \text{ mol}^{-1}$), $pH_{cathode}$ is the pH of the cathode and pH_{CEM} is the pH in the CEM membrane.

4) E_{ion} is the potential loss due to ionic losses.

$$E_{ion} (V) = j * \left(\frac{Thickness_{Feed}}{Conductivity_{Feed}} + \frac{Thickness_{Concentrate}}{Conductivity_{Concentrate}} + \frac{Thickness_{Cathode}}{Conductivity_{Cathode}} \right)$$

Where, j is the current density ($A \text{ m}^{-2}$), thickness (m) and conductivity ($S \text{ m}^{-1}$).

5) $E_{membrane}$ is potential loss occurring from the membrane.

$$E_{membrane} (V) = E_{cell} - \eta_{cathode} - \eta_{anode} - E_{pH} - E_{ion}$$

Where, E_{cell} is the measured cell voltage (V).

Transport number

The transport number was calculated based on the total applied charge (current) and the difference between the ion concentration of the influent and effluent. The transport number (t_i) was calculated for all ions in solution (except for protons and hydroxide). The transport of protons was defined as the difference between the total charged applied and the sum of the earlier calculated charge transported (i.e. Na^+ , K^+ , NH_4^+ , Mg^{2+} , Ca^{2+}).

$$t_i = \frac{\Delta C_i z_i F Q A t}{J t}$$

where ΔC_i is the cation concentration difference between influent and effluent (mol L^{-1}), z_i is the net charge of that cation (-).

Energy Input

$$Energy \text{ Input } (kJ \text{ g}_N^{-1}) = \frac{(j * E_{cell}) \times t}{TAN \text{ Transport Rate}}$$

Appendix B

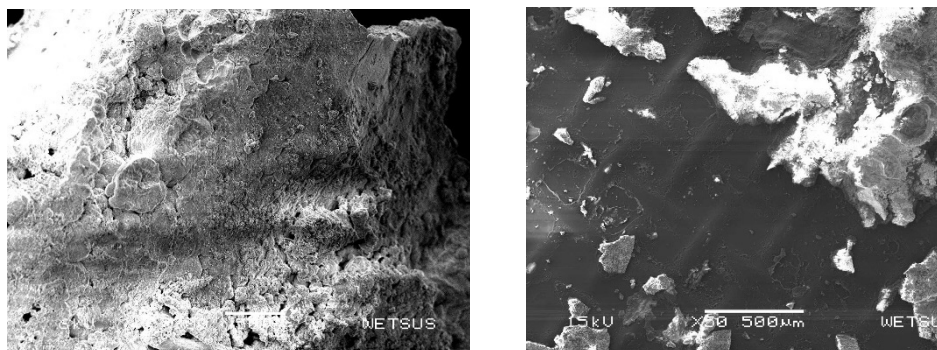


Figure A.1: Calcium Carbonate Precipitation on Cation Exchange Membrane. Scaling in the CEM was identified as calcite (CaCO_3) and was confirmed through SEM analysis. Scaling blocks the CEM, consequently increasing the membrane resistance, which leads to an increase in the energy consumption. Scaling is promoted by the high pH of our concentrate, limiting the process.

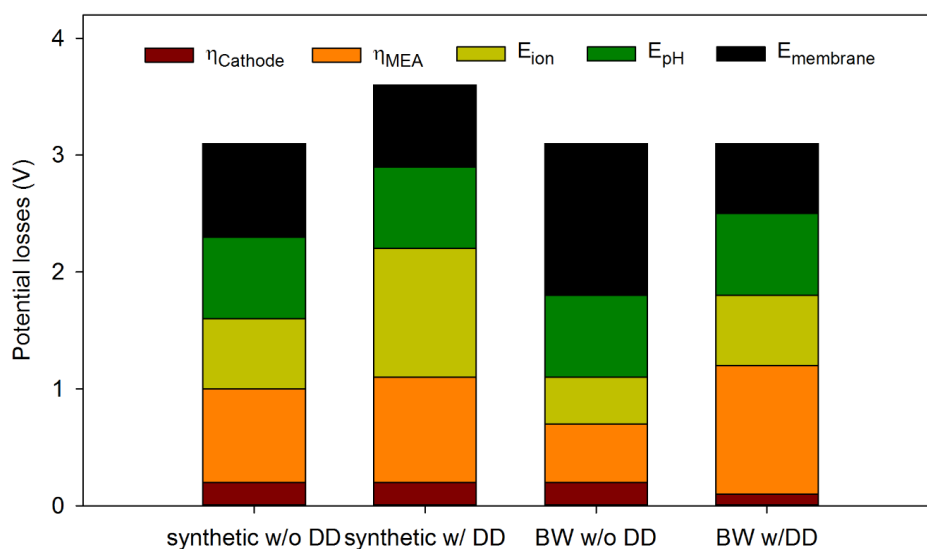


Figure A.2: Potential losses vs energy Input for Load ratio 1 while operating the ES with DD (w/ DD) and without DD (w/o DD) and synthetic influent and black Water.

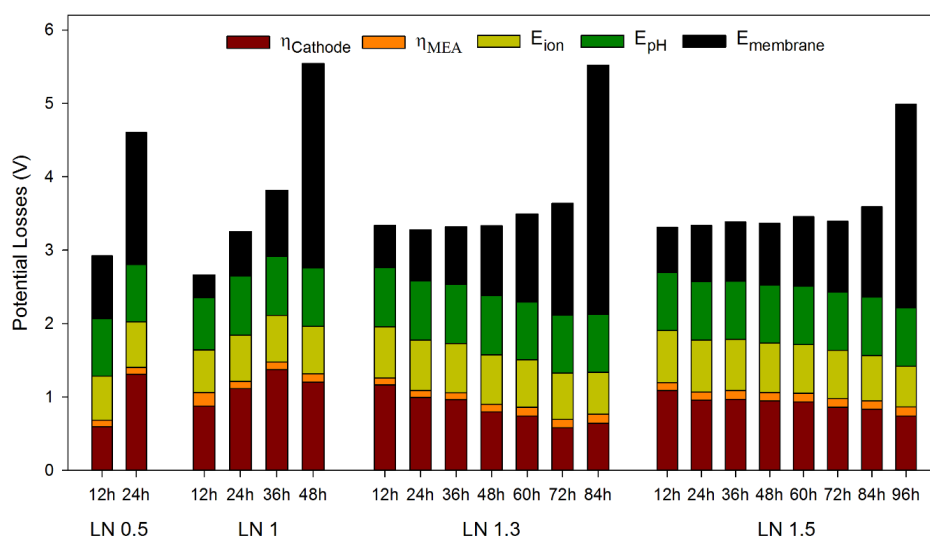
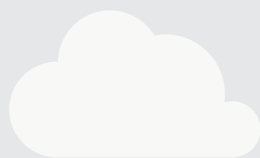
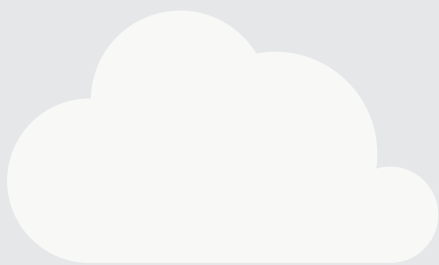


Figure A.3: Average potential losses measured every 12 hours of each experiment carried out at constant Load Ratio (0.5, 1, 1.2 and 1.5).

4



Chapter 4

Minimal bipolar membrane cell configuration for scaling up ammonium recovery

This Chapter has been published as:

Rodrigues, M., De Mattos, T.T., Sleutels, T., Ter Heijne, A., Hamelers, H.V.M., Buisman, C.J.N., Kuntke, P., 2020a. Minimal Bipolar Membrane Cell Configuration for Scaling up Ammonium Recovery. ACS Sustain. Chem. Eng. 8, 17359–17367.
<https://doi.org/10.1021/acssuschemeng.0c05043>



Abstract

Electrochemical systems for total ammonium nitrogen (TAN) recovery are a promising alternative compared with conventional nitrogen removal technologies. To make them competitive, we propose a new minimal stackable configuration using cell pairs with only bipolar membranes and cation exchange membranes. The tested bipolar electrodialysis (BP-ED) stack included six cell pairs of feed and concentrate compartments. Critical operational parameters, such as current density and ratio between applied current to nitrogen loading (load ratio), were varied to investigate the performance of the system using synthetic wastewater with high nitrogen content as influent ($\text{NH}_4^+ \approx 1.75 \text{ g L}^{-1}$). High TAN removal (>70%) was achieved for a load ratio higher than one. At current densities of 150 A m^{-2} and a load ratio 1.2, a TAN transport rate of $1145.1 \pm 14.1 \text{ g}_\text{N} \text{ m}^{-2} \text{ d}^{-1}$ and a TAN removal efficiency of 80% were observed. As the TAN removal was almost constant at different current densities, the BP-ED stack performed at a high TAN transport rate ($819.1 \text{ g}_\text{N} \text{ m}^{-2} \text{ d}^{-1}$) while consuming the lowest energy ($18.3 \text{ kJ g}_\text{N}^{-1}$) at load ratio 1.2 and 100 A m^{-2} . The TAN transport rate, TAN removal and energy input achieved by the minimal BP-ED stack demonstrated a promising new cell configuration for upscaling.

Introduction

Currently, we rely on energy intensive processes for ammonia production (Haber-Bosch process, $37 \text{ kJ g}_\text{N}^{-1}$) and subsequent nitrogen removal (nitrification/denitrification process, $46 \text{ kJ g}_\text{N}^{-1}$) in wastewater treatment plants (WWTP) ^{1,2}. For example, the sludge produced during the wastewater treatment is frequently processed by anaerobic digestion for methane production ³⁻⁵. After digestion, the sludge dewatering process results in a nitrogen rich stream known as reject water or centrate. The centrate contains between $400 - 2400 \text{ mg}_\text{N} \text{ L}^{-1}$ ⁶⁻⁸. Therefore, centrate requires further treatment before discharge, for example by the Anammox process (requiring an energy input of $16 \text{ kJ g}_\text{N}^{-1}$) ⁸⁻¹³.

Recently, electrodialysis (ED) has been proposed as an alternative to conventional TAN (total ammonium nitrogen) removal processes (nitrification/denitrification) as it allows subsequent nitrogen recovery instead of merely removing it ¹⁴⁻¹⁹. ED has already been demonstrated as one of the most energy efficient systems to remove nitrate from drinking water and wastewater ^{17,20,21}. ED is a separation process based on ion-exchange membranes where positive ions are transported through a cation exchange membrane (CEM) and negative ions are transported through an anion exchange membrane (AEM), due to an applied electric field ²². In recent years, the application of bipolar membranes (BPM) in ED technology has gained increasing attention, considering their unique behavior and properties such as high permselectivity and a high rate of water splitting ^{23,24}. BPMs dissociate water in protons and hydroxide which move through the cation and the anion layer of the BPM, respectively and thereby produce an acidic and an alkaline stream ^{25,26}. This allows for stacking of compartments with fewer electrodes while still supplying the protons/hydroxide also provided by the electrodes oxidation/reduction reactions. BPMs have a lower energy consumption compared to water electrolysis that produces hydrogen and oxygen gas at the electrodes (79.9 kJ mol^{-1} vs $198.5 \text{ kJ mol}^{-1}$) ²⁵. Other advantages of replacing the electrodes include the absence of reduction/oxidation species that could lead to unwanted by-products such as chlorine gas or halogenated organic compounds. In established bipolar ED (BP-ED) configuration, cell triplets (Acidic concentrate, diluate, alkaline concentrate) are used following the order: Anode | CEM | BPM | AEM | ... | CEM | BPM | AEM | cathode ^{27,28}. Ions are removed from the diluate stream, due to an applied electric field. Cations move from the diluate through the CEM towards the alkaline concentrate while anions move from the diluate through an AEM towards the acidic concentrate. This configuration of membranes (BPM, CEM and AEM) has previously been used in BP-ED processes such as desalination or reverse electrodialysis (RED) ^{23,29,30}. Pronk et al.,

2006 were first to report BP-ED for TAN recovery from urine in combination with a mass transfer unit (i.e., bubble columns or a gas-filled (hydrophobic) membrane) to obtain a product containing ammonium and phosphate ³¹. Their results showed that ammonia was removed from urine, but also undesired carbonate was recovered in the basic concentrate, limiting the purity of the product ²⁷. More recently, van Linden et al., 2020 operated a BP-ED system in batch containing 10 cell triplets (acid; diluate; base) and achieved up to 90% ammonium removal from synthetic medium (NH_4HCO_3 solution) at an energy input of $19 \text{ kJ g}_\text{N}^{-1}$ ²⁸.

To make the established BP-ED a more competitive technology for TAN recovery, we propose a new minimal cell configuration (Figure 1). The most important difference with previously reported BP-ED is that each cell pair in the stack has only two compartments instead of three, and no AEMs are employed except one facing the cathode. Therefore, no concentrated acid stream is formed. As a result, fewer membranes and compartments are needed and therefore the costs of the stack are reduced and less energy is required.

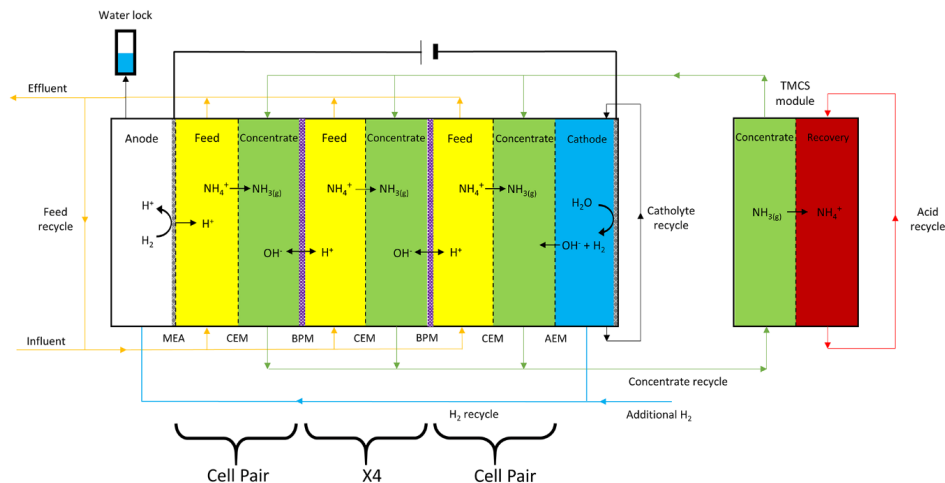


Figure 1. Scheme of the minimal cell configuration of the electro dialysis cell with a bipolar membrane (BPM) coupled with a cation exchange membrane (CEM) as cell pair. The minimal bipolar electro dialysis cell configuration includes 6 cell pairs of feed and concentrate compartments between the anode and cathode compartments. The BPM dissociates water into protons and hydroxyl ions. The cation side of the BPM supplies protons to the feed compartment. The protons protonate ammonia into ammonium, which can cross over the CEM to the concentrate compartment. On the other side, the anion side of the BPM, the hydroxyl ions pass to the concentrate compartment. Here the hydroxide reacts with the NH_4^+ , forming NH_3 . NH_3 can then be recovered in acid of the TMCS module (Transmembrane Chemisorption unit, Membrane stripping unit). The membrane electrode assembly supplies H^+ to the first feed compartment next to the anode. The anion exchange membrane works as a shielding membrane for the cathode (only OH^- was transported to the concentrate). The hydrogen gas formed at the cathode is then re-used at the anode, decreasing the energy requirement.

The anode supplies protons generated in the MEA to the adjacent feed compartment and at the cathode hydroxide ions cross through an AEM to the adjacent concentrate compartment. Inside the BP-ED stack, the BPMs supply protons to the feed and hydroxide ions to the concentrate compartment, thereby taking over the function of the electrodes (Figure 1). This leads to the formation of a pH gradient. The protons in the feed compartment, where the influent is supplied, protonate ammonia to ammonium which can be transported through the CEM towards the concentrate in direction of the cathode. The ammonium ions are then retained in the concentrate as they are blocked by the AEM side of the BPM, or by the AEM next to the cathode. Simultaneously, ammonium is deprotonated to ammonia in the concentrate as a result of hydroxide ions transported through the anion side of the bipolar membrane or the AEM from the cathode. The ammonia can then be recovered from the concentrate stream in the TMCS module (Transmembrane Chemisorption, membrane stripping unit).³² During membrane stripping, the ammonia is separated from the other cations in the concentrate and can be recovered in an acid solution as fertilizer $[(\text{NH}_4)_2\text{SO}_4]^{1,33}$.

In this BP-ED stack the hydrogen produced at the cathode was recycled to the anode and oxidized to provide energy to operate this system at low energy input. Hydrogen recycling has been shown to provide half of the energy required for TAN recovery³².

The main goal of this study is to assess the performance of this new minimal BP-ED stack configuration, consisting of 6 stacked cell pairs, for TAN recovery from synthetic wastewater. In this work, we demonstrate that stacking ED cell pairs enhances the TAN transport rate, TAN removal and recovery efficiency, at low energy consumption in a continuous operation mode.

Materials and methods

Setup configuration

The minimal BP-ED stack configuration comprised one anode, 6 feed compartments and 6 concentrate compartments (alternated) and one cathode. Figure 1 shows a schematic representation of the setup.

The ED stack materials were supplied by REDstack BV (Sneek, The Netherlands). The stack included a gas compartment for the anode and a cathode chamber. Both in the anode and cathode compartments, a Pt-coated titanium mesh electrode (9.8 cm x 9.8 cm x 0.2 cm, 5 mg Pt cm⁻² Magneto Special Anodes BV) was used. Twelve

polypropylene spacers (14 cm x 14 cm x 0.05 cm, 53% open) with a silicon gasket layer (2 cm x 14 cm) at two opposing sides for sealing were used as feed and concentrate compartments (DEUKUM GmbH, Frickenhausen, Germany).

The anode was separated from the feed compartment by a membrane electrode assembly (MEA). The MEA was composed of an electrode for gas oxidation, facing the anode, coated on a CEM, facing the feed side. The MEA was a commercial 14 cm x 14 cm Nafion N117 CEM coated with a 10 cm x 10 cm platinum Vulcan (carbon) catalyst (0.5 mg Pt cm⁻²) and an integrated gas diffusion layer (GDL) purchased from FuelCellsETC (College Station, TX, USA).

The feed compartments were separated from the concentrate compartments on one side by CEMs. The CEMs used were fumasep® FKB-PK-130 (14 cm x 14 cm, Fumatech BWT GmbH, Bietigheim-Bissingen, Germany). On the other side, BPMs (fumasep® FBM-PK, 14 cm x 14 cm, Fumatech BWT GmbH) were used to separate the concentrate compartment from the feed compartment.

The last concentrate compartment was separated from the cathode by an AEM (14 cm x 14 cm, fumasep® FAB-PK-130, Fumatech BWT GmbH). Thus, in total, 1 MEA, 6 CEMs, 5 BPMs and 1 AEM were used in the following order from anode to cathode: MEA| CEM| BPM| CEM| BPM| CEM| BPM| CEM| BPM| CEM| BPM| CEM| AEM. Each membrane had a projected surface area in contact with the electrolyte of 100 cm².

A TMCS module (Liquicell membrane contactor, EXF 8x2.5" model, 3M, Germany) with a membrane surface area of 1.4 m² was used for the recovery step, where the concentrate was recirculated on the lumen side and an acidic solution on the shell side of the membrane.

The H₂ was carried from cathode to anode by a 15 ml min⁻¹ flow of nitrogen gas. An external source (support cell) supplied 10% extra hydrogen gas to this recycling stream to compensate for any leakages in the main setup, as described in Kuntke et al., 2018¹.

During operation, a Memograph M RSG40 data logger (Endress+Hauser BV) recorded every minute the applied current and cell voltage of BP-ED and support cell, the pH and temperature in the feed, concentrate, catholyte and acid compartment and the conductivity in the feed compartment. Each compartment (feed, concentrate, cathode and acid) had its own pH sensor (Orbisint CPS11D) connected to a Liquiline CM444 transmitter (Endress+Hauser BV, Naarden, The Netherlands). A

conductivity sensor (QC205X EC electrodes and P915-85 – Controller (QjS-Prosence BV, Oosterhout, The Netherlands)) was placed in the feed compartment. The applied current was controlled by a power supply (ES 030-5, Delta Elektronika BV, Zierikzee, The Netherlands).

Operational conditions

Synthetic wastewater was used as influent, to study a solution with a defined and constant composition and to better quantify the transport over the membrane and avoid undesired phenomena such as scaling. The synthetic wastewater had the following composition: 12.8 mM KCl; 10.9 mM NaCl; 0.26 mM K_2SO_4 ; 18.7 mM NH_4Cl ; 46.2 mM $(NH_4)_2CO_3$. This composition was based on ion concentrations measured from real centrate collected from Rioolwaterzuiverings installatie (a WWTP) in the city of Heerenveen, Netherlands (See Appendix A – Table I).

All liquids were replaced at the beginning of each experiment. Initially, the concentrate was filled with synthetic influent solution and the cathode was filled with 0.1 M NaOH to increase the conductivity. The OH^- originated from the salt dissociation was negligible compared to the water dissociation at the BPMs and at the cathode electrode. A 3M H_2SO_4 solution was dosed continuously to the acid side of the TMCS to guarantee a concentration gradient between concentrate and acid, while maintaining a final product with pH 3.

All liquid compartments were recirculated at 4 cm s^{-1} (720 mL min^{-1}) to avoid mass transfer limitations.³⁴ (see Appendix B – Table S2).

Different current densities per electrode area (25 A m^{-2} - 150 A m^{-2}) were tested to quantify the transport rate over the CEMs. The current densities were selected within the membrane operation range recommended by the manufacturer, below the limiting current density. Additionally, different ratios between current and TAN loading (load ratio, LN) described by equation 1 were tested (0.4 – 1.7).¹⁴ These load ratios were selected to demonstrate the performance of the system under insufficient current (0.4), close to optimum (0.9-1.2) and excess of current (1.4-1.7) compared to TAN loading. The stack was operated with a continuous inflow of feed for each parameter tested for a minimum of 5 days, with the exception of 150 A m^{-2} . For this condition, the system was operated for 3 days due to the impracticality of the large influent volume needed for operation (approx. 74 L/d). All results show the average and standard deviation over 5 days of constant operation and of duplicate samples, unless stated otherwise.

Table 1. Load ratio and current densities applied to the stack.

Current density (A m ⁻²)	load ratio				
	0.4	0.9	1.2	1.4	1.7
25			X		
50	X	X	X	X	X
100		X	X	X	X
150			X		

Calculations

The load ratio was previously studied as a crucial parameter to characterize electrochemical systems for ammonium recovery and can be described by the following equation ¹⁴:

$$Ln = \frac{j A_e}{C_{TAN} Q F} \times 6 \quad (\text{Equation 1})$$

Where, j is current density (A m⁻²), is the projected surface area of the electrode (anode) (m²), 6 is the factor to account for 6 cell pairs, C_{TAN} is the concentration of TAN in the feed inflow (mol L⁻¹), the inflow rate (L min⁻¹), and is the Faraday constant (96 485 C mol⁻¹).

TAN transport rate per total CEM area in g_N m⁻² d⁻¹ for the ED system was calculated as:

$$TAN \text{ transport rate} = \frac{(C_{inf,TAN} Q_{inf} - C_{eff,TAN} Q_{eff})}{6 \times A_m} \quad (\text{Equation 2})$$

where $C_{inf,TAN}$ Q_{inf} is the influent TAN concentration (g_N L⁻¹), Q_{inf} is the influent flow rate (L d⁻¹), $C_{eff,TAN}$ Q_{eff} is the effluent TAN concentration (g_N L⁻¹), Q_{eff} is the effluent flow rate (L d⁻¹), and 6 is the number of CEMs used in the stack and A_m the area of one CEM (100 cm²). Water transport towards the concentrate was observed and quantified, meaning the effluent volume was smaller than the influent supplied therefore requiring the introduction of Q_{eff} .

TAN Removal efficiency in % for the BP-ED system is given by:

$$TAN \text{ Removal} = \frac{C_{inf,TAN} Q_{inf} - C_{eff,TAN} Q_{eff}}{C_{inf,TAN} Q_{inf}} \quad (\text{Equation 3})$$

TAN Recovery efficiency in % for the TMCS module:

$$TAN\ Recovery = \frac{C_{acid,TAN} Q_{acid}}{C_{inf,TAN} Q_{inf} - C_{eff,TAN} Q_{eff}} \quad (\text{Equation 4})$$

Where $C_{acid,TAN}$ is the TAN concentration in the final product ($\text{g}_N \text{ L}^{-1}$) and Q_{acid} is the volume of final product formed per day (L d^{-1}).

Energy consumption in kJ g_N^{-1} for the BP-ED system:

$$Energy\ consumption = \frac{(E_{cell} I_{cell} + E_{sup.cell} I_{sup.cell}) t}{TAN\ transport\ rate \times 6 \times A_m} \quad (\text{Equation 5})$$

Where E_{cell} is cell voltage (V), I_{cell} is applied current (A), $E_{sup.cell}$ is cell voltage of the support cell supplying the 10% additional hydrogen (V), $I_{sup.cell}$ is applied current of the support cell supplying the additional hydrogen (A), t is the number of seconds per day (86400 s d^{-1}). The TMCS energy consumption was not accounted as no caustic addition or temperature increase was used.

Analysis and measurements

IC cations analysis (Na^+ , K^+ , NH_4^+) and IC anions (SO_4^{2-} , Cl^- , NO_3^- , NO_2^-) were done daily for the influent, feed, concentrate, cathode and acid streams, using a Metrohm Compact IC Flex 930 instrument with a cation column (Metrosep C 4-150/4.0) and a Metrohm Compact IC 761 instrument with an anion column (Metrosep A Supp 5-150/4.0), respectively, each equipped with a conductivity detector (Metrohm Nederland BV, Schiedam, The Netherlands). Inorganic carbon was measured using TOC-L CPH, Shimadzu BENELUX, 's-Hertogenbosch (The Netherlands) for all samples. Last, pH and conductivity of all samples were also measured daily with handheld meters Seven Excellence S470, Mettler Toledo, Tiel, The Netherlands).

Results and discussions

The performance of the minimal BP-ED stack will be described when operated at different current densities and load ratios regarding TAN removal efficiency, TAN transport rate per total CEM area, energy consumption and TAN recovery efficiency. All results show the average and standard deviation over 5 days of constant operation and, of duplicate samples, unless stated otherwise.

High TAN removal efficiency from synthetic wastewater using the minimal BP-ED can be achieved for load ratio above 1.

Figure 2 shows the effect of the load ratio (ratio between current applied and the TAN loading) on the TAN removal efficiency, at current densities 50 A m^{-2} and 100 A m^{-2} .

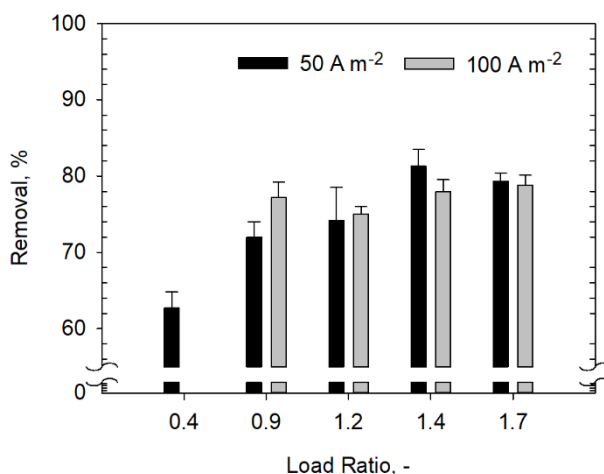


Figure 2. TAN removal efficiency obtained for different load ratios at 50 A m^{-2} and 100 A m^{-2} . The TAN removal efficiency increases with load ratio. Approximately 80% removal is achieved for a load ratio higher than 1, at both current densities.

For a load ratio of 0.4 at 50 A m^{-2} , 63% of TAN was removed from the influent (feed compartment) (Figure 2). For a load ratio above 0.9, TAN removal efficiencies of >70% were obtained, independent of the current density. When compared to previously described studies (Table 2), this BP-ED stack achieved a comparable or higher TAN removal efficiency^{17,19,35}.

Based on previous work of Rodriguez-Arredondo et al., 2017, a lower TAN removal of around 40% was expected at a load ratio of 0.4¹⁴. Besides the ion migration caused by the applied current, diffusion can play a significant role, as it has been demonstrated in other electrochemical ammonium treatment systems^{28,36}. A possible explanation for the additional removal observed here is ammonium diffusion from the feed towards

the concentrate in exchange for other ions that have accumulated in the concentrate solution, an exchange previously described as Donnan Dialysis (see Appendix D, Figure S1)^{37,38}. After ammonium is removed from the feed, it is converted to ammonia (NH_3) in the concentrate compartment. NH_3 is transported through the TMCS module, where a sulfuric acid solution is constantly recirculated, converting NH_3 back to ammonium and producing an ammonium sulfate solution. Ideally, all the ammonium transported over the CEM should be recovered in the acid, meaning the recovery should match the removal efficiency. However, TAN recovery was slightly lower than the TAN removal for lower current densities. The difference between TAN recovery and TAN removal can be due to losses in the system such as ammonia losses (volatilization) from the compartments³⁶. It was observed that the difference between TAN removal efficiency and TAN recovery can be avoided by operating at higher current densities as a high concentrate pH was achieved (pH>9.5 was achieved when operating at 100 A m^{-2} and 150 A m^{-2}). The pH of the concentrate compartment increased with an increasing current density, since cations (other than ammonium and protons) accumulate in the concentrate compartment and more OH^- ions are produced by the BPMs and the cathode³⁹. The high pH in the concentrate favors the conversion of ammonium to ammonia in the concentrate. Gustin et al., 2011 have shown that a minimum pH of 10 must be achieved to avoid a limitation on the ammonia recovery efficiency and consequently improve the amount of stripped ammonia-nitrogen and the TMCS performance⁴⁰.

At load ratio 1.2, the BP-ED stack maintains a high TAN transport rate while consuming the least energy.

Electrodialysis is an electricity driven system, which means that energy consumption is an important parameter that affects the system's economic feasibility. The energy consumption of an ED stack is determined by the system internal resistance and efficiency of ion transport across the membrane. Figure 3 presents the energy consumption for the complete stack and the TAN transport rate per total membrane area at 50 A m^{-2} at different load ratios.

An increase in energy consumption was observed between Load Ratio 0.4 and load ratio 0.9 as the TAN transport rate decreased (Figure 3). At load ratio 0.9, the energy consumption was $18.0 \pm 1.1 \text{ kJ g}_\text{N}^{-1}$, slightly decreasing to $17.0 \pm 0.4 \text{ kJ g}_\text{N}^{-1}$ when operating at load ratio 1.2 ($p = 0.04$, t-test). Additionally, the TAN transport rate slightly increased for load ratio 1.2 compared to 0.9. The same trend in the TAN transport rate as function of load ratio was previously observed by Kuntke et al., 2018 for a hydrogen recycling electrochemical system using only a single cell pair¹. In our study, it was observed that for load ratio 1.2, the system consumed the least energy (Figure 3) while reaching a high TAN removal efficiency of 74.2% (Figure 2).

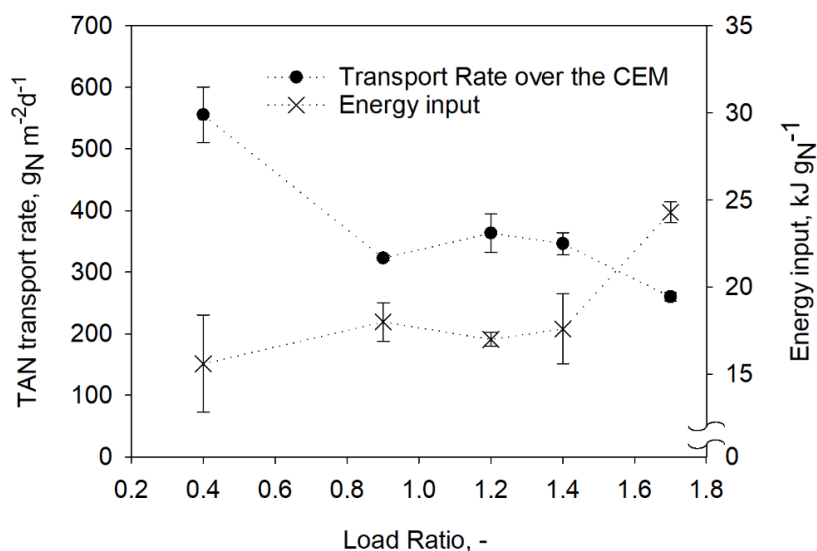


Figure 3. Energy input and TAN transport rate for different load ratios at 50 A m⁻². A dashed line was added between points to guide the reader. The minimum energy input was observed for load ratio 1.2, for a similar TAN transport rate obtained at LN 0.9 and 1.4 and without compromising the TAN removal previously described.

Again, the energy input increased from load ratio 1.4 to load ratio 1.7 as the TAN transport rate decreased. Rodríguez-Arredondo et al., 2017 previously showed that TAN could be removed from urine at LN 1.2 using an electrochemical system¹⁴. Rodríguez-Arredondo et al., 2017 demonstrated that operation at a Load Ratio higher than 1.2 increases significantly the energy consumption of the system without further benefit on the TAN removal and TAN transport rate¹⁴. In our study, we also found that for load ratio 1.7, the energy consumption of the system increased without extra benefit on the TAN removal rate and on the TAN removal efficiency and for this reason no higher load ratios were tested^{14,19}. When the current is much higher than the TAN loading supplied to an electrochemical system (LN >> 1.3), the Load Ratio model predicts the extra charge supplied is used to transport mostly other cations (i.e., H⁺, Na⁺, K⁺) instead of NH₄⁺.¹⁴ Based on the ion transport numbers (see Appendix D, Figure S1), the charge transported by H⁺ increased with Load Ratio in the BP-ED system. Hence, the removal efficiency no longer increases and consequently the TAN transport rate decreases, while the energy input increases.

The energy input can be also further analyzed using the ion transport numbers through the CEM, (see Appendix D, Figure S1). Ammonium ions are the main transported charge over the CEM for all load ratios. However, the percentage of current used to transport NH₄⁺ decreases with increasing load ratio. With increasing load ratio, the applied current is higher than the available amount of ammonium

in the feed that can be carried with the applied current. Therefore, protons will be transported, while the transport of potassium and sodium remains constant. This was previously observed in other electrodialysis studies, including other electrochemical systems for TAN recovery^{1,37,41}. The potential transport of anions over the CEM was measured but not detected.

Operation at high current density increased the TAN transport rate, without compromising the removal efficiency for the same load ratio.

Figure 4 shows the TAN transport rate per total CEM area and energy consumption at different current densities for load ratio of 1.2 as the previous results indicated a more successful operation at this condition.

The TAN removal rate increased almost proportionally with current density (Figure 4). The TAN transport rate was $202.1 \text{ g}_\text{N} \text{ m}^{-2} \text{ d}^{-1}$ at 25 A m^{-2} and increased to $1145.1 \text{ g}_\text{N} \text{ m}^{-2} \text{ d}^{-1}$ at 150 A m^{-2} . For the different current densities tested, the TAN removal efficiency was between 74.2% and 81.3% and did not significantly change with the applied current density ($p = 0.93$, t-test), (Table S3, Appendix C). Although the TAN removal efficiency was almost constant, the energy cost to achieve this result increased with increasing current density from $12.2 \text{ kJ g}_\text{N}^{-1}$ to $38.8 \text{ kJ g}_\text{N}^{-1}$.

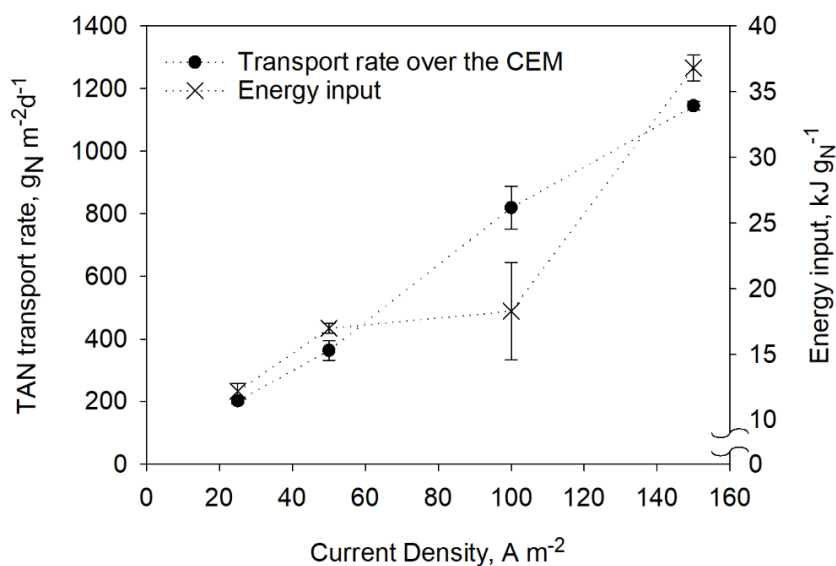


Figure 4. Transport rate per total installed CEM area and energy input at load ratio of 1.2 for different current densities. A dashed line was added between points to guide the reader. The TAN transport rate increased with current density. Also, the energy consumption gradually increase with current density, except at 100 A m^{-2} .

The ammonium transport number was constant and independent of the current density which also reflects in the TAN removal efficiency, (see Figure S2, Appendix D). Ammonium accounted for around 60% of the charge transported over the CEM. The internal resistance consisted of the anode and cathode overpotentials, ionic and pH losses and membrane potential ^{26,42}. The increase in current density amplifies particularly the membrane potential loss. The membrane potential increased as the transport of ions occurred against a higher concentration gradient between feed and concentrate (due to the accumulation of Na⁺ and K⁺ in the concentrate) ^{41,43,44}. At 25 A m⁻², the concentrations of Na⁺ and K⁺ in the concentrate solution reached 87 mM and 107 mM, respectively. At 100 A m⁻², the concentration of Na⁺ and K⁺ in the concentrate solution were 314 mM and 440 mM, respectively. Additionally, a water flux from feed to concentrate was observed for all the tested conditions. Water transport in ED was previously described by Tedesco et. al., 2017 as a result of (1) hydrostatic pressure difference across the membrane, (2) osmotic pressure difference across the membrane or (3) ion-water friction (Electro-osmosis) ^{24,45}. When operating the BP-ED stack at 150 A m⁻², the water transport was 12% higher than when operating at 50 A m⁻².

The BP-ED achieved 80% TAN removal while consuming approx. 18 kJ g_N⁻¹ at 50 and 100 A m⁻². Anammox process alone consumes 16 kJ g_N⁻¹ and when combined with Haber-Bosch it consumes 53 kJ g_N⁻¹ ^{19,46}. Therefore, the system developed during this work represents a much more energy efficient alternative technology to remove and recover nitrogen. Compared to similar electrochemical systems for TAN recovery, the BP-ED stack consumed either lower or comparable energy (see Table 2) ^{17,19,28}. Interestingly, in this minimal BP-ED stack, we observed an increase of the TAN transport rate with current density without compromising removal efficiency, while previous studies observed that a high TAN transport rate is only achieved in combination with lower TAN removal efficiency ^{1,32}. This result is supported by the constant NH₄⁺ transport number over the CEM (60%) and a positive consequence of the proposed BP-ED design improvement over other ED systems for TAN recovery.

Minimal bipolar electrodialysis stack including a CEM and BPM per cell pair is a feasible option for TAN recovery.

Table 2 includes some of the most recent developments on ED for TAN recovery which achieved high TAN removal at low energy consumption.

Table 2. TAN removal efficiency and other key operation parameters of ED like systems reported in literature.

	LN	j	Influent/amount N A.m ⁻² g.L ⁻¹	Mode ^(b)	Cell pairs	A _m cm ²	TAN transport rate g _N .m ² .d ⁻¹	TAN Removal %	Energy input kJ g _N ⁻¹	H ₂ recycling
Pronk et al., 2006 ³¹	-	-	Urine≈6.3	B	3 ^(c)	49	-	100	-	-
Desloover et al., 2012 ¹⁵	1.6	20	Digestate ^{(a)≈5}	C	1	64	90	58	16.7	✓
Luther et al., 2015 ³⁵	-	50	Urine ^{(a)≈5}	-	1	64	384	86.7	12.4	✓
Kuntke et al., 2017 ³²	1.3	50	Urine≈5.1	C	1	100	342.1	73	15.6	✓
Kuntke et al., 2018 ¹	1.3	100	Urine ^{(a)≈5.1}	C	1	400	598	58	23.4	✓
Tarpeh et al., 2018 ¹⁷	-	100	Urine≈4	C	1	64	-	60.6	30.6	-
Ward et al., 2018 ⁴⁷	-	20	Centrate ≈0.7	C	30 ^(c)	3.6x10 ⁴	129.6	78	18	-
Yan et al., 2018 ⁴⁸	-	2.9	Wastewater ^{(a)≈0.2}	B	2 ^(c)	189	-	65	4.5 ^(d)	-
Yan et al., 2020 ⁴⁹	-	200	Wastewater ^{(a)≈5}	B	2 ^(c)	189	-	99	7.9 ^(d)	-
van Linden et al., 2020 ²⁸	-	-	Diluate ^(a) NH ₄ HCO ₃ ≈1.5	B	10 ^(c)	640	-	85	18	-
This study	1.2	25	Wastewater ^{(a)≈2}	C	6 ^(c)	600	202.1	81.3	12.2	✓
This study	1.2	50	Wastewater ^{(a)≈2}	C	6 ^(c)	600	363.5	74.2	17	✓
This study	1.2	100	Wastewater ^{(a)≈2}	C	6 ^(c)	600	819.1	78	18.3	✓

(a) Synthetic Influent, (b) Operation Mode: B- Batch; C- Continuous, (c) system includes BPMs, (d) recalculated to kJ gN⁻¹

The minimal BP-ED cell configuration stack achieved a much higher TAN transport rate per membrane area compared to Kuntke et al., 2018, namely $819.1 \text{ g}_\text{N} \cdot \text{m}^2 \cdot \text{d}^{-1}$ at 100 A m^{-2} using synthetic wastewater, at a lower energy input. The minimal BP-ED cell configuration stack consumed slightly more energy per gram of nitrogen removed than Luther et al., 2015 and Kuntke et al., 2017, while transporting a higher amount of nitrogen per membrane area. The average TAN removal efficiency was 80%, which is comparable to the aforementioned studies. However, it is worth mentioning that these studies achieved similar energy input and TAN removal efficiency using a system with only 1 CEM.

Compared to previous BP-ED systems, the energy input and TAN removal were comparable.^{28,31} The use of a minimalistic approach for BP-ED using only 2 membranes per cell pair instead of three membranes is beneficial, as less membrane area and fewer compartments are used. As an AEM is more prone to biological fouling of negatively charge compounds, a longer performance is expected for the tested BP-ED configuration in our study⁵⁰. However, our minimal BP-ED configuration does not remove the anions presents in the wastewater.

During BP-ED operation, the pH increased in the concentrate compartment, allowing our minimal BP-ED combined with membrane stripping (transmembrane chemisorption, TMCS) to recover nitrogen by only requiring an acid solution and applied current. Unlike conventional ammonia (membrane) stripping processes for TAN recovery, no caustics addition and temperature increase were required BP-ED¹⁷. Additionally, although BP-ED still requires an acid to capture the ammonia, from the end-user point of view, the fertilizer formed is pure and consequently the product can be easily introduced in the market^{24,31}.

Overall, the minimal BP-ED operated in continuous feed flow at a higher current density, treating a larger volume of (synthetic) wastewater. The minimal BP-ED cell configuration stack treated up to 73 L d^{-1} and removed around 100 g of nitrogen per day at a load ratio 1.2 and a current density of 150 A m^{-2} . As previously described, the energy consumption per gram of nitrogen was similar to a conventional 1 cell pair ED system while improving the amount of nitrogen transported per membrane area. The use of BPMs guarantee a comparable energy input and together with hydrogen recycling, no harmful compounds are produced in this system, such as chlorine gas and halogenated organic compounds. As this BP-ED system operated at both high TAN transport rate and removal efficiency with low energy consumption, it is a promising solution towards upscaling of ammonia recovery from wastewater. Additionally, this more compact system with high treatment capacity can become

an interesting alternative to technologies such as conventional stripping or forward osmosis^{51–55}. The influence of bivalent ions found in centrate was not included in this study. Several studies previously demonstrated the scaling effects on a CEM when calcium and magnesium are present in the influent, even at low concentrations^{56–58}. Future research should focus on real wastewater to investigate the effects of scaling and (bio) fouling in this BP-ED stack for ammonia recovery and further scaling up with more cell pairs. Wastewaters with a high TAN concentration are the main focus for this minimal BP-ED configuration and further research might be needed when treating wastewater with a lower TAN concentration (less than 0.5 g L⁻¹).

Conclusion

In this work, we investigated a new cell configuration design for TAN recovery. A minimal BP-ED stack was built with cell pairs made of CEM and BPM instead of cell triplets with AEM, CEM and BPM. The minimal cell configuration was demonstrated to be energy efficient in TAN removal and recovery from synthetic wastewater. The minimal BP-ED cell configuration was stacked with 6 cell pairs and removed up to 80% of the supplied TAN during continuous operation. At a load ratio 1.2 and a current density of 100 A m⁻², the BP-ED stack treated 49 L d⁻¹ at a TAN transport rate of 819 g_N m⁻² d⁻¹ while consuming 18.3 kJ g_N⁻¹. The TAN transport rate and the treatment capacity were improved by increasing the current density without compromising the TAN removal efficiency. We demonstrated that this minimal BP-ED stack is a promising option for TAN recovery.

References

- (1) Kuntke, P.; Rodrigues, M.; Sleutels, T.; Saakes, M.; Hamelers, H. V. M. M.; Buisman, C. J. N. N. Energy-Efficient Ammonia Recovery in an Up-Scaled Hydrogen Gas Recycling Electrochemical System. *ACS Sustainable Chemistry and Engineering* **2018**, 6(6), 7638–7644. <https://doi.org/10.1021/acssuschemeng.8b00457>.
- (2) Maurer, M.; Schwegler, P.; Larsen, T. A. Nutrients in Urine: Energetic Aspects of Removal and Recovery. *Water Science and Technology* **2003**, 48 (1), 37–46. <https://doi.org/10.1017/S000748530002229X>.
- (3) Vlaeminck, S. E.; Terada, A.; Smets, B. F.; Van Der Linden, D.; Boon, N.; Verstraete, W.; Carballa, M. Nitrogen Removal from Digested Black Water by One-Stage Partial Nitrification and Anammox. *Environmental Science and Technology* **2009**, 43 (13), 5035–5041. <https://doi.org/10.1021/es803284y>.
- (4) S. Solomon, D. Qin, M. Manning, Z. Chen, M. Marquis, K.B. Averyt, M. T. and H. L. M. (eds.). *IPCC (2007) Climate Change 2007: The Physical Science Basis. Contribution of Working Group I to the Fourth Assessment Report of the Intergovernmental Panel on Climate Change.*; Cambridge, United Kingdom 996 pp., 2007.
- (5) Fux, C.; Siegrist, H. Nitrogen Removal from Sludge Digester Liquids by Nitrification/Denitrification or Partial Nitrification/Anammox: Environmental and Economical Considerations. *Water Science and Technology* **2004**, 50 (10), 19–26. <https://doi.org/10.2166/wst.2004.0599>.
- (6) Akhiar, A.; Battimelli, A.; Torrijos, M.; Carrere, H. Comprehensive Characterization of the Liquid Fraction of Digestates from Full-Scale Anaerobic Co-Digestion. *Waste Management* **2016**. <https://doi.org/10.1016/j.wasman.2016.11.005>.
- (7) Arnold, E.; Böhm, B.; Wilderer, P. A. Application of Activated Sludge and Biofilm Sequencing Batch Reactor Technology to Treat Reject Water from Sludge Dewatering Systems: A Comparison. *Water Science and Technology* **2000**, 41 (1), 115–122.
- (8) Constantine, T. A. North American Experience with Centrate Treatment Technologies for Ammonia and Nitrogen Removal. *Proceedings of the Water Environment Federation* **2014**, 2006 (7), 5271–5281. <https://doi.org/10.2175/193864706783763291>.
- (9) Janus, H. M.; Van Der Roest, H. F. Don't Reject the Idea of Treating Reject Water. *Water Science and Technology* **1997**, 35 (10), 27–34. [https://doi.org/10.1016/S0273-1223\(97\)00220-5](https://doi.org/10.1016/S0273-1223(97)00220-5).
- (10) Wang, H.; Liu, J.; He, W.; Qu, Y.; Li, D.; Feng, Y. Energy-Positive Nitrogen Removal from Reject Water Using a Tide-Type Biocathode Microbial Electrochemical System. **2016**. <https://doi.org/10.1016/j.biortech.2016.09.090>.
- (11) Kuntke, P.; Sleutels, T. H. J. A.; Rodríguez Arredondo, M.; Georg, S.; Barbosa, S. G.; ter Heijne, A.; Hamelers, H. V. M.; Buisman, C. J. N. (Bio)Electrochemical Ammonia Recovery: Progress and Perspectives. *Applied Microbiology and Biotechnology* **2018**, 102 (9), 3865–3878. <https://doi.org/10.1007/s00253-018-8888-6>.
- (12) Wu, X.; Modin, O. SI: Ammonium Recovery from Reject Water Combined with Hydrogen Production in a Bioelectrochemical Reactor. *Bioresource Technology* **2013**, 146, 530–536. <https://doi.org/10.1016/j.biortech.2013.07.130>.
- (13) Ek, M.; Bergström, R.; Bjurhem, J. E.; Björleinius, B.; Hellström, D. Concentration of Nutrients from Urine and Reject Water from Anaerobically Digested Sludge. *Water Science and Technology* **2006**, 54 (11–12), 437–444. <https://doi.org/10.2166/wst.2006.924>.
- (14) Rodríguez Arredondo, M.; Kuntke, P.; ter Heijne, A.; Hamelers, H. V. M. V. M.; Buisman, C. J. N. J. N. Load Ratio Determines the Ammonia Recovery and Energy Input of an Electrochemical System. *Water Research* **2017**, 111 (3), 330–337. <https://doi.org/10.1016/j.watres.2016.12.051>.
- (15) Desloover, J.; Abate Woldeyohannis, A.; Verstraete, W.; Boon, N.; Rabaey, K. Electrochemical Resource Recovery from Digestate to Prevent Ammonia Toxicity during Anaerobic Digestion. *Environmental Science and Technology* **2012**, 46 (21), 12209–12216. <https://doi.org/10.1021/es3028154>.

- (16) Pronk, W.; Biebow, M.; Boller, M. Electrodialysis for Recovering Salts from a Urine Solution Containing Micropollutants. *Environmental Science & Technology* **2006**, 40 (7), 2414–2420. <https://doi.org/10.1021/es051921i>.
- (17) Tarpeh, W. A.; Barazesh, J. M.; Cath, T. Y.; Nelson, K. L. Electrochemical Stripping to Recover Nitrogen from Source-Separated Urine. *Environmental Science and Technology* **2018**, 52 (3), 1453–1460. <https://doi.org/10.1021/acs.est.7b05488>.
- (18) van Linden, N.; Spanjers, H.; van Lier, J. B. Application of Dynamic Current Density for Increased Concentration Factors and Reduced Energy Consumption for Concentrating Ammonium by Electrodialysis. *Water Research* **2019**, 163, 114856. <https://doi.org/10.1016/j.watres.2019.114856>.
- (19) Kuntke, P.; Sleutels, T. H. J. A.; Rodríguez Arredondo, M.; Georg, S.; Barbosa, S. G.; ter Heijne, A.; Hamelers, H. V. M.; Buisman, C. J. N. (Bio)Electrochemical Ammonia Recovery: Progress and Perspectives. *Applied Microbiology and Biotechnology* **2018**, 102 (9), 3865–3878. <https://doi.org/10.1007/s00253-018-8888-6>.
- (20) Xu, D.; Li, Y.; Yin, L.; Ji, Y.; Niu, J.; Yu, Y. Electrochemical Removal of Nitrate in Industrial Wastewater. *Frontiers of Environmental Science and Engineering*. 2018. <https://doi.org/10.1007/s11783-018-1033-z>.
- (21) Graillon, S.; Persin, F.; Pourcelly, G.; Gavach, C. Development of Electrodialysis with Bipolar Membrane for the Treatment of Concentrated Nitrate Effluents. *Desalination* **1996**, 107 (2), 159–169. [https://doi.org/10.1016/S0011-9164\(96\)00155-5](https://doi.org/10.1016/S0011-9164(96)00155-5).
- (22) Strathmann, H. Electrodialysis, a Mature Technology with a Multitude of New Applications. *Desalination* **2010**, 264 (3), 268–288. <https://doi.org/10.1016/j.desal.2010.04.069>.
- (23) Yang, Y.; Gao, X.; Fan, A.; Fu, L.; Gao, C. An Innovative Beneficial Reuse of Seawater Concentrate Using Bipolar Membrane Electrodialysis. *Journal of Membrane Science* **2014**, 449, 119–126. <https://doi.org/10.1016/j.memsci.2013.07.066>.
- (24) Huang, C.; Xu, T. Electrodialysis with Bipolar Membranes for Sustainable Development. *Environmental Science and Technology* **2006**, 40 (17), 5233–5243. <https://doi.org/10.1021/es060039p>.
- (25) Ran, J.; Wu, L.; He, Y.; Yang, Z.; Wang, Y.; Jiang, C.; Ge, L.; Bakangura, E.; Xu, T. Ion Exchange Membranes: New Developments and Applications. *Journal of Membrane Science* **2017**, 522, 267–291. <https://doi.org/10.1016/j.memsci.2016.09.033>.
- (26) Sleutels, T. H. J. A.; Hamelers, H. V. M.; Rozendal, R. A.; Buisman, C. J. N. Ion Transport Resistance in Microbial Electrolysis Cells with Anion and Cation Exchange Membranes. *International Journal of Hydrogen Energy* **2009**, 34 (9), 3612–3620. <https://doi.org/10.1016/j.ijhydene.2009.03.004>.
- (27) Pronk, W.; Biebow, M.; Boller, M. Treatment of Source-Separated Urine by a Combination of Bipolar Electrodialysis and a Gas Transfer Membrane. *Water Science and Technology* **2006**, 53 (3), 139–146. <https://doi.org/10.2166/wst.2006.086>.
- (28) van Linden, N.; Bandinu, G. L.; Vermaas, D. A.; Spanjers, H.; van Lier, J. B. Bipolar Membrane Electrodialysis for Energetically Competitive Ammonium Removal and Dissolved Ammonia Production. *Journal of Cleaner Production* **2020**, 259, 120788. <https://doi.org/10.1016/j.jclepro.2020.120788>.
- (29) Pretz, J.; Staude, E. Reverse Electrodialysis (RED) with Bipolar Membranes, an Energy Storage System. *Berichte der Bunsengesellschaft für physikalische Chemie* **2010**, 102 (4), 676–685. <https://doi.org/10.1002/bbpc.19981020412>.
- (30) van Egmond, W. J.; Saakes, M.; Noor, I.; Porada, S.; Buisman, C. J. N.; Hamelers, H. V. M. Performance of an Environmentally Benign Acid Base Flow Battery at High Energy Density. *International Journal of Energy Research* **2018**, 42 (4), 1524–1535. <https://doi.org/10.1002/er.3941>.
- (31) Pronk, W.; Biebow, M.; Boller, M. Treatment of Source-Separated Urine by a Combination of Bipolar Electrodialysis and a Gas Transfer Membrane. *Water Science and Technology* **2006**, 53 (3), 139–146. <https://doi.org/10.2166/wst.2006.086>.

- (32) Kuntke, P.; Rodríguez Arredondo, M.; Widyakristi, L.; Ter Heijne, A.; Sleutels, T. H. J. A. J. A. H. J. A. J. A. J. A.; Hamelers, H. V. M. M. V. M. M.; Buisman, C. J. N. N. J. N. N. Hydrogen Gas Recycling for Energy Efficient Ammonia Recovery in Electrochemical Systems. *Environmental Science and Technology* **2017**, *51* (5), 3110–3116. <https://doi.org/10.1021/acs.est.6b06097>.
- (33) Christiaens, M. E. R.; Udert, K. M.; Arends, J. B. A.; Huysman, S.; Vanhaecke, L.; McAdam, E.; Rabaey, K. Membrane Stripping Enables Effective Electrochemical Ammonia Recovery from Urine While Retaining Microorganisms and Micropollutants. *Water Research* **2019**, *150*, 349–357. <https://doi.org/10.1016/j.watres.2018.11.072>.
- (34) Chehayeb, K. M.; Farhat, D. M.; Nayar, K. G.; Lienhard, J. H. Optimal Design and Operation of Electrodialysis for Brackish-Water Desalination and for High-Salinity Brine Concentration. *Desalination* **2017**, *420* (June), 167–182. <https://doi.org/10.1016/j.desal.2017.07.003>.
- (35) Luther, A. K.; Desloover, J.; Fennell, D. E.; Rabaey, K. Electrochemically Driven Extraction and Recovery of Ammonia from Human Urine. *Water Research* **2015**, *87*, 367–377. <https://doi.org/10.1016/j.watres.2015.09.041>.
- (36) Bandinu, G. L. Electrodialysis with Bipolar Membranes for Ammonia Recovery in Wastewater. *MSc Thesis* **2019**.
- (37) Rodrigues, M.; Sleutels, T.; Kuntke, P.; Hoekstra, D.; ter Heijne, A.; Buisman, C. J. N. J. N.; Hamelers, H. V. M. V. M. Exploiting Donnan Dialysis to Enhance Ammonia Recovery in an Electrochemical System. *Chemical Engineering Journal* **2020**, *395* (September 2019), 125143. <https://doi.org/10.1016/j.cej.2020.125143>.
- (38) Cox, J. A.; DiNunzio, J. E. Donnan Dialysis Enrichment of Cations. *Analytical Chemistry* **1977**, *49* (8), 1272–1275. <https://doi.org/10.1021/ac50016a056>.
- (39) Rozendal, R. A.; Hamelers, H. V. M.; Buisman, C. J. N. Effects of Membrane Cation Transport on PH and Microbial Fuel Cell Performance †. *Environmental Science & Technology* **2006**, *40* (17), 5206–5211. <https://doi.org/10.1021/es060387r>.
- (40) Guštin, S.; Marinšek-Logar, R. Effect of PH, Temperature and Air Flow Rate on the Continuous Ammonia Stripping of the Anaerobic Digestion Effluent. *Process Safety and Environmental Protection* **2011**, *89* (1), 61–66. <https://doi.org/10.1016/j.psep.2010.11.001>.
- (41) Rozendal, R. A. A.; Sleutels, T. H. J. A. H. J. A.; Hamelers, H. V. M. V. M.; Buisman, C. J. N. J. N. Effect of the Type of Ion Exchange Membrane on Performance, Ion Transport, and PH in Biocatalyzed Electrolysis of Wastewater. *Water Science & Technology* **2008**, *57* (11), 1757. <https://doi.org/10.2166/wst.2008.043>.
- (42) Veerman, J. The Effect of the NaCl Bulk Concentration on the Resistance of Ion Exchange Membranes-Measuring and Modeling. *Energies (Basel)* **2020**, *13* (8). <https://doi.org/10.3390/en13081946>.
- (43) Sleutels, T. H. J. A. J. A.; ter Heijne, A.; Kuntke, P.; Buisman, C. J. N. N.; Hamelers, H. V. M. Membrane Selectivity Determines Energetic Losses for Ion Transport in Bioelectrochemical Systems. *ChemistrySelect* **2017**, *2* (12), 3462–3470. <https://doi.org/10.1002/slct.201700064>.
- (44) Tedesco, M.; Hamelers, H. V. M.; Biesheuvel, P. M. Nernst-Planck Transport Theory for (Reverse) Electrodialysis: I. Effect of Co-Ion Transport through the Membranes. *Journal of Membrane Science* **2016**, *510*, 370–381. <https://doi.org/10.1016/j.memsci.2016.03.012>.
- (45) Tedesco, M.; Hamelers, H. V. M.; Biesheuvel, P. M. Nernst-Planck Transport Theory for (Reverse) Electrodialysis: II. Effect of Water Transport through Ion-Exchange Membranes. *Journal of Membrane Science* **2017**, *531* (September 2016), 172–182. <https://doi.org/10.1016/j.memsci.2017.02.031>.
- (46) Ahn, Y. H. Sustainable Nitrogen Elimination Biotechnologies: A Review. *Process Biochemistry* **2006**, *41* (8), 1709–1721. <https://doi.org/10.1016/j.procbio.2006.03.033>.
- (47) Ward, A. J.; Arola, K.; Thompson Brewster, E.; Mehta, C. M.; Batstone, D. J. Nutrient Recovery from Wastewater through Pilot Scale Electrodialysis. *Water Research* **2018**, *135*, 57–65. <https://doi.org/10.1016/j.watres.2018.02.021>.

- (48) Yan, H.; Wu, L.; Wang, Y.; Shehzad, M. A.; Xu, T. Ammonia Capture by Water Splitting and Hollow Fiber Extraction. *Chemical Engineering Science* **2018**, 192, 211–217. <https://doi.org/10.1016/j.ces.2018.07.040>.
- (49) Yan, H.; Wu, L.; Wang, Y.; Irfan, M.; Jiang, C.; Xu, T. Ammonia Capture from Wastewater with a High Ammonia Nitrogen Concentration by Water Splitting and Hollow Fiber Extraction. *Chemical Engineering Science* **2020**, 227, 115934. <https://doi.org/10.1016/j.ces.2020.115934>.
- (50) Sosa-Fernandez, P. A.; Miedema, S. J.; Bruning, H.; Leermakers, F. A. M.; Rijnaarts, H. H. M.; Post, J. W. Influence of Solution Composition on Fouling of Anion Exchange Membranes Desalinating Polymer-Flooding Produced Water. *Journal of Colloid and Interface Science* **2019**, 557, 381–394. <https://doi.org/10.1016/j.jcis.2019.09.029>.
- (51) Darestani, M.; Haigh, V.; Couperthwaite, S. J. J.; Millar, G. J. J.; Nghiem, L. D. D. Hollow Fibre Membrane Contactors for Ammonia Recovery: Current Status and Future Developments. *Journal of Environmental Chemical Engineering* **2017**, 5 (2), 1349–1359. <https://doi.org/10.1016/j.jece.2017.02.016>.
- (52) Saracco, G.; Genon, G. High Temperature Ammonia Stripping and Recovery from Process Liquid Wastes. *Journal of Hazardous Materials* **1994**, 37 (1), 191–206. [https://doi.org/10.1016/0304-3894\(94\)85048-8](https://doi.org/10.1016/0304-3894(94)85048-8).
- (53) Provolto, G.; Perazzolo, F.; Mattachini, G.; Finzi, A.; Naldi, E.; Riva, E. Nitrogen Removal from Digested Slurries Using a Simplified Ammonia Stripping Technique. *Waste Management* **2017**, 69 (5), 154–161. <https://doi.org/10.1016/j.wasman.2017.07.047>.
- (54) Littleton, H. X.; Strom, P. F.; Cowan, R. A.; Hill, C. H. M. Design and Operational Considerations for Ammonia Removal from Centrate by Steam Stripping. **2000**, No. c.
- (55) Holloway, R. W.; Childress, A. E.; Dennett, K. E.; Cath, T. Y. Forward Osmosis for Concentration of Anaerobic Digester Centrate. *Water Research* **2007**, 41 (17), 4005–4014. <https://doi.org/10.1016/j.watres.2007.05.054>.
- (56) Belashova, E.; Mikhaylin, S.; Pismenskaya, N.; Nikonenko, V.; Bazinet, L. Impact of Cation-Exchange Membrane Scaling Nature on the Electrochemical Characteristics of Membrane System. *Separation and Purification Technology* **2017**, 189 (May), 441–448. <https://doi.org/10.1016/j.seppur.2017.08.045>.
- (57) Thompson Brewster, E.; Ward, A. J.; Mehta, C. M.; Radjenovic, J.; Batstone, D. J. Predicting Scale Formation during Electrodialytic Nutrient Recovery. *Water Research* **2017**, 110, 202–210. <https://doi.org/10.1016/j.watres.2016.11.063>.
- (58) Asraf-Snir, M.; Gilron, J.; Oren, Y. *Scaling of Cation Exchange Membranes by Gypsum during Donnan Exchange and Electrodialysis*; Elsevier B.V., 2018; Vol. 567. <https://doi.org/10.1016/j.memsci.2018.08.009>.

Appendix A: Centrate composition

Table S1. Centrate composition collected in from Wastewater treatment plant (Rioolwaterzuiverings installatie) in the city of Heerenveen, Netherlands.

	<i>g L⁻¹</i>	<i>mM</i>
<i>Chloride</i>	1.64	46.2
<i>Nitrite</i>	Below the detection range	-
<i>Nitrate</i>	Below the detection range	-
<i>Sulphate</i>	0.02	0.2
<i>Inorganic carbon</i>	0.05	4.3
<i>COD</i>	0.9	28
<i>Total carbon</i>	0.05	4.3
<i>Iron (Fe²⁺/Fe³⁺)</i>	0.01	0.2
<i>Silicon</i>	0.03	0.2
<i>Manganese</i>	Below the detection range	-
<i>Sodium</i>	0.35	15.0
<i>Ammonium</i>	2.02	112.2
<i>Potassium</i>	0.40	10.3
<i>Magnesium</i>	0.03	1.3
<i>Calcium</i>	0.07	1.7

Appendix B: Recirculation Speed effect on the performance of the system

To guarantee that the recirculation rate was not limiting the systems' performance additional experiments were performed at different recirculation speeds for feed and concentrate compartments. These experiments had load ratio 1.2 and current density 100 A m^{-2} . Table S2 presents results from the experiments (A, B and C) in terms of TAN transport rate, TAN removal, and Energy consumption.

Table S2. Experiments A, B and C for different recirculation speeds.

	A	B	C
Recirculation speed (cm s^{-1})	0.33	1	4.0
TAN transport rate ($\text{g}_\text{N} \text{ m}^{-2} \text{ d}^{-1}$)	748.7	806.3	846.1
TAN removal (%)	70	75	79
Energy consumption ($\text{kJ g}_\text{N}^{-1}$)	29.5	23.3	24.4

Experiment A had a recirculation speed twelve times lower than C (three times lower than B) and this resulted in a higher resistance for the ion transport across the CEM membrane, compromising the TAN removal and increasing energy consumption. To avoid these limitations all experiments were performed at the higher recirculation speed of 4.0 cm s^{-1} .

Appendix C: Experiments performed in this study

Table S3. Overview of the tested conditions with the minimal BP-ED cell configuration for TAN recovery.

j (A m ⁻²)	LN	Tan Transport rate (g _n m ⁻² d ⁻¹)	TAN removal (%)	TAN Recovery (%)	Energy Input (kJ g _n ⁻¹)
25	1.2	202.1±8.9	81.3±3.1	41.8±2.2	12.2±0.6
50	0.4	555.4±45.6	62.7±2.1	78.1±23.5	15.6±2.8
	1.2	363.5±31.2	74.2±4.3	52.4±7.9	17.0±0.4
	0.9	323.5±4.0	72.0±2.0	61.0±2.0	18.0±1.1
	1.4	346.3±18.1	81.3±2.2	74.2±24.3	17.6±2.0
	1.7	260.2±6.9	79.3±1.1	72.3±7.9	24.3±0.6
100	0.9	909.6±30.6	77.2±2.0	59.4±23.6	29.8±1.2
	1.1	806.0±47.0	75.0±1.0	69.6±4.0	23.3±1.8
	1.2	819.4±67.4	77.9±1.6	67.0±9.0	18.3±3.7
	1.7	578.0±40.6	78.8±1.3	57.5±2.8	22.9±1.1
150	1.2	1145.1±14.1	80.4±0.3	76.1±11.4	36.8±1.0

Appendix D: Ion Transport Number

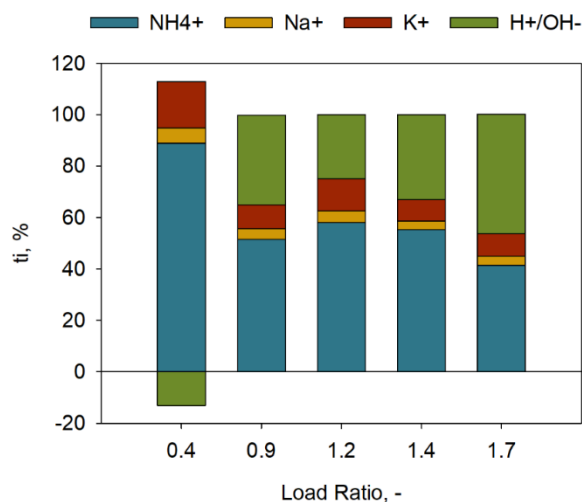


Figure S1. Ion transport across the CEM at different load ratios. Ammonium is the main charge transported over the cation exchange membrane. When operated at high load ratio, the proton becomes a considerable part of the charge transported over the CEM.

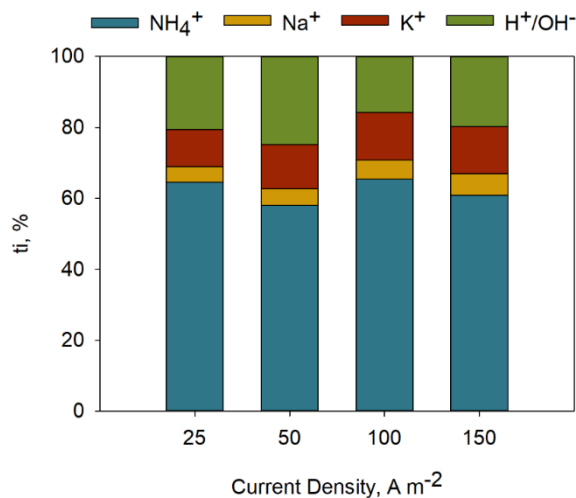
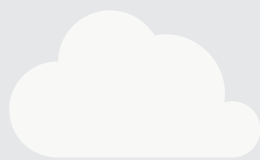
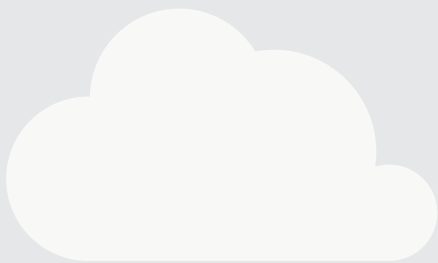


Figure S2. Ion transport over the CEM at different current densities. Ammonium is the main charge transported over the cation exchange membrane. The portion of ionic species transported is independent of the current density.

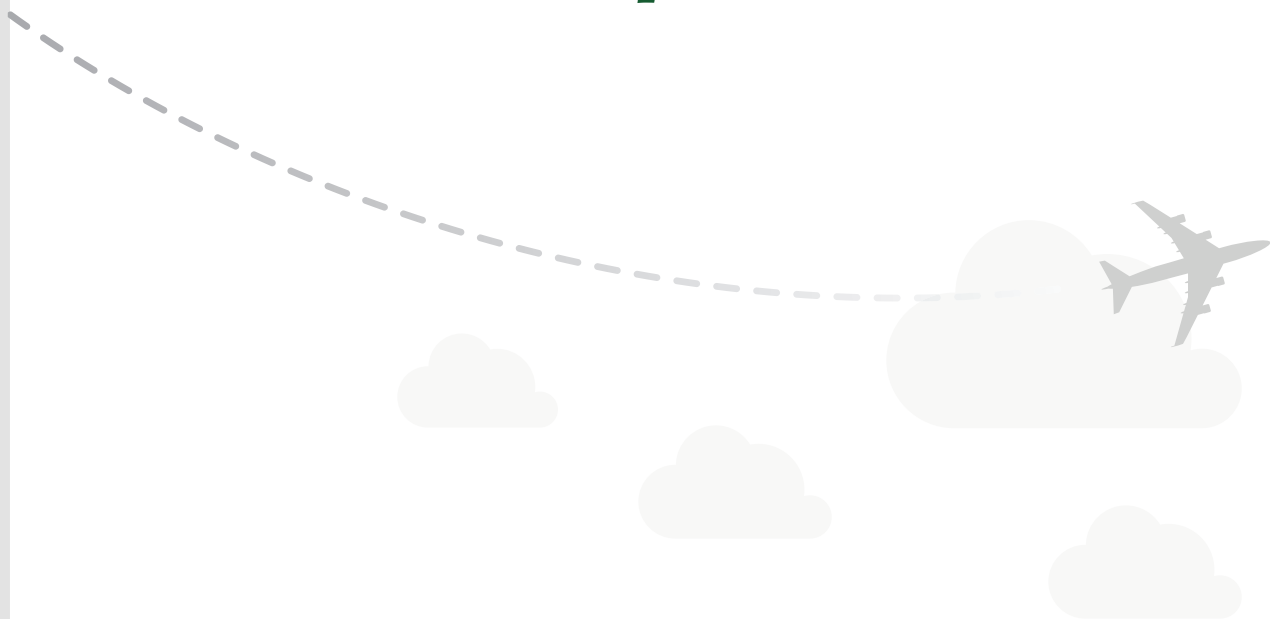
Additionally, water transport was observed from the feed compartment towards the concentrate compartment. 33% of water supplied as influent was transported to the concentrate while operating at 25 A m⁻² and 150 A m⁻²; 21% at 50 A m⁻² and 28% at 100 A m⁻².

5



Chapter 5

Effluent pH correlates with electrochemical nitrogen recovery efficiency at pilot scale operation



This Chapter has been submitted as:

Mariana Rodrigues, Sam Molenaar, Joana Barbosa, Tom Sleutels, Bert Hamelers,
Cees Buisman, Philipp Kuntke. Effluent pH correlates with electrochemical nitrogen
recovery efficiency at pilot scale operation

Abstract

A bipolar electrodialysis (BP-ED) pilot plant including 3.15 m² of cation exchange membrane and bipolar membrane each was operated for ammonia recovery. The pilot treated source-separated diluted urine (1 gNH₄⁺/L). Previously found set operation parameters for lab-scale such as current density and nitrogen load did not directly influence the stack performance. However, the effluent pH was directly related to the removal efficiency of the system. 80% nitrogen removal was achieved at a set effluent pH of 4. Operating under an effluent pH control strategy was more effective to control NH₄⁺ removal than controlling current density or nitrogen loading, as it accounts for fluctuation in wastewater availability and composition. The pilot plant removed up to 88% of the NH₄⁺ from urine and recovered around 700 g/day (from 1 m³ of urine). This was a significant improvement compared to the pilot plant previous performance on digestate. The energy consumption was around 13 Wh/g_N. The overall current efficiency was ~ 40% with most losses caused by parasitic ionic shortcut currents occurring at the hydraulic manifolds of the BP-ED stack. Therefore, the energy demand can be further decreased by preventing these ionic shortcuts in the new cell designs.

Introduction

Most of the nitrogen is produced in the Haber-Bosch (HB) process¹. The HB process was first demonstrated in 1909, and by 1913, ammonia was already produced at an industrial scale¹⁻⁴. As the natural nitrogen reserves (such as nitre deposits) were depleted there was an urgent need for the fast rollout of a process that could serve as a viable alternative for fertilizer production. The HB process is widely applied and remains almost unaltered after 100+ years. Nowadays, our attention has been slowly shifting from purely producing to also recovering nitrogen as the HB process is energy-intensive, and the natural gas required for the process is unevenly distributed worldwide^{2,5,6}. Further, the intensive use of N fertilizers is disrupting ecosystems through eutrophication⁷⁻⁹.

Ammonia recovery using electrochemical systems was previously demonstrated at lab-scale¹⁰⁻¹³. Yet, only a limited number of pilot studies were conducted. Ward et al used a 30 cell pair electrodialysis (ED) unit (total membrane area of 7.2 m²) for nutrient recovery (i.e., concentrated nitrogen and potassium product)¹⁴. Ferrari et al combined an electrodialysis with bipolar membranes cell including 65 cell pairs (3.15 m² membrane area) with two liquid/liquid membrane contactors¹⁵. The pilot produced a concentrated ammonium sulphate product. Nevertheless, both pilot installations demonstrated relatively short operation and performance decrease throughout the experiment.

Implementing a new technology like electrochemical systems for nitrogen recovery needs continuous further development. Certain features need to be optimized, such as operational flexibility, sustainability, safety, and economic competitiveness^{16,17}. So far, electrochemical systems in full-scale as treatment applications are rarely implemented successfully¹⁸⁻²⁰. However, the success of electrochemical nitrogen recovery depends on the performance at larger scale (removal/recovery, rate, and energy).

This study used the same bipolar electrodialysis pilot plant (Pilot BP-ED) used by Ferrari et al for ammonia recovery from source-separated urine. In contrast to the previous study, we explored how a pH-controlled operation mode improves the ammonium recovery and energy demand. We characterized the pilot plant performance regarding current efficiency, energy consumption, and nitrogen removal and identified new challenges of up-scaling for the (BP-)ED technology.

Materials and methods

Setup Configuration

A pilot-scale BP-ED cell unit consisting of a cross-flow stack (22X22 cm²) provided by REDstack BV (Sneek, The Netherlands) and two liquid/liquid membrane contactor (LLMC modules, 2.5 x 8 inch, type EXF, 3M Liqui- Cel™, NC, USA) were used in the pilot plant for ammonium recovery. The pilot installation is illustrated in Figure 1.

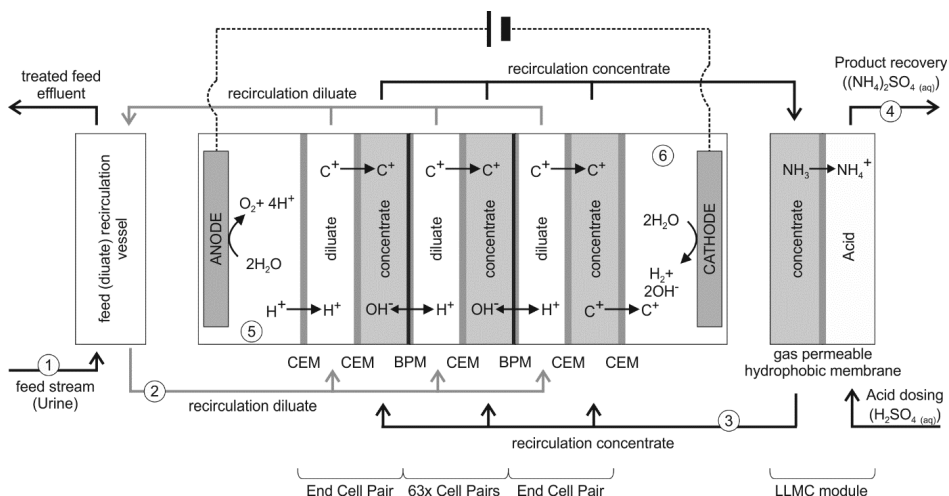


Figure 1. Adapted from Ferrari et al., 2022. The urine was supplied to the diluate compartments of the electrochemical cell. The current was applied to drive the ammonium in the urine through the cation exchange membranes into the concentrate solution. The concentrated solution is rich in ammonia gas due to the high pH. As a concentration gradient forms, the ammonia gas is extracted from the concentrate solution to concentrated sulphuric acid by using gas permeable membranes^{15,21}.

The BP-ED unit included, an anode compartment, 65 cell pairs of diluate and concentrate compartments, and a cathode compartment. The cell pairs were separated on one side by bipolar membranes (BPM) (FBM-PK, Fumatech GmbH, Germany) and on the other side CEM (FKB-PK130, Fumatech GmbH, Germany). The BPMs generate protons and hydroxide to diluate and concentrate, respectively (see Figure 1). NH₄⁺ is transported through the CEM from the diluate to the concentrate (towards the cathode). The diluate and concentrate compartments were created using polypropylene spacers (22 cm x 22 cm, thickness 0.05 cm, 53% open area) with a silicon gasket layer at two opposing sides for sealing (DEUKUM GmbH, Frickenhausen, Germany). The anode and cathode were two platinized titanium electrodes (22 cm x 22 cm MAGNETO Special Anodes B.V., Schiedam, The Netherlands). The anode and cathode compartments were shielded from the cell

pairs to minimize the transfer of chloride ions by two Nafion N117 membranes (22 cm x 22cm, Fuelcellsetc, TX, USA). The streams supply and recirculation and current supply are described in detail in Appendix A. After each run, a Clean In Place (CIP) strategy previously described by Federico et al was performed to guarantee the performance was not compromised¹⁵.

Operational Conditions

The pilot plant was supplied with urine collected in urine diverting toilets (Ecoflush, Wostman Ecology AB, Saltsjö-Boo, Sweden) installed in 15 households at Arneco (Arnhem, The Netherlands). The toilets have a separate collection for urine and apply a minimal flushing volume of 200 mL, therefore collecting diluted urine. The complex produces on average 100 L of diluted urine per day. To prevent filter clogging and increase the amount of NH_4^+ available, the urine was first collected in a 1 m³ storage tank that allowed for urea hydrolysis and settling suspended solids (Figure 1). The urine composition is provided in Table 1:

Table 1. Average urine composition collected at Arneco.

Analyte	Average Concentration (mg/L)
Chloride	344.3 ± 60.0
Nitrate	10.5
Phosphate	74.0 ± 16.2
Sulphate	216.0 ± 62.4
Inorganic Carbon	471.2 ± 61.9
Total Carbon	750.7 ± 100.3
Sodium	241.4 ± 38.5
Ammonium	921.9 ± 155.7
Potassium	258.3 ± 42.5
Magnesium	often below 10mg/L
Calcium	often below 10mg/L *

* Rarely 30 mg/L of Calcium were measured on the influent stream.

The performance of electrochemical systems is affected by the mode of operation (continuous or intermittent), current efficiency, and nitrogen loading (Load Ratio - L_N)²¹⁻²³. Firstly, we characterized the influence of current, loading, and mode of operation on the pilot BP-ED system (Table 2). After characterization the pilot was also operated under pH control, as we observed that the removal efficiency is related to the effluent pH. This was only possible after implementing a PID feedback loop

in the pilot plant operation system. The PID controller regulated the influent feed rate to assure a pre-set pH value of the effluent at the end of an intermittent current cycle. The current was applied in intermittent mode (50%, current on: 45 s and current off: 45 s) and at 100 A/m² during the pH-controlled runs. The length of the experiment was chosen as to allow uninterrupted operation given the available urine buffer at the site (~ 1 m³).

Table 2. Summary of the operational conditions conducted at the NEWBIES pilot plant when supplied with urine. The performance was characterized regarding current density, Load Ratio (L_N), intermittent and continuous current mode (CC). Later, the operation was extended to pH control.

Variable of interest	Studied Range	Fixed parameter
Current density (A/m ²)	50, 100 and 200	Load Ratio
Load Ratio (L_N)	0.5, 1, 1.5 and 2.5	Current Density
Current mode	CC, 50% intermittent and 75% intermittent	Current Density & Load Ratio
pH Control	pH effluent adjusted to 4	50% intermittent & 100 A/m ²

Analysis and measurements

Samples from the influent, effluent, concentrate, anolyte/catholyte, and acid were taken and analysed. All samples were filtered through a 0.45 µm filter prior to analysis and analysed in duplicate. Cations (NH₄⁺, Na⁺, K⁺, Ca²⁺, and Mg²⁺) and anions (SO₄²⁻, PO₄³⁻, NO₂⁻, NO₃⁻ and Cl⁻) were analysed using a Metrohm Compact IC Flex 930 instrument with a cation column (Metrosep C 4-150/4.0) and a Metrohm Compact IC 761 instrument with an anion column (Metrosep A Supp 5-150/4.0), respectively. Total and Inorganic carbon were measured using TOC-L CPH, Shimadzu BENELUX, 's-Hertogenbosch (The Netherlands).

Conductivity and pH of all process streams were measured and recorded per second by the PLCs data acquisition software (Labview) using in-line sensors (Easysense pH 32 and Inpro7100i, Mettler-Toledo,).

Calculations

All performance indicators (current efficiency, energy input, and removal efficiency) were calculated as described in ²¹.

Results & Discussion

Electrochemical systems performance can be improved by setting the effluent pH (dilate).

Unlike lab-scale studies, current and nitrogen loading (Load ratio) did not directly influence ammonia removal (see Appendix B) ²³. Nevertheless, during the characterization, a relation between nitrogen removal efficiency and the effluent pH of the stack was observed.

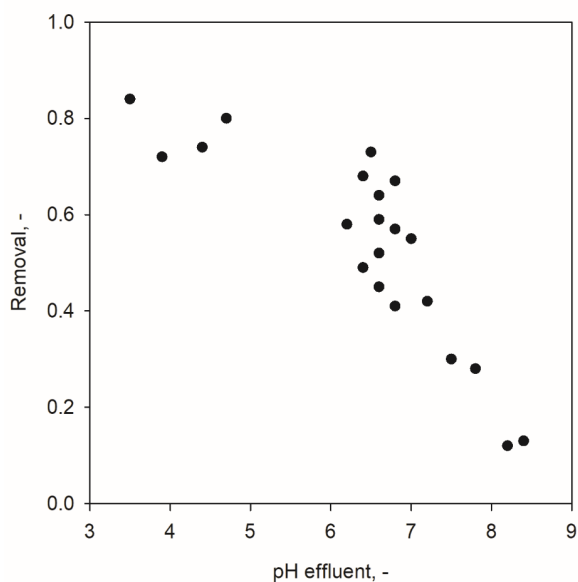


Figure 2. Nitrogen removal efficiency in function of the effluent pH. Higher ammonium removal efficiency was measured at lower effluent pH of the effluent.

Figure 2 shows the nitrogen removal efficiency in function of the effluent pH. Overall, we observed higher removal at lower effluent pHs. Ammonium removals of up to 80% were obtained when the pH of the effluent was around 4. Decreasing the alkalinity of the solution improves first the conversion of NH_3 to NH_4^+ . Second, it was previously demonstrated how in order to remove all ammonium ions from the diluate solution, all other cations needed to be depleted as well (model 1 reference).

Unlike previously observed at lab-scale, the removal efficiency was not directly correlated with load ratio or current density. This shows that the simplistic load ratio model previously described by Rodriguez-Arredondo et al 2017 has a limitation for the application on this more complex and variable wastewater (source separated urine). Rodriguez-Arredondo et al model was developed/validated for a more simple

and defined solution with little fluctuations, often obtained by pre-treatments and or synthetic formulations ^{22,23}. Therefore, a pilot operation under less controlled conditions requires a different and more simplistic approach, such as the pH control strategy.

High removal was achieved using effluent pH for process control.

Considering optimization between nitrogen recovery and energy consumption (see Table C1, Appendix C), the pilot operation was set for 100 A/m² and 50% intermittent mode. Additionally, the PLC was set to achieve an effluent pH of 4. The urine supply was controlled to guarantee the desired pH. Table 3 summarizes the pilot plant performance under this setting.

Table 3: Pilot performance under pH controlled operation.

Run	CD (A/m ²)	Removal efficiency (-)	Energy (Wh/g _N)	Mass recovered (g _N /d)	Volume treated (L/d)	Mass loaded (g _N /L)
1	100	0.80	13.6	348.8	630	434
2	100	0.88	13.4	269.6	423	307
3	100	0.83	12.7	702.5	1000	848

The pilot showed stable operation throughout these runs while removing up to 88% of the ammonium nitrogen from the influent and consuming on average 13 Wh/gN. This is a significant improvement compared to the 60% removal efficiency decreasing throughout the experiment to 30% achieved in the same pilot plant. According to the influent volume supplied and removal efficiency, the pilot was removing up to 700 g_N/day; a promising result compared with the operation using digestate (~560 g_N/day in continuous mode and ~130 g_N/day in intermittent mode) ¹⁵.

The energy consumption was comparable to ANAMMOX combined with the Haber-Bosch process ^{24,25}. In direct comparison with lab-scale electrochemical systems, the energy consumption was higher (2x) ^{12,26,27}.

During operation, an ammonium sulphate solution was produced (~ 145g/L, pH=3.5). Previous work by Rodrigues et al demonstrated that although acidic, the fertilizers produced by such BP-ED can be used for crop growth ²⁸. This combined electrochemical cell with LLMC can generate a product is free of unwanted sodium, as previously reported by ¹⁴.

Upscaling electrochemical systems for ammonia recovery leads to lower current efficiency due to ionic shortcut currents.

Figure 3 shows the current efficiency for ammonium, sodium, and potassium at different current densities (50, 100 and 200 A/m²) and Load ratio (1, 1.5 and 2.5).

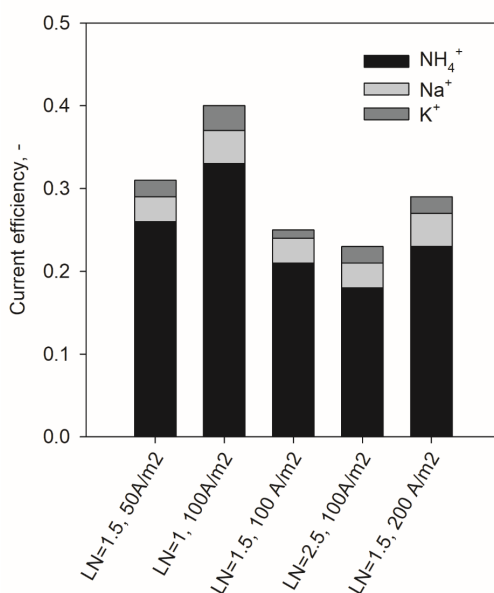


Figure 3. Ion current efficiency for the ions transported over the CEM (NH₄⁺, Na⁺ and K⁺), at different current densities (50, 100, and 200 A/m²) and Load ratio (1, 1.5 and 2.5). Calcium and magnesium current efficiencies were not included as these ion concentration were below detection range. Overall, the total current efficiency were often below 40%.

The ion transport was determined by measuring the change of ionic composition between influent and effluent. The sum of the current efficiency of all ions (ratio between charged removed over charged supplied) was often below 40% (Figure 3). Even considering the effect of Load Ratio and Current Density on the charge transported over the cation exchange membranes, this current efficiency is significantly lower than reported in previous studies^{21,27}. Around 60% of the total charge transport cannot be quantified based on the determined current efficiency. Ammonium was the main ion responsible for the charge transport in the BP-ED stack. Calcium and magnesium were often below the detection range, and the other cations (sodium and potassium) accounted for less than 10% of the charge transport. Previous studies reported up to 30% charge loss due to proton transport, ammonia diffusion, and/or anions leakage at similar operation conditions^{21,29,30}.

In this study, parasitic ionic shortcut currents through manifolds were the main phenomena causing the charge losses as proton transport, ammonia diffusion and anion leakage influences were not dominant. First, the pH of the diluate solution is not low enough for protons to play a substantial role in charge transfer. Secondly, ammonia diffusion was low as most nitrogen removed was measured in the acidic recovered solution. Finally, a low amount of anions was detected in the concentrate solution. A small anion leakage is expected as the CEM and BPM are known to have high permselectivity³¹.

The overall membrane/compartments resistance was high (around 41Ω), as 65 cell pairs are stacked. Additionally, the use of CEM/BPMs cell pairs have large resistance compared to normal ED (AEM/CEM) scenarios³². As, the diluate solution has a low conductivity (between 2 and 6 mS/cm) and the concentrate liquid has a high conductivity (higher than 20 mS/cm) salt bridges can form across the inlet manifolds or across the outlet manifolds. Instead of crossing the cation exchange membranes, the ions moved through the liquid from one compartment to another. This was not observed in earlier test with a similar stack design and only 6 cell pairs at the lab-scale²¹. This illustrates, it is essential to test technologies at larger pilot scale. Although the current efficiency aforementioned was particularly low for an BP-ED, we achieved up to 80% removal and energy below 8 Wh/gN comparable with previous studies^{10–12,26}.

Nevertheless, the simplicity of having an on/off system (no biology involved) that reaches equilibrium after a short period of time and can be controlled by an in-situ variable (effluent pH), makes BP-ED an attractive option for ammonia recovery of concentrated wastewater streams.

Conclusion

Nitrogen removal from buffered organic waste streams using bipolar electrodialysis systems has a high correlation with the effluent pH. Therefore, pilot-plants can be operated under pH control at a set current density. At pH 4, more than 80% of the nitrogen is removed. The energy consumption of electrochemical systems can be further improved by reducing ion shortcut currents through the manifolds and thereby improving current efficiencies.

References

- (1) Kyriakou, V.; Garagounis, I.; Vourros, A.; Vasileiou, E.; Stoukides, M. An Electrochemical Haber-Bosch Process. *Joule* **2020**, 4 (1), 142–158. <https://doi.org/10.1016/j.joule.2019.10.006>.
- (2) Smith, C.; Hill, A. K.; Torrente-Murciano, L. Current and Future Role of Haber-Bosch Ammonia in a Carbon-Free Energy Landscape. *Energy and Environmental Science* **2020**, 13 (2), 331–344. <https://doi.org/10.1039/c9ee02873k>.
- (3) Claudia Flavell-While. *Fritz Haber and Carl Bosch – Feed the World*. <https://www.thechemicalengineer.com/features/cewctw-fritz-haber-and-carl-bosch-feed-the-world/>.
- (4) Vaclav Smil. *Enriching the Earth: Fritz Haber, Carl Bosch, and the Transformation of World Food Production*; MIT Press, 2001.
- (5) Liu, X.; Elgowainy, A.; Wang, M. Life Cycle Energy Use and Greenhouse Gas Emissions of Ammonia Production from Renewable Resources and Industrial By-Products. *Green Chemistry* **2020**, 22 (17), 5751–5761. <https://doi.org/10.1039/d0gc02301a>.
- (6) Razon, L. F. Reactive Nitrogen: A Perspective on Its Global Impact and Prospects for Its Sustainable Production. *Sustainable Production and Consumption* **2018**, 15, 35–48. <https://doi.org/10.1016/j.spc.2018.04.003>.
- (7) Vitousek, P. M.; Aber, J. D.; Howarth, R. H.; Likens, G. E.; Matson, P. A.; Schindler, D. W.; Schlesinger, W. H.; Tilman, D. G. Human Alteration of the Global Nitrogen Cycle: Source and Consequences. *Ecol Appl* **1997**, 7 (3), 737–750. <https://doi.org/10.1038/nn1891>.
- (8) Mousavi, S. A. R.; Ibrahim, S.; Aroua, M. K. Bio-Electrochemical Denitrification -A Review. *International Journal of Chemical and Environmental Engineering* **2011**, 2 (2), 140–146.
- (9) Beckinghausen, A.; Odlare, M.; Thorin, E.; Schwede, S. From Removal to Recovery: An Evaluation of Nitrogen Recovery Techniques from Wastewater. *Applied Energy* **2020**, 263 (February), 114616. <https://doi.org/10.1016/j.apenergy.2020.114616>.
- (10) Tarpeh, W. A.; Barazesh, J. M.; Cath, T. Y.; Nelson, K. L. Electrochemical Stripping to Recover Nitrogen from Source-Separated Urine. *Environmental Science and Technology* **2018**, 52 (3), 1453–1460. <https://doi.org/10.1021/acs.est.7b05488>.
- (11) Desloover, J.; Abate Woldeyohannis, A.; Verstraete, W.; Boon, N.; Rabaey, K. Electrochemical Resource Recovery from Digestate to Prevent Ammonia Toxicity during Anaerobic Digestion. *Environmental Science and Technology* **2012**, 46 (21), 12209–12216. <https://doi.org/10.1021/es3028154>.
- (12) Christiaens, M. E. R.; Udert, K. M.; Arends, J. B. A.; Huysman, S.; Vanhaecke, L.; McAdam, E.; Rabaey, K. Membrane Stripping Enables Effective Electrochemical Ammonia Recovery from Urine While Retaining Microorganisms and Micropollutants. *Water Research* **2019**, 150, 349–357. <https://doi.org/10.1016/j.watres.2018.11.072>.
- (13) Rodrigues, M.; Paradkar, A.; Sleutels, T.; Heijne, A.; Buisman, C. J. N.; Hamelers, H. V. M.; Kuntke, P.; Donnan Dialysis for Scaling Mitigation from during Complex Electrochemical Wastewater Ammonium Recovery. *Water Research* **2021**, 117260. <https://doi.org/10.1016/j.watres.2021.117260>.
- (14) Ward, A. J.; Arola, K.; Thompson Brewster, E.; Mehta, C. M.; Batstone, D. J. Nutrient Recovery from Wastewater through Pilot Scale Electrodialysis. *Water Research* **2018**, 135, 57–65. <https://doi.org/10.1016/j.watres.2018.02.021>.
- (15) Ferrari, F.; Pijuan, M.; Molenaar, S.; Duinslaeger, N.; Sleutels, T.; Kuntke, P.; Radjenovic, J. Ammonia Recovery from Anaerobic Digester Centrate Using Onsite Pilot Scale Bipolar Membrane Electrodialysis Coupled to Membrane Stripping. *Water Research* **2022**, 218, 118504. <https://doi.org/10.1016/j.watres.2022.118504>.
- (16) Walsh, F. C.; Ponce de León, C. Progress in Electrochemical Flow Reactors for Laboratory and Pilot Scale Processing. *Electrochimica Acta* **2018**, 280, 121–148. <https://doi.org/10.1016/j.electacta.2018.05.027>.

- (17) Melnikov, S.; Loza, S.; Sharafan, M.; Zabolotskiy, V. Electrodialysis Treatment of Secondary Steam Condensate Obtained during Production of Ammonium Nitrate. Technical and Economic Analysis. *Separation and Purification Technology* **2016**, 157, 179–191. <https://doi.org/10.1016/j.seppur.2015.11.025>.
- (18) Radjenovic, J.; Sedlak, D. L. Challenges and Opportunities for Electrochemical Processes as Next-Generation Technologies for the Treatment of Contaminated Water. *Environmental Science and Technology* **2015**, 49 (19), 11292–11302. <https://doi.org/10.1021/acs.est.5b02414>.
- (19) Thompson Brewster, E.; Mehta, C. M.; Radjenovic, J.; Batstone, D. J. A Mechanistic Model for Electrochemical Nutrient Recovery Systems. *Water Research* **2016**, 94, 176–186. <https://doi.org/10.1016/j.watres.2016.02.032>.
- (20) Thompson Brewster, E.; Ward, A. J.; Mehta, C. M.; Radjenovic, J.; Batstone, D. J. Predicting Scale Formation during Electrodialytic Nutrient Recovery. *Water Research* **2017**, 110, 202–210. <https://doi.org/10.1016/j.watres.2016.11.063>.
- (21) Rodrigues, M.; De Mattos, T. T.; Sleutels, T.; Ter Heijne, A.; Hamelers, H. V. M.; Buisman, C. J. N.; Kuntke, P. Minimal Bipolar Membrane Cell Configuration for Scaling up Ammonium Recovery. *ACS Sustainable Chemistry and Engineering* **2020**, 8 (47), 17359–17367. <https://doi.org/10.1021/acssuschemeng.0c05043>.
- (22) Rodríguez Arredondo, M.; Kuntke, P.; ter Heijne, A.; Hamelers, H. V. M.; Buisman, C. J. N. Load Ratio Determines the Ammonia Recovery and Energy Input of an Electrochemical System. *Water Research* **2017**, 111 (3), 330–337. <https://doi.org/10.1016/j.watres.2016.12.051>.
- (23) Kuntke, P.; Sleutels, T. H. J. A.; Rodríguez Arredondo, M.; Georg, S.; Barbosa, S. G.; ter Heijne, A.; Hamelers, H. V. M.; Buisman, C. J. N. (Bio)Electrochemical Ammonia Recovery: Progress and Perspectives. *Applied Microbiology and Biotechnology* **2018**, 102 (9), 3865–3878. <https://doi.org/10.1007/s00253-018-8888-6>.
- (24) Maurer, M.; Pronk, W.; Larsen, T. A. Treatment Processes for Source-Separated Urine. *Water Research* **2006**, 40 (17), 3151–3166. <https://doi.org/10.1016/j.watres.2006.07.012>.
- (25) Pfromm, P. H. Towards Sustainable Agriculture: Fossil-Free Ammonia. *Journal of Renewable and Sustainable Energy* **2017**, 9 (3). <https://doi.org/10.1063/1.4985090>.
- (26) Gildemyn, S.; Luther, A. K.; Andersen, S. J.; Desloover, J.; Rabaey, K. Electrochemically and Bioelectrochemically Induced Ammonium Recovery. *Journal of Visualized Experiments* **2015**, No. 95, 1–12. <https://doi.org/10.3791/52405>.
- (27) Kuntke, P.; Rodrigues, M.; Sleutels, T.; Saakes, M.; Hamelers, H. V. M.; Buisman, C. J. N. N. Energy-Efficient Ammonia Recovery in an Up-Scaled Hydrogen Gas Recycling Electrochemical System. *ACS Sustainable Chemistry & Engineering* **2018**, 6 (6), 7638–7644. <https://doi.org/10.1021/acssuschemeng.8b00457>.
- (28) Rodrigues, M.; Lund, R. J.; ter Heijne, A.; Sleutels, T.; Buisman, C. J. N.; Kuntke, P. Application of Ammonium Fertilizers Recovered by an Electrochemical System. *Resources, Conservation and Recycling* **2022**, 181, 106225. <https://doi.org/10.1016/j.resconrec.2022.106225>.
- (29) Cord-Ruwisch, R.; Law, Y.; Cheng, K. Y. Ammonium as a Sustainable Proton Shuttle in Bioelectrochemical Systems. *Bioresource Technology* **2011**, 102 (20), 9691–9696. <https://doi.org/10.1016/j.biortech.2011.07.100>.
- (30) Liu, Y.; Qin, M.; Luo, S.; He, Z.; Qiao, R. Understanding Ammonium Transport in Bioelectrochemical Systems towards Its Recovery. *Scientific Reports* **2016**, 6 (December 2015), 1–10. <https://doi.org/10.1038/srep22547>.
- (31) Sarapulova, V.; Shkorkina, I.; Mareev, S.; Pismenskaya, N.; Kononenko, N.; Larchet, C.; Dammak, L.; Nikonenko, V. Transport Characteristics of Fujifilm Ion-Exchange Membranes as Compared to Homogeneous Membranes AMX and CMX and to Heterogeneous Membranes MK-40 and MA-41. *Membranes* **2019**, 9 (7), 1–23. <https://doi.org/10.3390/membranes9070084>.
- (32) Veerman, J.; Post, J. W.; Saakes, M.; Metz, S. J.; Harmsen, G. J. Reducing Power Losses Caused by Ionic Shortcut Currents in Reverse Electrodialysis Stacks by a Validated Model. *Journal of Membrane Science* **2008**, 310 (1–2), 418–430. <https://doi.org/10.1016/j.memsci.2007.11.032>.

Appendix A

The urine was supplied to the diluate compartment using a membrane pump (DDA 200-4, Grundfos Nederland B.V., Almere, The Netherlands). The 0.1 M Na_2SO_4 electrolyte solution (used as an electrolyte for both anode and cathode) was recirculated using a membrane pump (DDA 200-4, Grundfos). Membrane pumps (DDA 200-4) were also used to recirculate the diluate solution the concentrate solution and supply two TMCS. The TMCS were connected in parallel. Here, ammonia diffused through the gas permeable membrane and reacted with sulphuric acid forming ammonium sulfate (Figure 1). Concentrated sulphuric acid (37%, v/v) was continuously added by a membrane pump (DDA7.5-16, Grundfos) to form a concentrated ammonium sulphate solution and maintain the product pH at 2.5. The ammonium and other cations are transported through the CEM due to the current supplied to the ED module using a XYZ current supply (SM15K Delta Elektronika, Zierikzee, The Netherlands), with an upper limit of 330 V. A custom made PLC (Pro Control BV, De Rijp, the Netherlands) controlled all pilot functions (pumps, power supply, cleaning) and recorded operational data (volume, conductivity, pH, applied current and voltage). After each run, a cleaning in situ was applied in situ by flushing the diluate compartments with 1 M NaOH to remove organic fouling and flushing the concentrate compartments and TMCS units and lines with 1 M HCl to remove inorganic scaling deposits. The CIP was previously described¹⁵.

Appendix B

Figure B1 shows the energy consumption and nitrogen removal efficiency when the ED stack is operated continuously at different current densities (50, 100 and 200 A/m²).

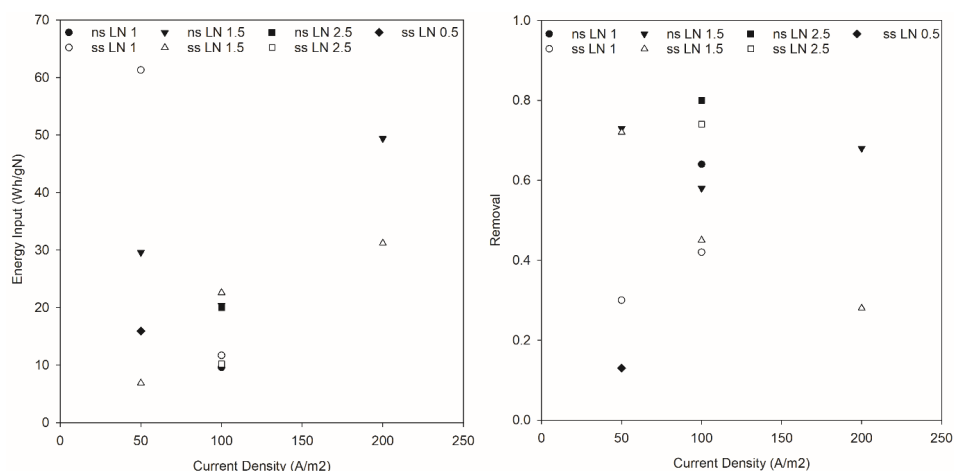


Figure B1. Energy input (left) and nitrogen removal (right) at different current densities (50, 100 and 200 A/m²). The current density effect was demonstrated at some different Load ratios (LN = 0.5, 1, 1.5 and 2.5) and in duplicate.

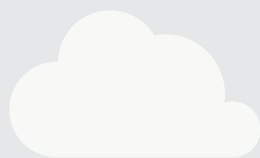
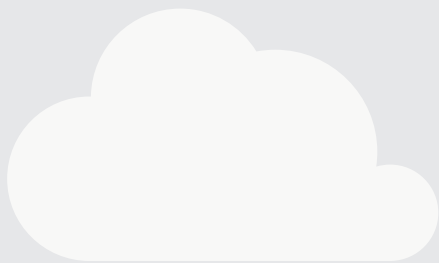
Appendix C

Table C1. Summary of all experiments performed and the respective performance regarding ammonium removal, current efficiency (for ammonium and total), energy consumption, mass recovered and loaded per day, and volume treated per day. The values presented are the average over the period considered.

Mode	CD	LN	pH effluent	Removal
CC	50	1.5	6.5	0.73
CC	50	1.5	3.9	0.72
CC	100	1	6.6	0.64
CC	100	1.0	7.2	0.42
CC	100	1.5	6.2	0.58
CC	100	1.5	6.6	0.59
CC	100	1.5	6.6	0.45
CC	100	2.5	4.7	0.80
CC	100	2.5	4.4	0.74
CC	200	1.5	6.4	0.68
INTERMITTENT 50%	100	1.5	6.6	0.52
INTERMITTENT 50%	100	1.5	6.4	0.49
INTERMITTENT 50%	100	1.5	6.8	0.57
INTERMITTENT 50%	100	2.5	3.5	0.84
INTERMITTENT 75%	100	1.5	6.8	0.67
INTERMITTENT 75%	100	1.5	6.8	0.41
INTERMITTENT 75%	100	1.5	7.0	0.55
pH control	100	n/a	-	0.80
pH control	100	n/a	-	0.88
pH control	100	n/a	-	0.83

-	-	Wh/g _N	g/day	L/day	g/day
tNH ₄ ⁺	ti total	Energy	total mass recovered	Volume treated	Mass loaded
0.26	0.31	29.6	678.0	730	935
0.20	0.25	6.9	510.8	730	713
0.33	0.40	9.6	1684.8	2193	2632
0.19	0.20	11.7	991.7	2192	2345
0.21	0.25	20.4	1082.0	1461	1870
0.25	0.29	19	1322.1	1461	2250
0.18	0.21	22.6	934.4	2023	2064
0.18	0.22	20.0	938.2	877	1175
0.13	0.16	10.2	686.7	877	929
0.23	0.29	49.4	2321.3	2922	3419
0.19	0.20	9.7	499.4	731	958
0.17	0.15	9.5	480.2	726	987
0.27	0.30	5.4	693.0	1027	1222
0.20	0.25	6.1	500.4	579	596
0.28	0.32	3.7	362.3	364	538
0.16	0.18	2.1	216.9	358	529
0.22	0.15	1.3	276.5	504	504
0.14	0.16	13.6	348.8	630	434
0.11	0.11	13.4	269.6	423	307
0.28	0.31	12.7	702.5	1000	848

6



Chapter 6

Effects of Current on the Membrane and Boundary layer selectivity in Electrochemical systems designed for nutrient recovery

This Chapter has been submitted as:

Mariana Rodrigues, Tom Sleutels, Philipp Kuntke, Cees Buisman, Bert Hamelers. Effects of Current on the Membrane and Boundary layer selectivity in Electrochemical systems designed for nutrient recovery



Abstract

During electrochemical nutrient recovery, current and ion exchange membranes (IEM) are used to extract an ionic species of interest (e.g., ion) from a mixture of multiple ions. The species of interest (ion 1) has an opposing charge to the IEM. When ion 1 is extracted from the solution, the species fractions at the membrane and the adjunct boundary layer are affected. Hence, the species transport through the electrochemical system (ES) can no longer be described as electrodialysis-like. A dynamic state is observed in the compartments where the ionic species are recovered. When the boundary layer-membrane interface is depleted, the IEM is at maximum current. If the ES is operated at a current higher than the maximum current, the fluxes of both ion 1 and other competing ions, with the same charge (ion 2), occur. This means, for example, ion 1 will be recovered, and the concentration of ion 2 will build up in time. Therefore, a steady state is never reached. Ideally, to prevent the effect of limiting current at the boundary layer-membrane interface, ES for nutrient recovery should be operated at low currents.

Introduction

Over the last decades, electrochemical systems (ES) have been developed for diverse fields, from the production of raw materials, energy production, and nutrient recovery¹⁻³. This diverse use of ES has led to several studies on, among others, the electrodes reactions, chemical efficiency, membrane resistance, and ion transport over the membrane⁴⁻⁹.

An ES is a system including a minimum of two electrodes immersed in a solution and connected through an electric circuit. Typically at the electrodes, reduction and oxidation reactions occur when current is applied. Consequently, electrons move through the external circuit, and charged species move in the solution accordingly to balance the charge in the system (maintain electro neutrality). The introduction of ion exchanges membranes (IEMs) in ESs allowed for membrane electrolysis and consequently the separation of charged molecules (i.e., ions) from the electrolyte or wastewater¹⁰⁻¹³. Additionally, as the IEMs block specific ions (co-ions), undesired reactions at the electrodes are prevented (e.g., chlorine gas formation at the anode).

In membrane electrolysis, counter-ions migrate through the IEMs due to the current, leading to the depletion of ions in one solution and enrichment in another solution. Three distinct operation regimes can be described for IEMs as a function of the current (density); (i) ohmic, (ii) limiting, and (iii) over-limiting current region¹⁴⁻¹⁶. In the ohmic region, increasing current density directly increases the charge transported per membrane area. An even higher current density will lead to a depletion of ions in the boundary layer. In this case, the ion concentration is close to zero on one side of the IEM, and the resistance increases. Here, the system operates at limiting current density, decreasing current efficiency for the desired ion transport. If we increase the current density further, the system operates at over-limiting current, and the conventional laws do not apply. A general limiting current density is often pre-established by the membrane manufacturer, using only known solutions of NaCl and a constant gradient between compartments¹⁷⁻¹⁹.

Depending on the application, IEMs can be operated at different current densities, 0.1 A m⁻² up to 1000 A m⁻²^{9,19,20}. Often, the current density is increased to improve the flux of ions (transport rate) over the IEM and therefore increase the treatment capacity. However, when increasing the current density while maintaining the amount of ions loaded to the system, the current efficiency will decrease as the system is in the limiting current regime^{21,22}.

When membrane electrolysis is implemented in, for example, resource recovery, the inclusion of membranes, the supply of different streams with extreme pH or variable compositions, or the need to operate in continuous mode, should be investigated^{11,22–24}. Furthermore, the pairing of membrane electrolysis with efficient extraction processes such as precipitation or stripping (i.e., gas permeable membranes) creates dynamic conditions within the system, as represented in Figure 1^{23,25–27}. This can cause low efficiency, limited ion transport, and high energy consumption. For example, during electrochemical ammonia recovery from wastewater, the transport of ammonium over the IEM is preferred (ammonium transport number equals one). However, it was previously observed that all cations in solution are transported through the cation exchange membrane (CEM) towards the cathode. While the NH_3 is removed from the cathode by a gas-permeable membrane, the other cations accumulate in the catholyte^{28–30}. The transport of other undesired charged species over the CEM lowers the current efficiency. Additionally, the catholyte does not reach equilibrium, influencing ion transport over the CEM, separating the anolyte from the catholyte. Here, the selectivity of the IEM results in different ion transport (behavior) than during electrodialysis^{12,31–33}.

In this work, we explore why more than one ionic specie is transported over an ion exchange membrane in some electrochemical systems, while the recovery process only recovers one species of interest. A simplified model was used to study how the ion fractions influence the ion transport over the boundary layer and CEM when increasing the current (density). We will also show that the ionic species transport over the boundary layer - membrane ensemble is affected by both the current (density) and anolyte (feed) composition and describe how we can maximize the transport (flux and efficiency) of the desired ion that is to be recovered from the catholyte.

Theoretical framework

This work describes the dynamic behavior of a quasi-steady-state membrane electrolysis system. Here, the system consists of a well-mixed anode compartment (with only monovalent ions), a boundary layer, an ideal IEM (meaning only counter-ions are transported through the membrane, as co-ion leakage over CEMs is very low compared to the total charge supplied; and the ions have equal mobility in the membrane, as their mobility, self-diffusion coefficients, and ionic Stokes radii are the same order of magnitude^{18,34,35}), a well-mixed catholyte, and an efficient extraction process at the cathode (Figure 1). The anolyte solution only includes monovalent ions (i.e., NH_4^+ , Na^+ and Cl^-). As the pH of the catholyte is alkaline the presence of bivalent cations would either cause inorganic scaling or require a pre-treatment, the transport over the membrane could not be characterized the same way^{36,37}. The catholyte includes

both counter-ions transported (i.e., NH_4^+ and Na^+). The hydroxyl ions (OH^-), generated during the electrode reaction, react with NH_4^+ and form a new species (i.e., $\text{NH}_3(\text{aq}) \Leftrightarrow \text{NH}_4^+ + \text{OH}^-$). The protons generated by the anode reaction will not be included in the model, as they behave similarly to NH_4^+ . Protons are also transported through the CEM and react with the OH^- at the catholyte. The influent is supplied continuously to the anode compartment, generating a treated effluent. On the other side of the IEM, a finite volume is recirculated in batch (catholyte). The concentrated solution formed at the cathode is recirculated over an extraction process, wherein this new species (NH_3) is recovered from the solution. The system described represents any system where current is applied; at least two cationic species (i.e., NH_4^+ , Na^+) are supplied to the anode compartment and transported to the cathode compartment through the CEM. In a second process, NH_3 is removed from the catholyte by a different process (e.g., NH_3 stripping, membrane extraction, etc.).

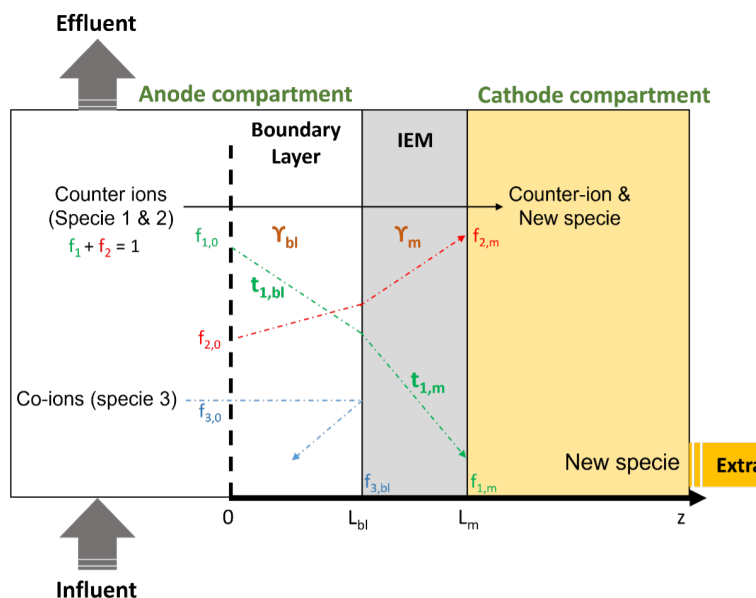


Figure 1. Scheme describing membrane electrolysis for ion recovery. Wastewater is supplied to an electrochemical system, including an ion exchange membrane (IEM) separating anolyte from the catholyte. Counter-ions are transported over an IEM due to the applied current (Y). A dimensionless current density (flux) is attributed to each region, boundary layer (Y_{bl}), and membrane (Y_m). Two counter-ions are supplied to the anode, and the sum of their fraction equals one. Once transported, ion 1 reacts and forms a new species, and ion 2 accumulates at the cathode. The new species is removed from the cathode due to an additional extraction process. Ion 3 represents all anions. The fraction of the different species (f) is characterized at the anolyte-boundary layer interface (0), boundary layer-membrane interface (L_{bl}), and at the membrane-catholyte interface (L_m). The relation between fraction (f), transport (t), and current (Y) will be established for ion 1.

To reduce the operation variables, we will present all parameters dimensionless.

Dimensionless Nernst-Planck equation

When current is applied, the transport of ions is driven by the concentration gradient over the membrane and the potential gradient between anode and cathode. This transport is commonly described by the Nernst-Planck equation. We considered three main species: Ion 1, NH_4^+ , either recovered or consumed at the cathode side. Ion 2, Na^+ represents the sum of all other cations accumulated at the cathode side. Ion 3, Cl^- representing the sum of all anions. Additionally, T^+ is the sum of all cations (NH_4^+ and Na^+) and T^- the sum of all anions (in this case, Cl^-). In the considered system, the ions are supplied to the anode compartment, where a boundary layer near the CEM is formed due to applied current. The counter-ions move through the boundary layer, into the IEM, and finally to the catholyte. In our model, we characterized the transport of these ions through the boundary layer and the membrane, in a first instance separately and then combined. For all equations, the following notations are used: C = concentration, f = fraction. The first subscript (i) represents the ion. The second subscript (z) represents the location of the ionic species: o is anolyte solution - boundary layer interface, bl is the boundary layer - CEM interface, and m is the CEM - catholyte solution interface. L_{bl} boundary layer thickness, L_m membrane thickness, and z is a dimensionless distance from anolyte to catholyte where the ions move.

For the described system, the anode is in steady-state, and therefore we can write the Nernst-Planck equation as:

$$\frac{df_i}{dz} = -\gamma_i - q_i f_i \frac{d\phi}{dz} \quad (\text{Equation 1})$$

Where f_i is the ion fraction expressed as the ratio of the total counter-ion concentration ($C_{T,o}$); q_i is the ion charge (in this case, it is always one as only monovalent ions are considered); γ_i is the dimensionless transported current of the ion given by (equation 2), and ϕ is the dimensionless potential expressed as $\phi = E.F.R.Temp$ (where E is potential, R is the gas constant, $Temp$ is the temperature, and F is Faraday's constant).

Dimensionless Operational Parameters

Different operational parameters, such as the applied current, can be controlled when membrane electrolysis is used for ion recovery. This current relates to the ions transported through the membrane, and it will determine the effluent concentration. To make the current (γ) dimensionless, we considered the same variables as for the individual fluxes previously described:

$$\gamma_{i,z} = \frac{I}{C_{T,z}} \frac{L_z}{D_{i,z}} \quad (\text{Equation 2})$$

Where I is the molar current density ($\text{mol.m}^{-2}.\text{s}^{-1}$), $D_{i,z}$ is the ion diffusion coefficient at location z ($\text{m}^2.\text{s}^{-1}$).

Ion 1 transport number at the boundary layer - IEM ensemble

The ion transport number (t_i) can be derived for the combined boundary layer (bl) – IEM ensemble at the anode side and for the IEM. First, the relationships for the boundary layer and IEM are derived separately, and later, these are combined.

Boundary layer, selectivity, and limiting current

As previously stated, in the anolyte, three ions are assumed to be present ($1= \text{NH}_4^+$, $2= \text{Na}^+$, and $3= \text{Cl}^-$), of which the NP equation describes the transport. Considering an ideal selective membrane, we assume that the flux of Cl^- through the CEM is zero. This means that the ratio of the flux of total anions and total cations ($\frac{df_T}{dz}$) can be described as:

$$\frac{df_T}{dz} = f_T \frac{d\phi}{dz} \quad (\text{Equation 3})$$

Furthermore, we also know that the transported current (γ) equals the total flux of cations through the CEM and that the sum of the fractions of ion 1 and ion 2 is one, therefore:

$$\frac{df_T}{dz} = -\gamma_{bl} - f_T \frac{d\phi}{dz} \quad (\text{Equation 4})$$

Combining equations 3 and 4 gives a linear solution for the counter-ion concentration and thus, also for the sum of ions 1 and 2:

$$f_T(z) = 1 - \frac{\gamma_{bl}}{2} z \quad (\text{Equation 5})$$

As the fraction of total anions (γ) at the anode solution-boundary layer interface is one, we find the first constraint, which is the maximum current density at the boundary layer-membrane interface ($\gamma_{bl} \leq 2$). At the boundary layer, we have both counter and co-ions flux. As Cl^- cannot move through the CEM, it enhances the flux of T^+ to compensate the gradient between the bulk and the membrane and therefore sets a maximum current for the boundary layer of two (twice the flux of T^+). This maximum current can be achieved when the counter-ion concentration becomes zero at the boundary layer-membrane interface ($z=\text{bl}$). If the membrane allows a certain co-ion transport (leakage), the transport of counter-ions will slightly decrease³⁵.

Using the relationship described in equation 5, we can find the ordinary differential equations (ODE) for ion 1:

$$\frac{df_1}{dz} = f_1 \left(\frac{\gamma_{bl}}{2 - \gamma_{bl}z} \right) - \gamma_{bl}t_1 \quad (\text{Equation 6})$$

From the solution of equation 6 [d'Alembert equation], we can find the fraction of ion 1 at the membrane interface.

$$f_{1,bl} = \frac{\left(f_{1,0} - \left(1 - \left(1 - \frac{\gamma_{bl}}{2} \right)^2 \right) t_1 \right)}{1 - \frac{\gamma_{bl}}{2}} \quad (\text{Equation 7})$$

As the fraction cannot become negative, at the boundary layer, the following constraint limits the ion transport:

$$\frac{f_{1,0}}{t_1} \geq 1 - \left(1 - \frac{\gamma_{bl}}{2} \right)^2 \quad (\text{Equation 8})$$

Furthermore, this sets a maximum current through the boundary layer that is reached when the transport of ion 1 is higher than its fraction and vice-versa, namely:

$$\gamma_{bl} = 2 \left(1 - \sqrt{1 - \frac{f_{1,0}}{t_1}} \right), \text{ for } t_1 \geq f_{1,0} \quad (\text{Equation 9})$$

$$\gamma_{bl} = 2 \left(1 - \sqrt{1 - \frac{1 - f_{1,0}}{1 - t_1}} \right), \text{ for } t_1 \leq f_{1,0} \quad (\text{Equation 10})$$

The first equation (equation 9) represents the maximum current when the transport number of ion 1 is higher than its fraction in the anolyte. Therefore, there is a limited amount of ion 1. This means that the current can be considered as over-limiting current. There is current available to transport more ions even though the anode solution is depleted.

The second equation (equation 10) represents the situation when the transport of ion 1 is lower than its fraction. This can be considered the ohmic limited region for the counter ion transport.

Membrane selectivity and current relationship

We will also investigate the effect of current on the ion transport through the CEM. Additionally, the catholyte of an ES for ammonia recovery has such a pH ($\text{pH} \gg 10$) that the concentration of NH_4^+ can be considered zero.

We assumed an ideal CEM and anolyte composition with only monovalent ions. At the catholyte-membrane interface, the total fractions of all ions equals the fractions in the solution. However, inside the CEM, the total concentration of the ionic species equals the fixed charge of the IEM. We also know that the sum of the fractions of all cations equals one ($f_1 + f_2 = 1$). The NP equation for both ions 1 and 2 thus gives:

$$\frac{d\varphi}{dz} = -(\gamma_1 + \gamma_2) \quad (\text{Equation 11})$$

Since all ions considered are monovalent, the sum of the ionic fluxes equals the current in the membrane (γ_m). When adding this to equation 1, we thus find:

$$\frac{df_i}{dz} = -\gamma_i + f_i \gamma_m \quad (\text{Equation 12})$$

The solution of this equation and the resulting ion transport are:

$$f_i = \frac{\gamma_i}{\gamma_m} + \left(f_{i,bl} - \frac{\gamma_i}{\gamma_m}\right) e^{\gamma_m z} \quad (\text{Equation 13})$$

Mind that $\frac{\gamma_i}{\gamma_m}$ is the transport number of i (current efficiency of the desired ion). From equation 12, we can calculate the transport number as both the concentration on the anode side ($f_{i,bl}$) and the concentration on the cathode side ($f_{i,m}$) of the membrane are known as well as the applied current density. The transport number (t_i) is presented in equation 14:

$$t_i = \frac{\gamma_i}{\gamma_m} = \frac{f_{i,bl} e^{\gamma_m} - f_{i,m}}{e^{\gamma_m} - 1} \quad (\text{Equation 14})$$

If we consider the transport obtained in equation 14, the fraction of ion 2 in the membrane ($f_{2,m}$) is related to the fraction of ion 2 in the boundary layer ($f_{2,bl}$):

$$f_{2,m} = f_{2,bl} e^{\gamma_1} \quad (\text{Equation 15})$$

However, the sum of the counter-ion fractions is maximally one, which sets a maximum current through the membrane ($\gamma_{m,max}$). This means that when the fraction of ion 2 at the cathode is near one, the ion 1 that can be transported towards the cathode is still fraction dependent. This maximum current in the membrane allowing a steady-state, equals:

$$\gamma_{m,max} = \ln\left(\frac{1}{f_{2,bl}}\right) = \ln\left(\frac{1}{1 - f_{1,bl}}\right) \quad (\text{Equation 16})$$

This means that when the current at the membrane is below the maximum current, the transport number of ion 1 is one (for $\gamma_m \leq \gamma_{m,max}$). For currents higher than $\gamma_{m,max}$ and assuming ion 1 is entirely extracted from the cathode ($f_{1,m} = 0$), we then find a new relation for t_1 :

$$t_1 = \frac{f_{1,bl}}{1 - e^{-\gamma_m}} \quad \text{for } \gamma_m \geq \gamma_{m,max} \quad (\text{Equation 17})$$

Boundary layer-Membrane ensemble

Overall, we observe that the boundary layer and IEM each present a maximum current (γ_{bl} and γ_m). This means each layer has its own influence on the ion transport number. So far, we have discussed the boundary layer and membrane selectivity separately, but they both determine the overall ion transport. In the system, the total flux through the boundary layer is the same as the total flux through the CEM. As γ_{bl} has a constant maximum value (equation 9), we will further express the membrane current as a function of the boundary layer current ($\gamma_m = \alpha \gamma_{bl}$). The value of α represents the ratio between the flux of ions through the membrane and the boundary layer:

$$\alpha = \left(\frac{C_T}{X} \right) \left(\frac{L_m}{L_{bl}} \right) \left(\frac{D_{bl}}{D_m} \right) \quad (\text{Equation 18})$$

From equation 14, it is possible to observe that the selectivity of the boundary layer-membrane ensemble is dependent on (i) the concentration of ions in the membrane solution, (ii) on the thickness of both regions, and (iii) both the diffusion coefficients in the membrane and the boundary layer. By combining equation 8 and equation 18, we find that the ion transport number for ion 1 from the anolyte through the ensemble to the catholyte can be described as:

$$t_1 = \frac{f_{1,0}}{1 - \left(1 - \frac{\gamma_{bl}}{2} \right)^2 e^{-\alpha \gamma_{bl}}} \quad (\text{Equation 19})$$

Here, we see that the transport number is directly proportional to the fraction, while the denominator accounts for the effects of current and the size of the boundary layer. For ease of notation, we will further write equation 19 as:

$$t_1 = \frac{f_{1,0}}{H(\alpha, \gamma_{bl})} \quad (\text{Equation 20})$$

Where H is the combined selectivity function of the boundary layer-membrane ensemble. The boundary layer- membrane selectivity shows how an ion (ion 1) is transported preferentially over the other (ion 2). Figure 2 shows the effect of α on selectivity as a function of the current.

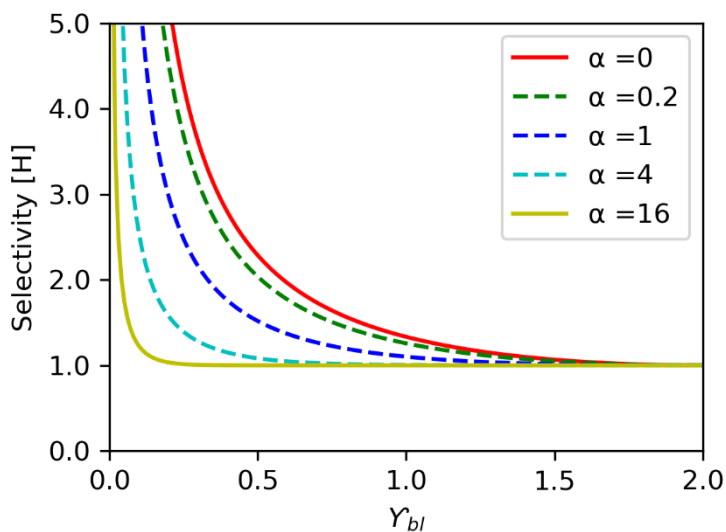


Figure 2. The effect of the boundary layer-membrane properties (represented in α) on the selectivity (H) as a function of the current (γ) (Equation 20). Different α were considered. With the current increase, the selectivity tends to one.

Figure 2 shows the lower the current (γ) is, the more selective is the IEM for ion 1. Additionally, it shows a non-selective region for higher currents (H is ~ 1). Once this current is reached, the physical properties of the IEM and boundary layer do not affect the system, and the fractions influence the transport in the anolyte solution. However, the smaller the α , the higher the current we can operate the system before a reduction of the selectivity occurs.

As the fraction of ions in solution is maximum one, equation 20 is only valid if the fraction of ion 1 in the anolyte is equal to or smaller than the combined selectivity:

$$f_{1,0} \leq 1 - \left(1 - \frac{\gamma_{bl}}{2}\right)^2 e^{-\alpha\gamma_{bl}} \quad (\text{Equation 21})$$

For a smaller current ($\gamma \leq \gamma_{\max}$), this relationship does not hold, and the transport number of ion 1 equals one, as described in equation 13. The combination of boundary layer and IEM always allows a current, such that $\gamma_{bl} \leq 2$. The ideal α is close to zero. It represents the situation when the selectivity is only affected by the membrane properties, meaning the highest selectivity possible is observed (no current effect).

Results & Discussion

In practical applications, the main interest is maximizing the removal and membrane transport of the species recovered towards the cathode to improve the extraction process. Using the relationships established above, we will describe how the transport is affected by current and, consequently, how an inverse selectivity is observed at the boundary layer and CEM for certain conditions. The effect of the maximum current on the transport of the recovered ion 1 in the catholyte will be described at different ion fractions in the influent (f_i) for both the boundary layer and CEM. Additionally, a maximum current for the membrane electrolysis system on the different selectivity (α) is established.

The boundary layer acts as a pre-selective region before the ions cross the membrane.

The model established that the studied system has a maximum current in the boundary layer due to the depletion of ions in the anolyte-boundary layer interface. Figure 3 shows $\gamma_{bl,max}$ (maximum dimensionless current) through the boundary layer expressed as function a of the ion transport number of ion 1 (t_1) for different fractions of ion 1 at the anode ($f_{i,0}$). For example, when f_i is 0.3, 30% in solution is NH_4^+ and 70% is Na^+ .

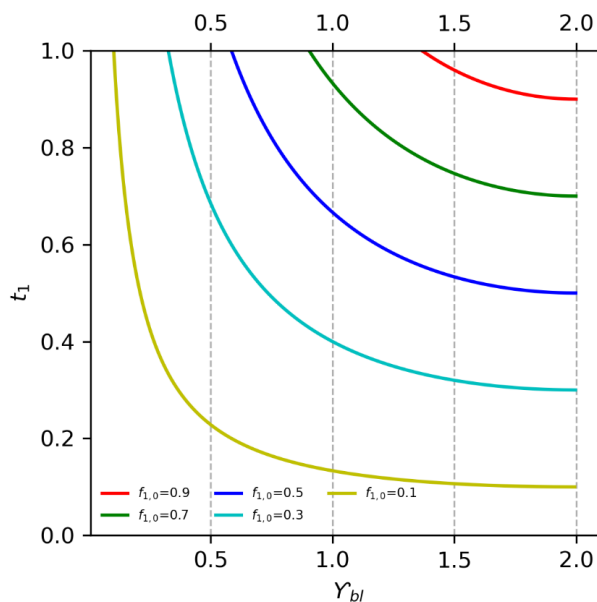


Figure 3. Limiting current (Y_{bl}) at the boundary layer as a function of the ion 1 transport number (t_1) in relation to the current was described at different ion fractions in the influent solution. Overall, the ion transport number decreases with the current.

When the transport number of ion 1 equals its fraction in the influent solution, the system can be operated at the highest current, see Figure 3.

As ion 1 is recovered, we are especially interested in those situations where the transport number is higher than the fraction ($t_1 > f_1$) at the anolyte solution. This would mean that a higher removal/extraction of ion 1 could be achieved independent of its fraction in solution (the system is more selective). The maximum current is smaller due to either ion 1 or ion 2 depletion in all other cases. This means the boundary layer limits the ions in the boundary-layer membrane interface (L_{bl}) and consequently acts as a selective region itself.

The maximum current shifts according to the fraction of ion 1 in solution (equation 9). A high transport number of ion 1 can only be observed at currents lower than this maximum current when the fraction of ion 1 is higher than its transport. Thus, a maximum flux of ion 1 is determined by the fraction of ion 1 in the anolyte ($f_{1,o}$) and the maximum current.

In the membrane, the exclusive transport ($t_1=1$) of ion 1 only occurs at low current densities.

Equation 17 was used to calculate the transport number of the ions through the membrane. Figure 4 shows the transport number as function of the current through the membrane.

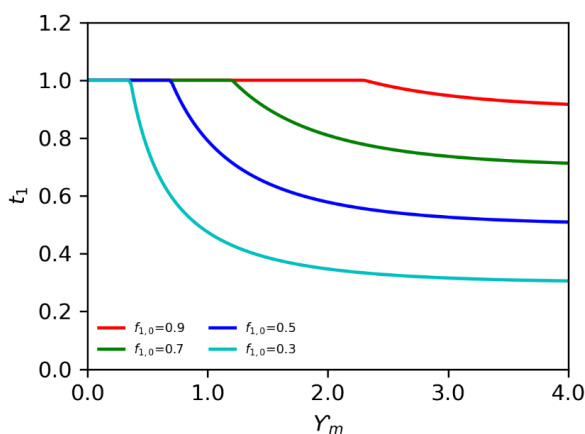


Figure 4. Ion 1 transport number as function of the current (Y_m) through the CEM at different ion fractions in the influent solution. Initially, the ion 1 transport number is equal to one. Once we reach a certain current, the transport number decreases. The higher the ion 1 fraction, the higher the currents we can reach..

Figure 4 shows that the exclusive transport of ion 1 ($t_1=1$) over the CEM only occurs when its fraction is lower than the transport number and at low currents, as the transport is both a function of current and fraction. When current increases, the maximum transport number achieved equals the fraction of ion 1 in the anolyte solution ($f_{1,o}$). Here, we are in a limiting current regime for ion 1, and transport of ion 2 occurs.

The transport of cations over the CEM is limited by the conditions obtained at the membrane interfaces with both anolyte and catholyte. We assumed an ideal CEM, where no anions are transported. However, the fraction of ion 2 ($f_{2,c}$) in the catholyte is close to one, while the fraction of ion 1 ($f_{1,c}$) is assumed to be equal to zero as it is removed/extracted from the cathode. This means that the ion 2 concentration gradient over the membrane increases while the ion 1 concentration decreases. When a current lower than the maximum current is used, the transport of Na^+ is slowed down by an increase of the concentration gradient in the membrane. This results in selective transport of ion 1. However, the effect is diminished when the current increases. When we operate the system at a current higher than the maximum membrane current ($\gamma_{m,\max}$), we will always observe both the transport of ion 1 and ion 2. The accumulation of ion 2 in the cathode creates a concentration gradient over the membrane that opposes the electric field strength. However, the ion fraction can be maximally one and sets the maximum current through the membrane ($\gamma_{m,\max}$).

Steady-state in the catholyte would only occur when the transport number of ion 2 is zero (meaning no Na^+ would be transported) and when the fraction of ion 2 at the cathode side equals the fraction at the boundary layer ($\gamma_m=0$) (equation 15). However, in many practical examples, a flux of both ion 1 and ion 2 towards the cathode is observed^{21,22,38–40}. Meaning most studies are operating above limiting current.

Membrane electrolysis paired with an extraction process should be operated well below the limiting current density.

Additional to the boundary-layer membrane ensemble effect on the selectivity, a maximum current can be established to achieve a certain fraction at the anolyte, while the ion 1 transport number is one.

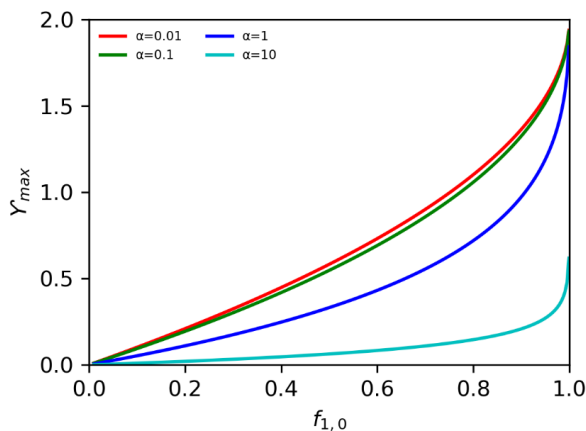


Figure 5. Maximum current (Y_{max}) the ES can operate at different fraction of ion 1 in the anolyte, while maintaining exclusive transport of ion 1 ($t_1=1$). The influence was characterized for different α . When the solution is depleted, no current can be applied (zero current, zero fraction). The higher the fraction in the anolyte, the higher the current the system can be operated.

Figure 5 shows the maximum current the system can be operated to achieve a certain ion 1 fraction at different boundary-layer membrane properties ratio (α), while the transport of ion 1 over the membrane equals one. Firstly, the maximum current of the system should be decreased to match the fraction of ion 1 in the anolyte. Furthermore, removing ion 1 entirely from the anode is more difficult as the system becomes ion depleted at the boundary layer for lower fractions, particularly when α is further from ideal ($\alpha > 0$).

At low current, the boundary layer and membrane ensemble is extremely selective as only ion 1 is transported ($t_1=1$). When we increase the current, we observe that the double layer- membrane ensemble selectivity (H , equation 20) plays a role, and the transport number of ion 1 as it decreases with increasing current.

The equation below gives the maximum current:

$$I_{max} = \frac{D_m X}{L_m} \ln \left(\frac{1}{1 - f_{0,1}} \right) \quad (\text{Equation 22})$$

Considering the IEM data compiled by ^{41,42}, where for a Nafion CEM, the fixed charge (X) for a CEM is 4 mol L⁻¹; the D_m is 5 E-12; and an average membrane thickness of 1 E-4 m, we can calculate the maximum current density. From equation 2, and assuming 70% of the cations in solution is ammonium (as found in urine and reject water ^{43,44}), the maximum current density is approximately 23 A m⁻². Although a higher limiting current value of the IEM was previously quantified (>200 A.m⁻²) ^{42,45}, the exclusive transport of NH₄⁺ ($t_1=1$) can only be achieved at a current density below 23 A m⁻².

When it comes to the boundary layer versus membrane properties included in the parameter α , the ideal case is α close to zero. Here, the system can achieve the highest transport for ion 1 at the maximum limiting current, meaning a selective IEM with infinite high conductivity (e.g., by reducing the membrane thickness) and/or a boundary layer with thickness close to zero (e.g., by increasing the liquid recirculation speed). Besides the physical characteristics of the membrane, α is influenced by the thickness and diffusivity of the boundary layer, parameters that are affected, for example, by the recirculation speed of the solution in the compartment^{9,46} or by the ion concentration in the system (a characteristic of the wastewater)^{29,47}.

The model provides a simplified description for all membrane electrolysis where a dynamic cathode is imposed by the extraction of one of its species. What we often see in practical examples is that several cationic species are transported over the CEM when operating an electrochemical system for nutrient recovery^{10,22,48}. If only one ion is of interest, ideally, we would like to have a transport number of one ($t_i=1$) as this would mean a high recovery and high current efficiency. However, the transport of a single species over the CEM is rarely reached. Here, while only considering the Nernst-Planck equation to describe the fluxes, we see that this can be the result of a competing ion 2 and the fact that the ion 1 is constantly removed from the catholyte. In order to maintain the flux of ion 1, we need the flux of ion 2, therefore, t_i is never equal to one. We need to keep the flux of Na^+ to keep a certain flux of NH_4^+ . Consequently, this flux is related to a maximum current. In equilibrium, a constant removal of ions occurs from the anolyte (constant composition) through the CEM, but the catholyte concentrations are variable (a steady state is never reached). At present, most electrochemical recovery processes are performed at higher current densities ($>20 \text{ A.m}^{-2}$), and therefore, observe the transport of all cationic species, meaning an inefficient use of energy^{25,49}. Ammonium is often the most transported charge (around 60%) over the cation exchange membrane. If sufficient current is applied, the ammonium transport often matches its fraction in wastewater such as urine or reject water (60-70%)^{21,22,25,39}.

Conclusion

Using the Nernst-Planck equation, we predicted that during electrochemical ion recovery, the transport of a single ionic species of interest through an IEM could only be achieved at low current densities. Once the maximum current is surpassed, the concentration gradient formed over the membrane results in the transport of the different species from the anolyte solution. When operating an ES, we should consider both the properties of the IEM/boundary layer (here described as α) as well as the selectivity of both regions.

References

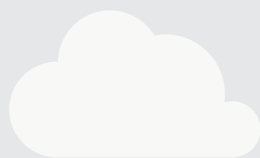
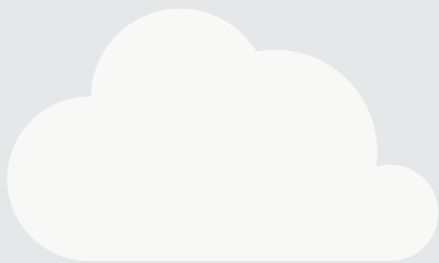
- (1) Holyst, R.; Poniewierski, A. Electrochemical Systems. In *Thermodynamics for Chemists, Physicists and Engineers*; Springer Netherlands: Dordrecht, 2012; pp 245–263. https://doi.org/10.1007/978-94-007-2999-5_11.
- (2) Grotheer, M.; Alkire, R.; Varjtan, R.; Srinivasan, V.; Weidner, J. Industrial Electrolysis and Electrochemical Engineering. *Electrochemical Society Interface* **2006**, 15 (1), 52–54. <https://doi.org/10.1149/2.f15061if>.
- (3) Muster, T. H.; Jermakka, J. Electrochemically-Assisted Ammonia Recovery from Wastewater Using a Floating Electrode. *Water Science and Technology* **2017**, 75 (8), 1804–1811. <https://doi.org/10.2166/wst.2017.060>.
- (4) Długolecki, P.; Ogonowski, P.; Metz, S. J.; Saakes, M.; Nijmeijer, K.; Wessling, M. On the Resistances of Membrane, Diffusion Boundary Layer and Double Layer in Ion Exchange Membrane Transport. *Journal of Membrane Science* **2010**, 349 (1–2), 369–379. <https://doi.org/10.1016/j.memsci.2009.11.069>.
- (5) Tedesco, M.; Hamelers, H. V. M.; Biesheuvel, P. M. Nernst-Planck Transport Theory for (Reverse) Electrodialysis: I. Effect of Co-Ion Transport through the Membranes. *Journal of Membrane Science* **2016**, 510, 370–381. <https://doi.org/10.1016/j.memsci.2016.03.012>.
- (6) He, X.; Li, N. Lattice Boltzmann Simulation of Electrochemical Systems. *Computer Physics Communications* **2000**, 129 (1), 158–166. [https://doi.org/10.1016/S0010-4655\(00\)00103-X](https://doi.org/10.1016/S0010-4655(00)00103-X).
- (7) Stephens, L. I.; Mauzeroll, J. Demystifying Mathematical Modeling of Electrochemical Systems. *Journal of Chemical Education* **2019**, 96 (10), 2217–2224. <https://doi.org/10.1021/acs.jchemed.9b00542>.
- (8) Liu, Y.; Qin, M.; Luo, S.; He, Z.; Qiao, R. Understanding Ammonium Transport in Bioelectrochemical Systems towards Its Recovery. *Scientific Reports* **2016**, 6 (December 2015), 1–10. <https://doi.org/10.1038/srep22547>.
- (9) la Cerva, M.; Gurreri, L.; Tedesco, M.; Cipollina, A.; Ciofalo, M.; Tamburini, A.; Micale, G. Determination of Limiting Current Density and Current Efficiency in Electrodialysis Units. *Desalination* **2018**, 445 (July), 138–148. <https://doi.org/10.1016/j.desal.2018.07.028>.
- (10) Rozendal, R. A. A.; Leone, E.; Keller, J.; Rabaey, K. Efficient Hydrogen Peroxide Generation from Organic Matter in a Bioelectrochemical System. *Electrochemistry Communications* **2009**, 11 (9), 1752–1755. <https://doi.org/10.1016/j.elecom.2009.07.008>.
- (11) de Paepe, J.; de Pryck, L.; Verliefde, A. R. D.; Rabaey, K.; Clauwaert, P. Electrochemically Induced Precipitation Enables Fresh Urine Stabilization and Facilitates Source Separation. *Environmental Science & Technology* **2020**, 54 (6), 3618–3627. <https://doi.org/10.1021/acs.est.9b06804>.
- (12) Sleutels, T. H. J. A.; ter Heijne, A.; Kuntke, P.; Buisman, C. J. N.; Hamelers, H. V. M. Membrane Selectivity Determines Energetic Losses for Ion Transport in Bioelectrochemical Systems. *ChemistrySelect* **2017**, 2 (12), 3462–3470. <https://doi.org/10.1002/slct.201700064>.
- (13) Lu, S.; Li, H.; Tan, G.; Wen, F.; Flynn, M. T.; Zhu, X. Resource Recovery Microbial Fuel Cells for Urine-Containing Wastewater Treatment without External Energy Consumption. *Chemical Engineering Journal* **2019**, 373 (January), 1072–1080. <https://doi.org/10.1016/j.cej.2019.05.130>.
- (14) Káňavová, N.; Machuča, L.; Tvrzník, D. Determination of Limiting Current Density for Different Electrodialysis Modules. *Chemical Papers* **2014**, 68 (3). <https://doi.org/10.2478/s11696-013-0456-z>.
- (15) Krol, J.; Wessling, M.; Strathmann, H. Concentration Polarization with Monopolar Ion Exchange Membranes: Current-Voltage Curves and Water Dissociation. *Journal of Membrane Science* **1999**, 162 (1–2), 145–154. [https://doi.org/10.1016/S0376-7388\(99\)00133-7](https://doi.org/10.1016/S0376-7388(99)00133-7).
- (16) Strathmann, H.; Grabowski, A.; Eigenberger, G. Ion-Exchange Membranes in the Chemical Process Industry. *Industrial & Engineering Chemistry Research* **2013**, 52 (31), 10364–10379. <https://doi.org/10.1021/ie4002102>.

- (17) Hosseini, S. M.; Madaeni, S. S.; Khodabakhshi, A. R. Heterogeneous Cation Exchange Membrane: Preparation, Characterization and Comparison of Transport Properties of Mono and Bivalent Cations. *Separation Science and Technology* **2010**, 45 (16), 2308–2321. <https://doi.org/10.1080/01496395.2010.497792>.
- (18) Luo, T.; Abdu, S.; Wessling, M. Selectivity of Ion Exchange Membranes: A Review. *Journal of Membrane Science* **2018**, 555, 429–454. <https://doi.org/10.1016/j.memsci.2018.03.051>.
- (19) Tanaka, Y. Limiting Current Density of an Ion-Exchange Membrane and of an Electrodialyzer. *Journal of Membrane Science* **2005**, 266 (1–2), 6–17. <https://doi.org/10.1016/j.memsci.2005.05.005>.
- (20) Długolecki, P.; Anet, B.; Metz, S. J.; Nijmeijer, K.; Wessling, M. Transport Limitations in Ion Exchange Membranes at Low Salt Concentrations. *Journal of Membrane Science* **2010**, 346 (1), 163–171. <https://doi.org/10.1016/j.memsci.2009.09.033>.
- (21) Rodríguez Arredondo, M.; Kuntke, P.; ter Heijne, A.; Hamelers, H. V. M.; Buisman, C. J. N. Load Ratio Determines the Ammonia Recovery and Energy Input of an Electrochemical System. *Water Research* **2017**, 111 (3), 330–337. <https://doi.org/10.1016/j.watres.2016.12.051>.
- (22) Rodrigues, M.; Sleutels, T.; Kuntke, P.; Hoekstra, D.; ter Heijne, A.; Buisman, C. J. N.; Hamelers, H. V. M. Exploiting Donnan Dialysis to Enhance Ammonia Recovery in an Electrochemical System. *Chemical Engineering Journal* **2020**, 395 (April), 125143. <https://doi.org/10.1016/j.cej.2020.125143>.
- (23) Kappel, C.; Yasadi, K.; Temmink, H.; Metz, S. J.; Kemperman, A. J. B.; Nijmeijer, K.; Zwijnenburg, A.; Witkamp, G.-J.; Rijnaarts, H. H. M. Electrochemical Phosphate Recovery from Nanofiltration Concentrates. *Separation and Purification Technology* **2013**, 120, 437–444. <https://doi.org/10.1016/j.seppur.2013.10.022>.
- (24) Gao, R.; Benetton, X. D.; Varia, J.; Mees, B.; du Laing, G.; Rabaey, K. Membrane Electrolysis for Separation of Cobalt from Terephthalic Acid Industrial Wastewater. *Hydrometallurgy* **2020**, 191, 105216. <https://doi.org/10.1016/j.hydromet.2019.105216>.
- (25) Kuntke, P.; Sleutels, T. H. J. A.; Rodríguez Arredondo, M.; Georg, S.; Barbosa, S. G.; ter Heijne, A.; Hamelers, H. V. M.; Buisman, C. J. N. (Bio)Electrochemical Ammonia Recovery: Progress and Perspectives. *Applied Microbiology and Biotechnology* **2018**, 102 (9), 3865–3878. <https://doi.org/10.1007/s00253-018-8888-6>.
- (26) Lei, Y.; Du, M.; Kuntke, P.; Saakes, M.; van der Weijden, R.; Buisman, C. J. N. Energy Efficient Phosphorus Recovery by Microbial Electrolysis Cell Induced Calcium Phosphate Precipitation. *ACS Sustainable Chemistry & Engineering* **2019**, 7 (9), 8860–8867. <https://doi.org/10.1021/acssuschemeng.9b00867>.
- (27) Giddey, S.; Badwal, S. P. S.; Kulkarni, A. Review of Electrochemical Ammonia Production Technologies and Materials. *International Journal of Hydrogen Energy*. Elsevier Ltd 2013, pp 14576–14594. <https://doi.org/10.1016/j.ijhydene.2013.09.054>.
- (28) Kuntke, P.; Rodríguez Arredondo, M.; Widyakristi, L.; ter Heijne, A.; Sleutels, T. H. J. A. J. A.; Hamelers, H. V. M.; Buisman, C. J. N. N. Hydrogen Gas Recycling for Energy Efficient Ammonia Recovery in Electrochemical Systems. *Environmental Science & Technology* **2017**, 51 (5), 3110–3116. <https://doi.org/10.1021/acs.est.6b06097>.
- (29) Kuntke, P.; Rodrigues, M.; Sleutels, T.; Saakes, M.; Hamelers, H. V. M.; Buisman, C. J. N. N. Energy-Efficient Ammonia Recovery in an Up-Scaled Hydrogen Gas Recycling Electrochemical System. *ACS Sustainable Chemistry & Engineering* **2018**, 6 (6), 7638–7644. <https://doi.org/10.1021/acssuschemeng.8b00457>.
- (30) Rodrigues, M.; de Mattos, T. T.; Sleutels, T.; ter Heijne, A.; Hamelers, H. V. M.; Buisman, C. J. N.; Kuntke, P. Minimal Bipolar Membrane Cell Configuration for Scaling up Ammonium Recovery. *ACS Sustainable Chemistry and Engineering* **2020**, 8 (47), 17359–17367. <https://doi.org/10.1021/acssuschemeng.0c05043>.
- (31) Cherif, A. T.; Gavach, C.; Cohen, T.; Dagard, P.; Albert, L. Sulfuric Acid Concentration with an Electro-Electrodialysis Process. *Hydrometallurgy* **1988**, 21 (2), 191–201. [https://doi.org/10.1016/0304-386X\(88\)90004-7](https://doi.org/10.1016/0304-386X(88)90004-7).

- (32) Strathmann, H. Electrodialysis, a Mature Technology with a Multitude of New Applications. *Desalination* **2010**, 264 (3), 268–288. <https://doi.org/10.1016/j.desal.2010.04.069>.
- (33) Arola, K.; Ward, A.; Mänttari, M.; Kallioinen, M.; Batstone, D. Transport of Pharmaceuticals during Electrodialysis Treatment of Wastewater. *Water Research* **2019**, 161, 496–504. <https://doi.org/10.1016/j.watres.2019.06.031>.
- (34) Luo, T.; Roghman, F.; Wessling, M. Ion Mobility and Partition Determine the Counter-Ion Selectivity of Ion Exchange Membranes. *Journal of Membrane Science* **2020**, 597, 117645. <https://doi.org/10.1016/j.memsci.2019.117645>.
- (35) Kristensen, M. B.; Bentien, A.; Tedesco, M.; Catalano, J. Counter-Ion Transport Number and Membrane Potential in Working Membrane Systems. *Journal of Colloid and Interface Science* **2017**, 504, 800–813. <https://doi.org/10.1016/j.jcis.2017.06.010>.
- (36) Ward, A. J.; Arola, K.; Thompson Brewster, E.; Mehta, C. M.; Batstone, D. J. Nutrient Recovery from Wastewater through Pilot Scale Electrodialysis. *Water Research* **2018**, 135, 57–65. <https://doi.org/10.1016/j.watres.2018.02.021>.
- (37) Xie, M.; Shon, H. K.; Gray, S. R.; Elimelech, M. Membrane-Based Processes for Wastewater Nutrient Recovery: Technology, Challenges, and Future Direction. *Water Research* **2016**, 89, 210–221. <https://doi.org/10.1016/j.watres.2015.11.045>.
- (38) Zhang, C.; Ma, J.; Song, J.; He, C.; Waite, T. D. Continuous Ammonia Recovery from Wastewaters Using an Integrated Capacitive Flow Electrode Membrane Stripping System. *Environmental Science and Technology* **2018**, 52 (24), 14275–14285. <https://doi.org/10.1021/acs.est.8b02743>.
- (39) Luther, A. K.; Desloover, J.; Fennell, D. E.; Rabaey, K. Electrochemically Driven Extraction and Recovery of Ammonia from Human Urine. *Water Research* **2015**, 87, 367–377. <https://doi.org/10.1016/j.watres.2015.09.041>.
- (40) Darestani, M.; Haigh, V.; Couperthwaite, S. J.; Millar, G. J.; Nghiem, L. D. Hollow Fibre Membrane Contactors for Ammonia Recovery: Current Status and Future Developments. *Journal of Environmental Chemical Engineering* **2017**, 5 (2), 1349–1359. <https://doi.org/10.1016/j.jece.2017.02.016>.
- (41) Veerman, J.; de Jong, R. M.; Saakes, M.; Metz, S. J.; Harmsen, G. J. Reverse Electrodialysis: Comparison of Six Commercial Membrane Pairs on the Thermodynamic Efficiency and Power Density. *Journal of Membrane Science* **2009**, 343 (1–2), 7–15. <https://doi.org/10.1016/j.memsci.2009.05.047>.
- (42) Veerman, J. The Effect of the NaCl Bulk Concentration on the Resistance of Ion Exchange Membranes—Measuring and Modeling. *Energies (Basel)* **2020**, 13 (8). <https://doi.org/10.3390/en13081946>.
- (43) Zamora, P.; Georgieva, T.; Salcedo, I.; Elzinga, N.; Kuntke, P.; Buisman, C. J. N. Long-Term Operation of a Pilot-Scale Reactor for Phosphorus Recovery as Struvite from Source-Separated Urine. *Journal of Chemical Technology and Biotechnology* **2017**, 92 (5), 1035–1045. <https://doi.org/10.1002/jctb.5079>.
- (44) Wang, H.; Liu, J.; He, W.; Qu, Y.; Li, D.; Feng, Y. Energy-Positive Nitrogen Removal from Reject Water Using a Tide-Type Biocathode Microbial Electrochemical System. *Bioresource Technology* **2016**, 222, 317–325. <https://doi.org/10.1016/j.biortech.2016.09.090>.
- (45) Berezina, N. P.; Kononenko, N. A.; Dyomina, O. A.; Gnusin, N. P. Characterization of Ion-Exchange Membrane Materials: Properties vs Structure. *Advances in Colloid and Interface Science* **2008**, 139 (1–2), 3–28. <https://doi.org/10.1016/j.cis.2008.01.002>.
- (46) Casademont, C.; Farias, M. A.; Pourcelly, G.; Bazinet, L. Impact of Electrodialytic Parameters on Cation Migration Kinetics and Fouling Nature of Ion-Exchange Membranes during Treatment of Solutions with Different Magnesium/Calcium Ratios. *Journal of Membrane Science* **2008**, 325 (2), 570–579. <https://doi.org/10.1016/j.memsci.2008.08.023>.

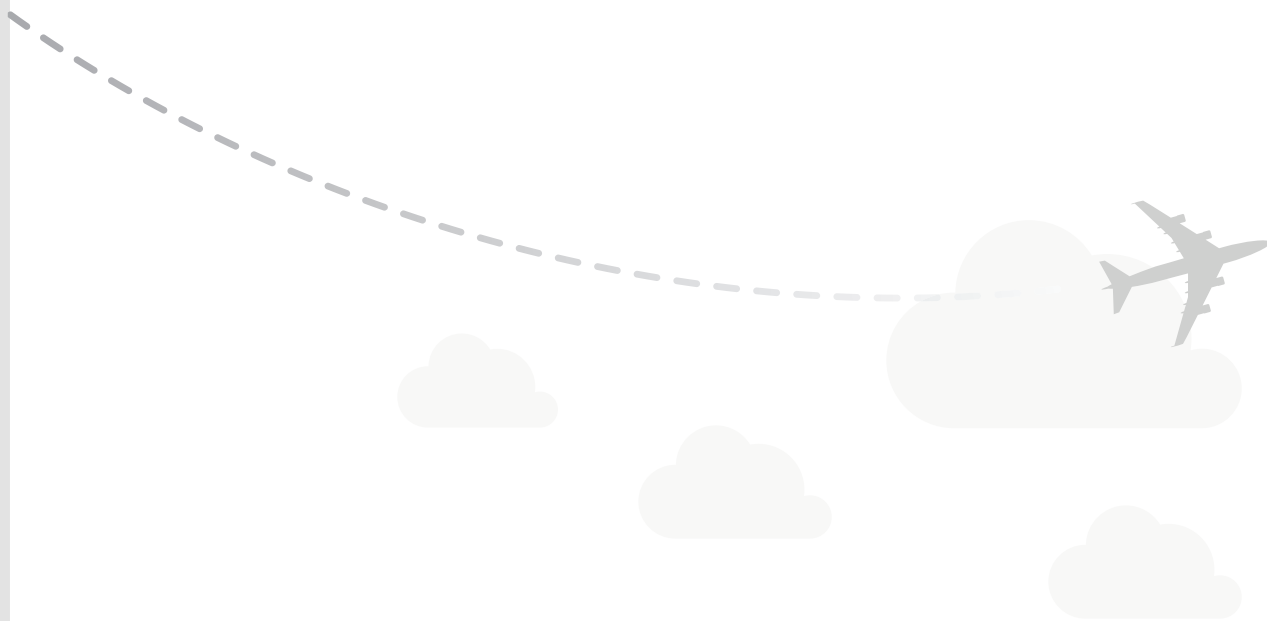
- (47) Desloover, J.; Abate Woldeyohannis, A.; Verstraete, W.; Boon, N.; Rabaey, K. Electrochemical Resource Recovery from Digestate to Prevent Ammonia Toxicity during Anaerobic Digestion. *Environmental Science and Technology* **2012**, 46 (21), 12209–12216. <https://doi.org/10.1021/es3028154>.
- (48) Christiaens, M. E. R.; Udert, K. M.; Arends, J. B. A.; Huysman, S.; Vanhaecke, L.; McAdam, E.; Rabaey, K. Membrane Stripping Enables Effective Electrochemical Ammonia Recovery from Urine While Retaining Microorganisms and Micropollutants. *Water Research* **2019**, 150, 349–357. <https://doi.org/10.1016/j.watres.2018.11.072>.
- (49) Tarpeh, W. A.; Barazesh, J. M.; Cath, T. Y.; Nelson, K. L. Electrochemical Stripping to Recover Nitrogen from Source-Separated Urine. *Environmental Science and Technology* **2018**, 52 (3), 1453–1460. <https://doi.org/10.1021/acs.est.7b05488>.

7



Chapter 7

Critical transport regimes during electrochemical ammonia recovery



This Chapter has been submitted as:

Mariana Rodrigues, Tom Sleutels, Philipp Kuntke, Cees Buisman, Bert Hamelers.
Critical transport regimes during electrochemical ammonia recovery.

Abstract

Electrochemical systems (ES) are an emerging technology for ammonia recovery; and, a complete insight on their control, essential process, and performance is still lacking. A simplified model of the transport over the cation exchange membrane (CEM) during electrochemical ammonia recovery was developed, considering crucial control parameters (e.g., current, loading, wastewater supplied). Four transport regimes were identified for electrochemical ammonia recovery: 1) transport of only NH_4^+ ; 2) transport of NH_4^+ and Na^+ ; 3) transport NH_4^+ and H^+ and 4) transport of the Na^+ , NH_4^+ , and H^+ . These transport regimes are directly linked to the system's performance regarding removal efficiency, flux over the CEM, and energy demand. Overall, a high removal efficiency comes at the cost of a high energy demand, particularly when a high treatment capacity (i.e., high current density) is desired to reduce the investment costs. The buffer fraction in solution affects at which under conditions the four transport regimes occur. Therefore, considering only the current and total cation loading is insufficient to predict the performance. The transport regimes described in this model explain why so far, the desired combination of high removal efficiency at low energy consumption and high current density was never observed.

Introduction

The interest in more sustainable paths has slowly shifted the production of reactive nitrogen towards nitrogen recovery. At the same time, the required energy input for nitrogen removal processes and related nitrous oxide emissions in our wastewater treatment plants increase the need for sustainable nitrogen recovery processes ¹⁻³.

Among the different nitrogen recovery technologies, electrochemical systems (ES) have been proposed as a viable option for nitrogen recovery ⁴⁻⁷. So far, ES development focused on low energy input (around 16kJ/g^N; comparable to ANAMMOX) and to achieve efficient nitrogen removal (up to 90%) from different wastewaters ⁸. The observed wide performance range of ES, make their implementation for ammonia recovery challenging.

Tarpeh et al reported 61% nitrogen removal from urine when operating continuous mode at 100 A m⁻², and 93% nitrogen removal when running in batch mode ⁹. Rodrigues et al reported 80% nitrogen removal when supplying synthetic urine continuously at varying inflow rates ¹⁰. Van Linden et al demonstrated operating with a dynamic (variable) current density could enhance ammonium concentration from synthetic reject water ¹¹. Several other studies describe ammonia recovery at different inflow rates and current densities resulting in considerable differences in obtained removal efficiency and energy consumptions ^{8,12-15}.

So far, there have been no reports of simultaneously high removal efficiency (>> 90%) at a high current density (>> 100 A/m²) and low energy consumption (below ANAMMOX energy consumption, 16 kJ/g_N). It somehow seems these performance efficiencies rule each other out. To scale up ES, it is crucial to understand the relationships between the key performance parameters and the system controls (applied current and inflow rate). However, there is no sufficient insight on how these system controls impact the key performance parameters.

Chapter 6 described how the selectivity of the boundary layer/membrane and the extraction of ammonium from the cathode affect the ion transport over the CEM. Once a certain current is reached, the transport of other (unwanted) counter-ions occurs and the current efficiency decreases. Above a certain current, the boundary layer and membrane selectivity is lost, and the transport number corresponds to the ions fraction in the wastewater supplied.

In this study, we extended the previously developed model in Chapter 6 with the presence of buffer, the dynamic composition of the anode, and the transport of uncharged species over the CEM and their effect on the transport number over the CEM. This extended model describes the relation between removal efficiency, energy consumption, and treatment capacity during electrochemical ammonia recovery. From the model, we identify four different transport regimes during electrochemical ammonia recovery and the window of operation where a high removal efficiency can be achieved at the lowest energy consumption. Furthermore, the presence of buffer in wastewater was identified as a crucial point to achieve a certain performance.

Electrochemical system for nitrogen recovery: theoretical framework

The electrochemical ammonia recovery system considered here includes any ES where a CEM separates two compartments, a constant current is applied to transport ammonium towards the cathode, and an efficient ammonia extraction process (i.e., membrane stripping), represented in Figure 1. The system is continuously fed on the anode side with wastewater. The anodic reaction generates protons (H^+) to acidify the supplied wastewater. The cathodic reaction generates hydroxide ion (OH^-) that reacts with ammonium (NH_4^+) to form ammonia gas (i.e.: $NH_4^+ + OH^- \rightarrow NH_3(g) + H_2O$). The cathode side is operated in batch (a finite volume recirculated over the compartment). While the anode side continuously generates an effluent (i.e.: treated wastewater). The influent supplied represents any wastewater containing ammonium, sodium (representing all other cations), a buffer specie (e.g.: bicarbonate or acetate), and chloride (representing all other anions). When the buffer is depleted, the anolyte accumulates H^+ from the anode reaction. In electrochemical ammonia recovery, cations are transported over a CEM to the cathode. At the cathode compartment, NH_3 is removed, while Na^+ accumulates. The Cl^- and the buffer species in the anode are not transported over the CEM. At the cathode, two species are “consumed”; both NH_4^+ is deprotonated (and extracted) and H^+ are neutralized by OH^- formed in the cathodic reaction.

In Chapter 6, the current applied to the system is described dimensionless (Y , Equation S1, appendix B). Additionally, a transition current (Y_t) was defined, as the maximum current where the transport of an ionic specie 1 is equal to 1 ($t_1=1$). Above the transition current, the transport is a function of the fraction of ions in solution and of the selectivity of the boundary layer and membrane $H(\alpha)$ where α represents the ratio between the membrane and boundary layer properties (Equation S3, Appendix B).

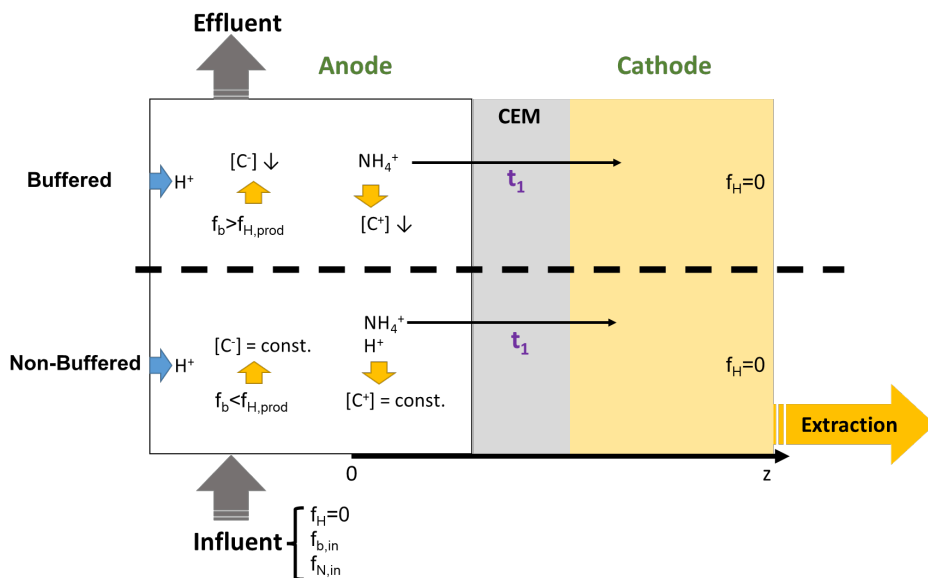


Figure 1. Evolution of concentration of ionic species in the anolyte for the buffered and non-buffered case. In both cases, protons (H^+) are produced at the anode and completely consumed at the cathode ($f_H=0$). The influent (in) is supplied to the anode. In the buffered case, as the H^+ fraction ($f_H=0$) is lower than the buffer fraction ($f_b>0$) in the anolyte, and NH_4^+ is transported over the CEM, the concentration of the cations ($[C^+]$) decreases. The transport of specie 1 (t_1) includes only the transport of NH_4^+ . The buffer (e.g.: H_2CO_3 , HCO_3^- , CO_3^{2-}) is part of the total anions. Thus, because of the buffer's reaction with H^+ , the total concentration of anions ($[A^-]$) at the anode is lowered. In the non-buffered case, the buffer is depleted ($f_b=0$), and H^+ are in excess ($f_H>0$). Therefore, protons replace other cations transported over the CEM, keeping the $[C^+]$ constant. In the non-buffered case, the H^+ concentration builds up and both NH_4^+ and H^+ can be transported over the CEM. We also assume a small diffusion flux of NH_3 from the cathode towards the anode. The total anion concentration ($[A^-]$) is also constant, as it is only dependent on Cl^- (here representing all other anions) and not on the buffer.

The previous model described an ideal case where NH_4^+ , Na^+ and Cl^- represented all ionic species (Chapter 6). However, wastewater is a complex matrix with variable composition including buffer species that affect the transport number. Additionally, the H^+ produced at the anode can react with the buffer present in the influent (bicarbonate or acetate). Therefore, the previous model will be extended. Two cases will be distinguished (see Figure 1). One a buffered case, where the buffer is present, and all H^+ produced from the electrode reaction are “neutralized” by the buffer specie. Two a non-buffered case, where the concentration of H^+ is not negligible, and these H^+ are available for transport. To determine whether there is still buffer present, we can write for the overall buffer balance:

$$0 = f_{b,in} - \eta f_{b,in} - L_T + t_N \beta L_T \quad (\text{Equation 1})$$

Where $f_{b,in}$ is the fraction of buffer in the influent, is the transport of NH_4^+ , η is the ratio between the total cation/anion concentration at the anode-boundary layer interface and the total cation/anion concentration of the influent (Appendix C, equation S4), L_T is the total cation loading ratio (Equation S2, Appendix A) and β is a possible ammonia diffusion towards the anode(described in Appendix D). The first term represents the buffer supplied, the second term represents the remaining buffer in the anode, and the third term accounts for the H^+ produced (current and loading dependent). The fourth term ($t_N\beta L_T$) is the ammonia diffusion towards the anode, as NH_3 also has a buffer capacity (this can occur when the NH_3 extraction at the cathode is insufficient). As in an ideal situation a maximum extraction is desired, the model will be studied with a low β .

It is important to note that the H^+ and NH_4^+ behave similarly. Both are monovalent cations, and both have a practically zero concentration in the cathode compartment, as they are both “consumed”. Therefore, we can set up the ammonium nitrogen fraction (f_N), the proton fraction (f_H) and the fraction of specie 1 ($f_1=f_N+f_H$). The same applies to the balance for NH_4^+ , H^+ , and its sum as species 1. Adding the individual balances and considering the buffer balance (Appendix E, equation S12 and S13), we get the balance of species 1 in a buffered and not buffered case:

$$\eta f_1 = \begin{cases} f_{N,in} - L_T(1 - \beta)t_N, & \text{for the buffered case} \\ f_{N,in} - f_{b,in} + L_T(1 - t_1), & \text{for the non - buffered case} \end{cases} \quad (\text{Equation 2})$$

Ions transported through the CEM

When we apply this extended model to electrochemical ammonia recovery, four different situations can be distinguished. The first two situations are defined by the transition current conditions. When below this transition current condition, the transport of NH_4^+ is 1 ($t_1=1$), and when above this transition current the transport efficiency of NH_4^+ is smaller than 1 ($t_1<1$). The second two situations are defined by the presence of buffer. When buffer is present, all H^+ are taken up by the buffer and no H^+ are transported. When buffer is depleted, the produced H^+ will be also transported. Table 1 provides an overview of all conditions and the expected transport number.

Table 1: Ions transported during electrochemical NH_4^+ removal.

	$t_1 = 1$	$t_1 \leq 1$
buffer present	NH_4^+ is transported	NH_4^+ & Na^+ are transported
buffer depleted	NH_4^+ & H^+ are transported	NH_4^+ & Na^+ & H^+ are transported

To give insight about the ES operation, in the sections below, we will define the limits of each transport regime (line) with respect to the dimensionless current (Υ) and total cation loading ratio (L_T).

When buffer is present and if operated below the transition current only the transport of NH_4^+ occurs. Once the transition current is reached, and buffer is still present, Na^+ is also transported through the CEM. When the buffer supply is insufficient and the anolyte solution is near depletion of NH_4^+ and Na^+ , the H^+ resulting from the electrode reaction are also transported over the CEM.

The Na transport exclusion line

In the previously reported model (Chapter 6) a transition current was established where Na^+ (here representing all other cations) is transported over the CEM ($t_1 < 1$). Here, we need to distinguish two situations: 1) buffer is present or 2) buffer is depleted.

a) Buffer is present

In Chapter 6, we established that the transport number is directly proportional to the specie 1 fraction (t_1), while the denominator accounts for the effects of current and the size of the boundary layer (Equation 3). For ease of notation, the transport equation was further distinguished as:

$$t_1 = \frac{f_{1,0}}{H(\alpha, \gamma)} \quad (\text{Equation 3})$$

in which $H(\alpha, \gamma)$ is the combined selectivity function and it can be described as:

$$H(\alpha, \gamma) = 1 - \left(1 - \frac{\gamma t}{2}\right)^2 e^{-\alpha \gamma t} \quad (\text{Equation 4})$$

When the transport number of specie 1 is one ($t_1=1$), and buffer is present, there is no Na^+ transport. We know from the balance equation for species 1 (Equation 2), and the relationship between the transport number and the combined selectivity function (H , Equation 4) formed by the boundary layer-membrane ensemble (Equation 3) that the transport of NH_4^+ can be described as:

$$t_N = \frac{f_{N,in}}{\eta H(\alpha, \gamma, \eta) + L_T(1-\beta)} = 1 \quad (\text{Equation 5})$$

Solving for H and from the buffer equation (Equation 2), the relation above gives the selectivity for NH_4^+ :

$$H_1 = \frac{f_{N,in} - L_T(1-\beta)}{1 - L_T(1-\beta)} \quad (\text{Equation 6})$$

This equation can be used to calculate the current that gives an exclusive transport of specie one (NH_4^+ ; $t_1=1$) at certain L_T . Since the influent has multiple components, $f_{1,in} < 1$, and thus the selectivity will decrease with increasing L_T and become eventually zero, yielding a zero current. This implies that for a higher value of L_T (meaning more current is available than cations loaded to the system), the t_1 is always lower than one, and Na^+ transport will occur (depletion).

b) Buffer is depleted

Once the buffer is depleted, new assumptions need to be considered due to the excess of H^+ generated at a higher applied current. This implies that if the buffer fraction supplied (L_b) is smaller than the ammonium fraction supplied, the buffer will be depleted first. Substituting buffer fraction supplied in the relation for gives a value for function H that can be used to determine the current where the buffer gets depleted. For all currents at L_b smaller than the Y_t , we will have $t_1=1$ and $f_b=0$.

If the buffer is depleted, H^+ will be available for transport, and we must look for $t_1=1$, to find the points where no Na^+ transport takes place (i.e.: Na^+ transport occurs at higher currents depending on the buffer).

$$\eta f_1 = f_{1,in} - f_{b,in} + L_T(1 - t_1) \quad (\text{Equation 7})$$

Again if $t_1=1$ and $\eta = 1 - f_{b,in}$ we get:

$$f_1 = \frac{f_{1,in} - f_{b,in}}{1 - f_{b,in}} = \frac{f_{N,in} - f_{b,in}}{1 - f_{b,in}} \quad (\text{Equation 8})$$

Since f_1 is always positive, and if $f_{N,in} > f_{b,in}$ there will be a f_1 where $t_1=1$.

For even higher currents, as the selectivity equals one (Chapter 6), an over limiting current area can also be defined, where the model assumptions no longer applied.

Buffer Transition line

Finally, we want to identify the transition points that are characterized by both the buffer and the H^+ concentration being zero. On this transition line, as the buffer is depleted, we know that $\eta = 1 - f_{b,in}$. Now, if we consider the case when the NH_4^+ transport is less than one (≤ 1), we can establish the current at where the system gets the buffer depleted:

$$H(\alpha, \gamma, \eta) = \frac{L_b}{\eta} \left(\frac{\beta f_{N,in}}{L_b - f_{b,in}} - (1 - \beta) \right) \quad (\text{Equation 9})$$

An increase of L_T with increasing f_N , will reflect on the buffer term. Consequently, the NH_3 diffusion from cathode towards the anode, takes away protons, reducing the buffer consumption. Hence, from S13, Appendix E, we can find the L_T at which the transition current is reached on the buffer and non-buffered cases.

$$\eta = L_{b,m} \left(\frac{\beta f_{N,in}}{L_{b,m} - f_{b,in}} - (1 - \beta) \right) \quad (\text{Equation 10})$$

Equation 10 gives the $L_{b,m}$ at which the transition current can be calculated.

Considering the previous equations and assuming a fixed fraction of ammonium ($f_i=0.7$) and buffer ($f_b=0.5$) in the feed solution while keeping the boundary layer – membrane relation ($\alpha=1$), and the amount of ammonia returning to the feed solution ($\beta=0.1$) constant, four transport regimes can be outlined (see Figure 2).

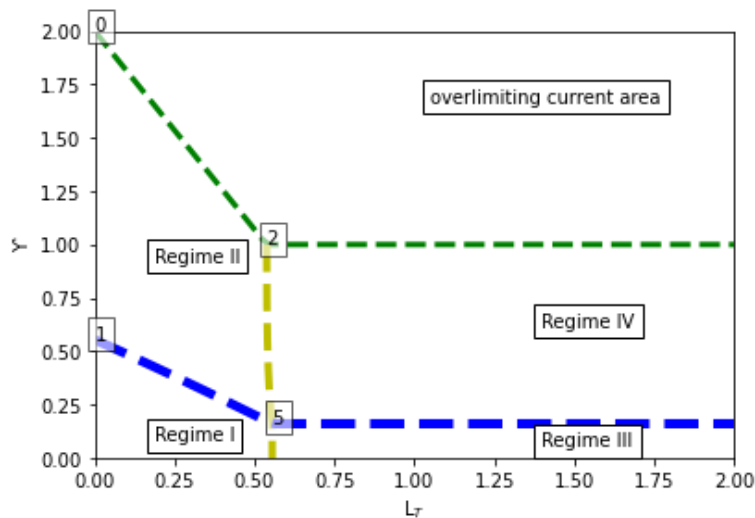


Figure 2. Ion transport regimes at different L_T and Y , when $f_N > f_b$. Here, four regions are distinguished, where only certain species are transported: Regime 1 - NH_4^+ transport, Regime 2 - NH_4^+ and Na^+ (where sodium represents all other monovalent cation excluding protons) transport, Regime 3 - NH_4^+ and H^+ transport, and Regime 4 – transport of all cationic species.

As described in Table 1, while operating in Regime 1, only NH_4^+ is transported and there is enough buffer to neutralize all H^+ produced at the anode. When increasing Y , the transport number of NH_4^+ is lower than 1, also Na^+ is transported (Regime 2). Once the buffer is depleted, H^+ will be transported together with either only NH_4^+ (regime 3) or together with NH_4^+ and all other cations (Regime 4). Regimes 3 and 4 occur when the L_T is increased.

The yellow line represents the buffer transition line, where the buffer is equal to the amount of produced H^+ . The blue line represents the Na^+ exclusion line and the border conditions where all charge transported is NH_4^+ ($t_i=1$). The green line represents the transition current. Here, the selectivity of the boundary layer-membrane ensemble equals one. Above the green line, the over transition current area, the model assumptions no longer apply as for example water splitting may¹⁶.

Performance Parameters

An ES performance can be described by several parameters (removal efficiency, transport number, specific membrane flux, and energy use). In order to characterize the relation between transport regimes, ammonium-nitrogen (sum of ammonia and ammonium nitrogen) removal and energy input, and consequently predict its performance, several parameters were calculated.

Removal

The nitrogen removal efficiency is given by:

$$K_N = 1 - \frac{C_N}{C_{N,in}} \quad (\text{Equation 11})$$

Where C_N is the ammonium-nitrogen effluent concentration (mol/dm^3) and $C_{N,in}$ is the influent ammonium-nitrogen concentration (mol/dm^3).

N membrane flux

The nitrogen flux over the cation exchange membrane is given by:

$$F_N = \gamma t_N \quad (\text{Equation 12})$$

Energy consumption

A minimum energy consumption was also considered to establish the performance of the ES. This energy is origination from work needed for the transport of NH_4^+ over the CEM. Additionally, the pH difference is also of great importance. Since the pH in

the anode is not the pH of the catalyst, we assume a fixed value for the (scaled) pH difference (ψ_{pH} , 14). For simplicity, we derive for a minimum expected dimensionless energy demand.

$$E_N = \frac{1}{t_N} \left(\frac{\gamma_i}{\eta} d_c - 2 \ln \left(\eta - \frac{\gamma_i}{2} \right) + \psi_{\text{pH}} \right) \quad (\text{Equation 13})$$

In this equation $d_c = 2L_{\text{bl}}$ is the scaled thickness of the compartment and accounts for the ohmic loss, the second term accounts for the boundary layer and membrane and the third term accounts for the pH difference.

Assumptions

Nitrogen ($f_N=0.7$) and buffer fractions ($f_b=0.5$ and $f_b=0.1$) were selected according to results often measured in concentrated streams such as urine or reject water^{8,9,17}. The ratio between the membrane and the boundary layer transport ($\alpha=1$) was selected assuming the membrane properties relate equally to the behavior observed in the boundary layer (Chapter 6). Additionally, a constant ammonia diffusion towards the anode ($\beta=0.1$) was considered, as this has previously been reported^{11,14}.

Results & Discussion

The model was analyzed considering the two most important cases often presented in literature (an influent with high ammonium fraction and high or low buffer fraction). Aforementioned, the nitrogen fraction considered was 0.7 and the buffer fractions were 0.5 and 0.1.

High removal efficiency, low energy consumption or high treatment capacity cannot be achieved simultaneously.

Figure 3 shows the expected performance at a certain current and total cation loading ratio. The performance parameters presented include the transport regime (A), ammonium transport numbers (B), ammonium-nitrogen removal efficiency (C), fraction of ammonium-nitrogen in the effluent (D), membrane flux (E), and energy consumption (F). Figure 3 resulted from the model developed in this study. All variables are dimensionless.

Figure 3, graph A and B represent the transport regime and the ammonium transport number, respectively. As described in Figure 2 there are four distinct transport regimes, the exclusive NH_4^+ transport over the CEM only occurs at low Υ and low L_T for Regime I (see Figure 3, graphs A and B). With Υ increase, other cationic species will move through the CEM, so we observe a change in the transport regime and the transport number decreases. This can occur due to a depletion effect related to transition current (Na^+ is transported – Regime 2, light blue). On the other hand, when increasing L_T the transport is also affected either due to a buffer limitation (H^+ is transported – Regime 3, light red) or due to a combination of both sodium and protons transport (Regime 4, dark red). Overall, the supplied charge is not only used for NH_4^+ but also for other cations and the transport number decreases (t_i). Consequently, this will influence the energy demand of the system.

Figure 3, graphs C and D show the ammonium removal efficiency and its fraction on the effluent of the ES. Depending on the transport regime, the removal is influenced by transport number (t_i), buffer in the influent, L_T and Υ . According to the present model, to remove all ammonium-nitrogen from wastewater, the solution needs to be depleted of other cationic species too (Regime 4). Furthermore, the removal increases with L_T (less cations supplied per amount of charge applied).

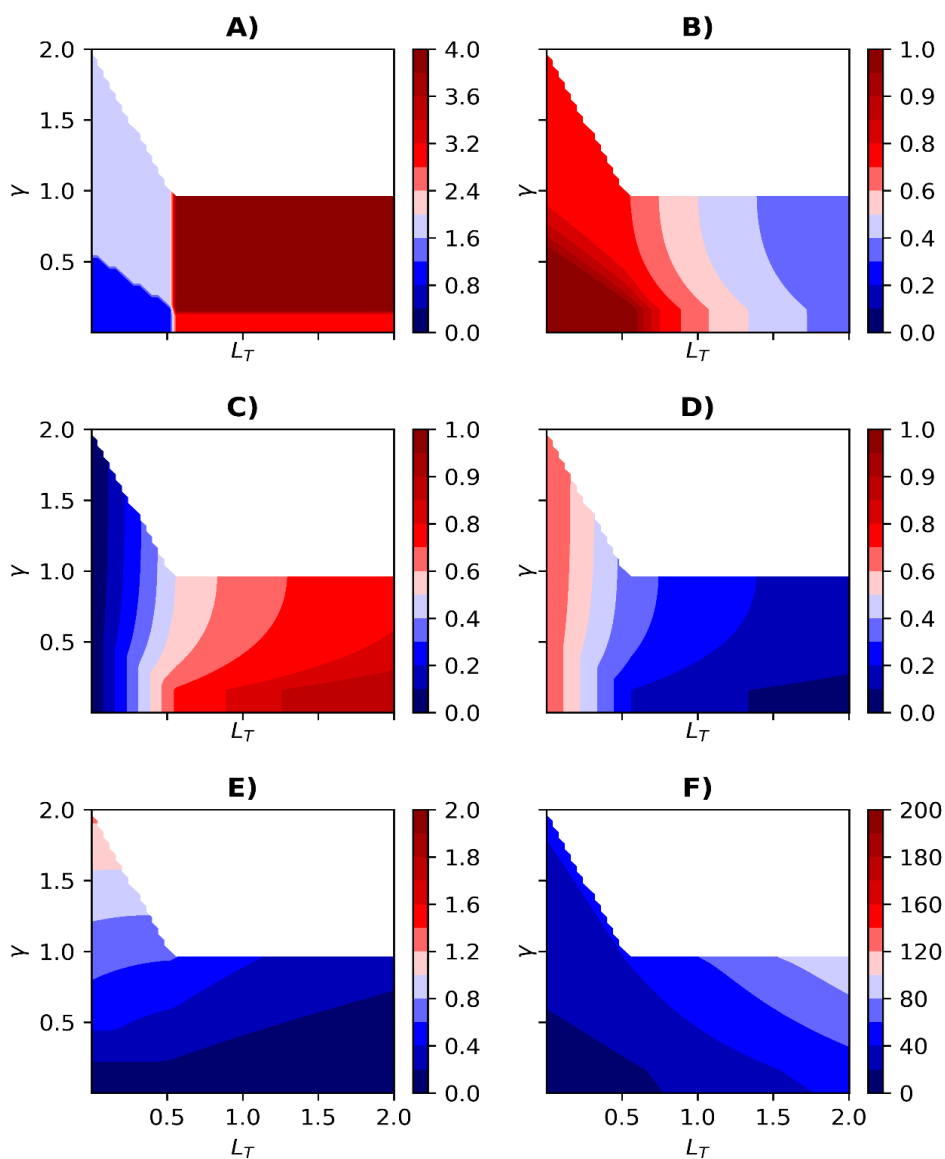


Figure 3. Current and total cation loading ratio influence on several performance parameters for electrochemical ammonia recovery systems (A - transport regime, B - ammonium transport numbers, C - ammonium-nitrogen removal efficiency, D - fraction of ammonium-nitrogen on the effluent, E - membrane flux, F - energy consumption) when the fraction of nitrogen ($f_N=0.7$) is higher than the fraction of buffer ($f_b=0.5$). The performance increases from blue to red.

Figure 3 (graph E) shows that the flux increases with the Υ which is expected as more charge is transported over the same membrane area. A high NH_4^+ transport number ($t_1=1$) can only be observed at low currents and low L_T . Once, the system starts transporting other ionic species (different regimes), the ammonium flux is lower. Consequently, the energy demand is dependent on the NH_4^+ transport efficiency and the flux over the membrane. The combination of decreasing NH_4^+ transport number at higher flux translates into a higher energy demand per ammonium-nitrogen removed (see Figure 3, graph F). Either increasing the current or the L_T will gradually increase the energy consumption of the system, meaning more energy needs to be applied to remove the same amount of ammonium nitrogen. Overall, in Figure 3, we can see that the performance parameters relate differently with Υ and L_T .

The buffer in solution plays an important role on the transport regimes and severely limits the removal efficiency.

To see the effect of buffer, the transport regime (A), ammonium transport numbers (B), ammonium-nitrogen removal efficiency (C), fraction of ammonium-nitrogen on the effluent (D), membrane flux (E), and energy consumption (F) were also characterized at a lower buffer fraction ($f_b=0.1$) compared to Figure 3, see Figure 4.

Figure 4 (graph A) shows the effect of a lower buffer fraction ($f_b=0.1$) on the transport regimes. Compared to Figure 2 and Figure 3, graph A, Regime 3 and Regime 4 occur at a lower L_T , when there is less buffer in the influent solution. This is expected, less H^+ are needed from the electrode reaction to neutralize all buffer in solution. Furthermore, the Na^+ exclusion line and the transition current line occur at a higher current ($\Upsilon \sim 0.5$ vs $\Upsilon \sim 0.25$ for the sodium exclusion line). This means the system can operate at higher current before transporting Na^+ through the CEM or reaching complete depletion (transition current).

Particularly for the removal (Figure 4, graph C), it will be no longer possible to reach conditions where all nitrogen can be removed ($>80\%$) for such low amount of buffer. Therefore, the system becomes less adequate for a situation where high removal is desired. Overall, for the other performance parameters, a low buffer fraction shifts the regions to lower L_T . Therefore, ideal conditions such as a low energy demand or high flux, are not accessible anymore for high Υ and L_T .

The presence of buffer is often not considered as a defining parameter for the performance of electrochemical ammonia recovery systems, nevertheless we identify it as a crucial aspect to achieve a certain performance.

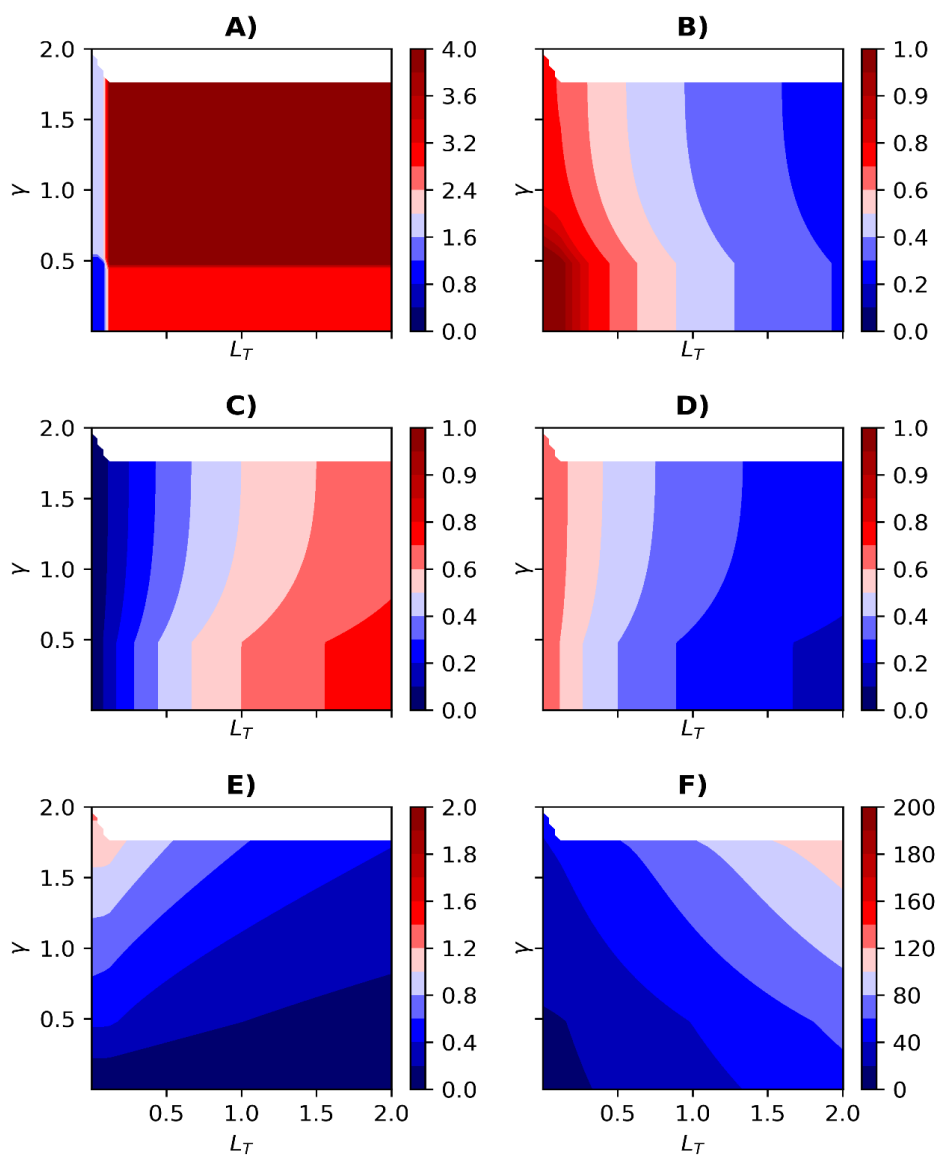


Figure 4. Current and total cation loading ratio influence on several performance parameters for electrochemical systems (A - transport regime, B - ammonium transport numbers, C - ammonium-nitrogen removal efficiency, D - fraction of ammonium-nitrogen on the effluent, E- membrane flux, F - energy consumption) when the buffer fraction is very low ($f_b=0.1$). The performance increases from blue to red.

An “engineering approach” on electrochemical ammonium-nitrogen recovery resulted in studies converging into similar performance.

As most studies aim for a high NH_4^+ removal (>90%), at the lowest energy consumption (approximately ≥ 18 kJ/gN, equivalent to of 80 – 100 in Figure 3, graph E), while treating more influent, we observe most studies in Regime 4 (high L_T and high currents) (see Table S1, Appendix F) ^{7,8}. On the other hand, although different operation parameters are set among studies, a similar performance was observed.

This model confirms that we must consider simultaneously several characteristics (such as current, influent composition, amount of ammonium-nitrogen, buffer in the influent, and total cation loading ratio) to successfully apply electrochemical ammonia recovery systems. Furthermore, studies often report insufficient experimental details for an extensive analysis using our model and some information (i.e. current or loading, dynamics of transport such as membrane characteristics or recirculation flow) are also hard to acquire. Fortunately, transport numbers can be measured and used to assess the regime. Information on the regime can be used to deduct in which direction operational parameters must be changed to achieve a certain desired performance. Also, the parameters describing cell characteristics could be used as a starting point to improve the design aspects, like membrane characteristics, boundary layer thickness, etc.

When implementing an electrochemical ammonia recovery system, the desired output (efficiency) should be first considered before selecting the operation parameters. High removal can only be achieved at a higher cation loading ratio (L_T), higher than the ion fraction, at low current (Υ) and only when the buffer capacity of the anolyte is depleted (Regime 3). At these conditions, NH_4^+ is no longer the only charged specie transported over the CEM. For example, if the ES is used to recover only part of the ammonium-nitrogen of digestate at a wastewater treatment plant and therefore needs to treat a large volume, higher current densities at $L_T=1$ should be selected. On the other hand, if it is required to recover all the ammonium-nitrogen from the supplied wastewater, the system can be only operated at low current densities. At $L_T \sim 1.5$, this will lead to higher energy input per mol of ammonia. Additionally, the buffer in waste streams will determine how effective the ammonium-nitrogen can be recovered.

Conclusion

The definition of four transport regimes allowed to establish the relation between different performance parameter with the control parameters (current (Y) and total cation loading ratio (L_T)) during electrochemical ammonia recovery. The model further describes how these regimes are affected by the presence of buffer and the applied current. Consequently, 4 transport regimes can be distinguished: Regime 1 - NH_4^+ transport, Regime 2 - NH_4^+ and Na^+ (where sodium represents all other monovalent cation excluding protons) transport, Regime 3 - NH_4^+ and H^+ transport, and Regime 4 – transport of all cationic species. A high ammonium-nitrogen removal (>90%) can only be obtained at low current density or at the cost of a high energy input. This is linked to the ion transport observed over the cation exchange membrane. The four transport regime areas shift due to the fraction of buffer in the influent, and this consequently affects the window of operation where a certain removal or energy consumption can be achieved. The model demonstrates how the increase in treatment capacity through an increase of applied current is affecting the removal efficiency and energy demand. Furthermore, this model will be helpful to optimize electrochemical ammonia recovery in terms of energy costs, capital cost, and performance.

References

- (1) Maurer, M.; Schwegler, P.; Larsen, T. A. Nutrients in Urine: Energetic Aspects of Removal and Recovery. *Water Science and Technology* **2003**, 48 (1), 37–46. <https://doi.org/10.1017/S000748530002229X>.
- (2) US-EPA. *Greenhouse Gas Emissions*. <https://www.epa.gov/ghgemissions/overview-greenhouse-gases>.
- (3) Sutton, M. A.; Oenema, O.; Erisman, J. W.; Leip, A.; van Grinsven, H.; Winiwarter, W. Too Much of a Good Thing. *Nature* **2011**, 472 (7342), 159–161. <https://doi.org/10.1038/472159a>.
- (4) Pronk, W.; Biebow, M.; Boller, M. Treatment of Source-Separated Urine by a Combination of Bipolar Electrodialysis and a Gas Transfer Membrane. *Water Science and Technology* **2006**, 53 (3), 139–146. <https://doi.org/10.2166/wst.2006.086>.
- (5) van Linden, N.; Bandinu, G. L.; Vermaas, D. A.; Spanjers, H.; van Lier, J. B. Bipolar Membrane Electrodialysis for Energetically Competitive Ammonium Removal and Dissolved Ammonia Production. *Journal of Cleaner Production* **2020**, 259, 120788. <https://doi.org/10.1016/j.jclepro.2020.120788>.
- (6) Rodríguez Arredondo, M.; Kuntke, P.; ter Heijne, A.; Hamelers, H. V. M.; Buisman, C. J. N. Load Ratio Determines the Ammonia Recovery and Energy Input of an Electrochemical System. *Water Research* **2017**, 111 (3), 330–337. <https://doi.org/10.1016/j.watres.2016.12.051>.
- (7) Liu, Y.; Deng, Y. Y.; Zhang, Q.; Liu, H. Overview of Recent Developments of Resource Recovery from Wastewater via Electrochemistry-Based Technologies. *Science of the Total Environment* **2021**, 757, 143901. <https://doi.org/10.1016/j.scitotenv.2020.143901>.
- (8) Kuntke, P.; Sleutels, T. H. J. A.; Rodríguez Arredondo, M.; Georg, S.; Barbosa, S. G.; ter Heijne, A.; Hamelers, H. V. M.; Buisman, C. J. N. (Bio)Electrochemical Ammonia Recovery: Progress and Perspectives. *Applied Microbiology and Biotechnology* **2018**, 102 (9), 3865–3878. <https://doi.org/10.1007/s00253-018-8888-6>.
- (9) Tarpeh, W. A.; Barazesh, J. M.; Cath, T. Y.; Nelson, K. L. Electrochemical Stripping to Recover Nitrogen from Source-Separated Urine. *Environmental Science and Technology* **2018**, 52 (3), 1453–1460. <https://doi.org/10.1021/acs.est.7b05488>.
- (10) Rodrigues, M.; Sleutels, T.; Kuntke, P.; Hoekstra, D.; ter Heijne, A.; Buisman, C. J. N.; Hamelers, H. V. M. Exploiting Donnan Dialysis to Enhance Ammonia Recovery in an Electrochemical System. *Chemical Engineering Journal* **2020**, 395 (April), 125143. <https://doi.org/10.1016/j.cej.2020.125143>.
- (11) van Linden, N.; Spanjers, H.; van Lier, J. B. Application of Dynamic Current Density for Increased Concentration Factors and Reduced Energy Consumption for Concentrating Ammonium by Electrodialysis. *Water Research* **2019**, 163, 114856. <https://doi.org/10.1016/j.watres.2019.114856>.
- (12) Kuntke, P.; Rodrigues, M.; Sleutels, T.; Saakes, M.; Hamelers, H. V. M.; Buisman, C. J. N. N. Energy-Efficient Ammonia Recovery in an Up-Scaled Hydrogen Gas Recycling Electrochemical System. *ACS Sustainable Chemistry & Engineering* **2018**, 6 (6), 7638–7644. <https://doi.org/10.1021/acssuschemeng.8b00457>.
- (13) Yang, K.; Qin, M. The Application of Cation Exchange Membranes in Electrochemical Systems for Ammonia Recovery from Wastewater. *Membranes (Basel)* **2021**, 11 (7), 494. <https://doi.org/10.3390/membranes11070494>.
- (14) Thompson Brewster, E.; Jermakka, J.; Freguia, S.; Batstone, D. J. Modelling Recovery of Ammonium from Urine by Electro-Concentration in a 3-Chamber Cell. *Water Research* **2017**, 124, 210–218. <https://doi.org/10.1016/j.watres.2017.07.043>.
- (15) Christiaens, M. E. R.; Udert, K. M.; Arends, J. B. A.; Huysman, S.; Vanhaecke, L.; McAdam, E.; Rabaey, K. Membrane Stripping Enables Effective Electrochemical Ammonia Recovery from Urine While Retaining Microorganisms and Micropollutants. *Water Research* **2019**, 150, 349–357. <https://doi.org/10.1016/j.watres.2018.11.072>.

- (16) de Valenca, J. C. Overlimiting Current Properties at Ion Exchange Membranes, University of Twente, Enschede, The Netherlands, 2017. <https://doi.org/10.3990/1.9789036543149>.
- (17) Desloover, J.; Abate Woldeyohannis, A.; Verstraete, W.; Boon, N.; Rabaey, K. Electrochemical Resource Recovery from Digestate to Prevent Ammonia Toxicity during Anaerobic Digestion. *Environmental Science and Technology* **2012**, 46 (21), 12209–12216. <https://doi.org/10.1021/es3028154>.

Appendix A

The dimensionless applied current (γ) and the total cation loading ratio (L_T - ratio between the applied current density and the amount that is added to the system in the form of ionic charge), are described below:

$$\gamma = \frac{I}{C_{T,z}} \frac{L_z}{D_{i,z}} \quad (\text{Equation S1})$$

$$L_T = \frac{I}{Q} \frac{A}{C_T} \quad (\text{Equation S2})$$

Where I is the molar current density ($\text{mol}/(\text{m}^2 \cdot \text{s})$), D_x is the ion diffusion coefficient in the z (m^2/s), z is the dimensionless distance where the ions move from anode to cathode, Q is influent flow (m^3/s), and A is the membrane area (m^2).

Appendix B

$$\alpha = \left(\frac{C_T}{X} \right) \left(\frac{L_m}{L_{bl}} \right) \left(\frac{D_{bl}}{D_m} \right) \quad (\text{Equation S3})$$

Where C_T is the total cation/anion concentration (mol/dm^3), X is the fixed charge for cation exchange membrane (mol/L), L_m is the membrane thickness (m), L_{bl} is the boundary layer thickness (m), and D_{bl} and D_m are the boundary layer and membrane diffusion coefficients, respectively (m^2/s).

Appendix C

Extrapolating the concentration at the anode compartment

The influent composition of the electrochemical system was assumed to be known, while the anolyte composition needs to be predicted as this changes as a result of the operation. Therefore, we used the composition of the influent as the basis to deduce the anolyte concentrations. To account for this distinction, we introduce a new factor (η):

$$\eta = \frac{C_T}{C_{T,in}} \quad (\text{Equation S4})$$

Where C_T is the total cation/anion concentration at the anode-boundary layer interface and $C_{T,in}$ is the total cation/anion concentration of the influent.

Appendix D

Cathode Balance (NH₃ transport/extraction)

To determine how much NH₃ diffuses “back” from the cathode to the anode, due to the concentration gradient between cathode and anode. In this model, we assumed a steady-state meaning a constant current applied and a constant NH₄⁺ transport from anode through the cation exchange membrane and through the gas permeable membrane at constant operation conditions. Furthermore, we consider such a high cathode pH that the ammonium concentration is zero. At the anode, we assumed a neutral or acidic pH such that the concentration of ammonia is zero. This way, the transport through the gas permeable membrane can be related to a current in the same way as the transport for the cation exchange membrane:

$$\gamma_{N,s} = -k_s f_{N,Lm} \quad (\text{Equation S5})$$

Where $\gamma_{N,s}$ is the equivalent current of the nitrogen (NH₃/NH₄⁺) transported through the gas permeable membrane, k_s is a diffusion constant for the gas permeable membrane and $f_{N,Lm}$ is the NH₄⁺ fraction at the cation exchange membrane and cathode interface (_{Lm}). Considering that no nitrogen accumulates in the cathode, the nitrogen balance in the cathode for a steady state is:

$$t_{NH4+\gamma} + \gamma_{N,m} + \gamma_{N,s} = 0 \quad (\text{Equation S6})$$

Where the first term represents the nitrogen removed from the influent and transported through the CEM, the second term represents the nitrogen that moves back to the anode through the cation exchange membrane and the third term represents the nitrogen transported through the LLMC(gas permeable membrane). The ammonia transport from cathode to the anode is only concentration driven, as the NH₃ concentration in the anode is zero and it can be written as:

$$\gamma_{N,m} = k_m (-f_{N,Lm}) \quad (\text{Equation S7})$$

Combining these relationships we can establish how much nitrogen is lost from the cathode to the anode:

$$f_{N,Lm} = \frac{t_{NH4+\gamma}}{k_m + k_s} \quad (\text{Equation S8})$$

This concentration determines how much of the NH_3 is transported back to the anode over the CEM. This means that the N transport can be written as:

$$\gamma_{N,m} = \frac{k_m}{k_m + k_s} t_{\text{NH}_4^+} \gamma = -\beta t_{\text{NH}_4^+} \gamma \quad (\text{Equation S9})$$

This shows if we use a well-designed LLMC unit, the nitrogen transport across the LLMC is basically equal to the ammonium transport over the CEM. Moreover, we assume that this NH_3 transport does not interfere with the ion transport. Instead, the effect of ammonia diffusion will be accounted for via the balance equation of the buffer at the anode compartment as β .

Appendix E

Anode Balance - the buffer effect

When the buffer is present, the protons concentration is zero and increases with current until the buffer is depleted. Moreover, the anode concentrations were scaled to fractions with the total concentration in the anode by the factor η described in Eq. S4. From the buffer balance (Equation 2), we know buffer remains present for the following condition:

$$L_T \leq \frac{f_{b,in}}{1 - \beta t_{\text{NH}_4^+}} \quad (\text{Equation S10})$$

We also know that the total concentration of anions consists of the non-buffering anions (Cl^-) that remain in solution (no transport, no conversion) and the buffer that can be converted. The total anolyte concentration is thus determined by this non-reactive part ($1 - f_{b,in}$) and the remaining buffer:

$$\eta = (1 - f_{b,in}) + f_b \eta = 1 - L_T (1 - \beta t_{\text{NH}_4^+}) \quad (\text{Equation S11})$$

Using Eq. S10 and S11, we can get relationships for the buffer total concentration in the anode total concentration:

$$\eta = 1 - (1 - \beta t_{\text{NH}_4^+}) L_T \text{ for } L_T \leq \frac{f_{b,in}}{1 - \beta t_{\text{NH}_4^+}} \quad (\text{Equation S12a})$$

$$\eta = 1 - f_{b,in} \text{ for } L_T \geq \frac{f_{b,in}}{1 - \beta t_{\text{NH}_4^+}} \quad (\text{Equation S12b})$$

Where the first equation S12a defines the buffered case and S12b the non-buffered case.

The balance of ammonium-nitrogen can then be described as:

$$\eta f_N = f_{N,in} - L_T(1 - \beta)t_{NH4+} \quad (\text{Equation S13})$$

Where the total ammonium-nitrogen concentration ($f_{N,in}$) includes the fraction removed from the anode ($\eta \cdot f_N$) and the fraction returning from the cathode ($L_T(1-\beta)t_{NH4+}$)

In the same way, we can write the balance of protons and distinguish the buffered and non-buffered cases:

$$\eta f_H = \begin{cases} 0 & , \quad L_T \leq \frac{f_{b,in}}{1-\beta t_{NH4+}} \\ (f_{H,in} - f_{b,in}) + L_T(1 - t_H - \beta t_{NH4+}), & L_T \geq \frac{f_{b,in}}{1-\beta t_{NH4+}} \end{cases} \quad (\text{Equation S14})$$

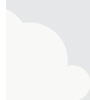
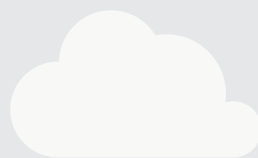
Where the fraction of protons (f_H) in the anode in the buffered case is zero. When the buffer is depleted at the anode, the proton fraction equals the fraction of protons neutralized by the buffer ($f_{H,in} - f_{b,in}$) plus the additional fraction produced at the anode (current dependent). Mind that if $f_{H,in} > 0$, that $f_{b,in} = 0$ and vice versa, as we assume that the (anionic) buffer directly binds to the proton.

Appendix F

Table S1. Studies applying electrochemical ammonia recovery and the respective current and current density, total cation loading ratio, ammonium-nitrogen fraction, buffer fraction and removal efficiency. The dimensionless current and total cation loading ratio were estimated considering a fixed boundary layer-membrane thickness (0.0006m).

Study	wastewater	i (A/m ²)	Y	L _T	f _N	f _b	Removal
(Desloover et al., 2012)	Digestate (synthetic)	10	0,14	0,003	0,33	0	0,19
	Digestate (synthetic)	30	0,43	0,31	0,33	0	0,41
	Digestate	10	0,14	0,26	0,33	n/a ^(COD)	0,38
	Digestate	20	0,29	0,52	0,33	n/a ^(COD)	0,58
	Digestate	30	0,43	0,78	0,33	n/a ^(COD)	0,63
(Luther et al., 2015)	Urine (synthetic)	30	0,22	0,6	0,82	0,41	0,53
	Urine (synthetic)	50	0,37	1	0,82	0,41	0,81
	Urine	40	0,3	1,09	0,82	0,41	0,75
(Gildemyn et al., 2015)	synthetic	30	1,25	0,07	0,08	n/a ^(PO₄⁻)	0,41
(Kuntke et al., 2017)	urine (after P recovery)	10	0,18	0,83	0,64	0,81	0,82
	urine (after P recovery)	20	0,35	0,77	0,64	0,81	0,73
	urine (after P recovery)	50	0,88	0,83	0,64	0,81	0,73
(Rodríguez Arredondo et al., 2017)	urine (after P recovery)	20	0,29	1,82	0,67	0,51	0,89
	urine (after P recovery)	50	0,74	4,35	0,67	0,51	0,92
	urine (after P recovery)	50	0,74	0,79	0,67	0,51	0,63
(Christiaens et al., 2017)	urine	20	0,22	0,32	0,65	0,47	0,86
	urine	20	0,22	0,32	0,65	0,47	0,68
(Christiaens et al., 2019)	urine	20	0,22	0,36	0,72	0,01 ^(PO₄⁻)	0,49

8



Chapter 8

General discussion



The work described in this thesis provides scientific insight into the development of electrochemical systems for ammonia recovery from concentrated wastewater streams. Following the insights given in the previous chapters, the technical limitations and possible future research for electrochemical ammonia recovery are summarized in this chapter. Lastly, a general discussion about the implementation of ammonia recovery is presented.

1. Thesis outcomes and future research

a. ES versus other technologies

The acceptance of new technologies such as ES is strongly dependent on their economic competitiveness. Table 1 compares the ammonia removal efficiency, energy consumption, technological maturity and capacity, cost and (by-)products (fertilizers and emissions) between ES, Haber-Bosch (HB) combined with ANAMMOX, and thermal stripping with acid adsorption (Strip.). Even though there are many nitrogen recovery technologies in development, thermal stripping with acid adsorption was selected as nitrogen recovery technology as it was already demonstrated at pilot-scale and produces the same product as ES ¹. Recovery efficiency was not included in the comparison presented in Table 1 as this parameter is often identical to the removal efficiency ^{1,2}.

Apart from economic feasibility, ANAMMOX has been used as nitrogen removal technology over the last two decades, and it is included in many WWTPs. Besides, ANAMMOX reactors have an estimated longevity of around 20 years ⁶. Based on Table 1, it is farfetched to assume that ES will fully replace the combination of HB and ANAMMOX ⁷⁻¹⁰. For ES to become economically feasible, the energy price has to rise. Nevertheless, ES can decrease the current dependency on HB and ANAMMOX. ES allows for an adjustable ammonia removal efficiency at a lower energy consumption (considering production and removal energy), forming a product ready to be applied as fertilizer ¹¹. Besides, the application of ES can be extended from our centralized WWTPs in source separated sanitation settings. Lastly, both ES and stripping are more environmental friendly when compared to HB+ANAMMOX as these do not emit N₂O.

Regarding the required energy (see Table 1), ES has an immense advantage compared to thermal stripping. Moreover, high removals were often not reported at pilot scale for thermal stripping (>80%), and the energy consumption of this technology needs to be considerably improved.

Although deepening knowledge by means of scientific research is crucial, recent literature reviews have acknowledged the most import step towards the implementation of ES to be more pilot testing and stakeholders' acceptance (including citizens, politicians and farmers) ^{1,12,13}.

Table 1. Comparison regarding Energy consumption, maturity, and nitrogen price between ES and HB + ANAMMOX and vacuum thermal stripping (Strip.) for removals efficiencies above and below 80%.

Process	HB + ANAMMOX	Strip.	ES	
Nitrogen removal efficiency	<80% ⁽²⁾	< 80%	> 80%	< 80% > 80%
Energy (kJ/g _N)	50 - 58 ⁽³⁾	0 - 105	100 - 200	4.7 - 13.3 ⁽⁵⁾ 22 - 46 ⁽⁴⁾
TRL	9	5-7	4-5	5-8
Maturity ⁽¹⁾	+++	++	+ / ++	++ ++
Cost (€/kg _N)	0.8 ⁽⁴⁾	1.9 - 3.2		2.65 ⁽⁶⁾
Product	no product (NH ₃ →N ₂)	Ammonium sulphate		Ammonium sulphate
Chemical consumption	CH ₄ or H ₂ , (might require buffer and substrate dosing)	H ₂ SO ₄ , NaOH, CaOH		H ₂ SO ₄ , NaOH, HCl
GHG Emissions	CO ₂ , N ₂ O	CO ₂		CO ₂
Reference	3	3	4	Chapter 5

n/a – not applicable

+++ - full scale, ++ - pilot scale, + - lab-scale

Operational parameters such as temperature, pH, nitrogen concentration, and carbon concentration influence significantly the stability of a high nitrogen removal rate in ANAMMOX ⁵.

Energy consumption of both HB and ANAMMOX, as ANAMMOX does not allow nitrogen recovery. Individually, HB consumes ~37kJ/g_N and ANAMMOX consumes ~16kJ/g_N.

Cost uniquely for ANAMMOX.

The energy consumption was during intermittent operation (on/off current).

This value was estimated considering the costliest stand out items: 1) Cost of stripping acid (sulfuric) The acid choice has a direct effect on the composition of the product. If a different acid is used (for example, hydrochloric acid or nitric acid), this results in a different price as well as a different product. 2) Cost of electricity ED stacks (Stack PSUs): Energy consumption is not expected to decrease much further, as the experiments aimed to optimize the specific stack. The amount of energy required is, strongly dependent on the concentration of nitrogen in the rejection water and is also strongly related to the desired removal percentage. 3) Depreciation of ED membranes (over 10 years). 4) Cost of electric pumps: Current lab practice was used to calculate the pump capacities.

b. Electrochemical ammonia recovery: finding the operational “sweet spot”

A 100% ammonium removal efficiency is almost never reported ^{2,14}. Even, Donnan dialysis only offered limited improvements when it comes to ammonium removal efficiency (Chapter 2 and 3). Furthermore, the performance got further diminished once the system membrane area was increased by stacking (Chapter 5).

The transport of cations and anions through ion exchange membranes was often characterized in electrodialysis ¹⁵. However, during nitrogen recovery, as cation and gas can coexist in solution, its behavior transcends the normal regimes and makes the process more challenging and is therefore an interesting study object. Electrochemical nitrogen recovery plays with the pH peculiarity between the equilibrium of the NH_4^+ and the NH_3 (gas form).

Studies have reported NH_3 as a proton shuttle or claimed ammonia “back” diffusion as the main mechanism responsible for the low ammonium removal ^{16–18}. Chapter 7 demonstrates how increasing the current contributes to the transport of different ionic species over the cation exchange membrane (CEM). The performance of electrochemical systems is therefore dependent on current, loading, and buffer capacity. Overall, high removal efficiency requires more energy ^{2,19}. Four transport regimes were outlined regarding current and total cation loading ratio, where (i) only NH_4^+ is transported, (ii) NH_4^+ and Na^+ are transported, (iii) NH_4^+ and H^+ are transported, or (iv) all cations are transported over the CEM. This allowed us to understand: i) why other species compete with ammonium over the CEM, although ammonium is the most concentrated specie; ii) why the nitrogen removal is limited (80%) or energy-intensive; and iii) how the ratio of the species present influence the transport. Therefore, when implementing ES for ammonia recovery, it is necessary to evaluate the characteristics of the wastewater supplied to the system, the desired removal, and scale (treatment capacity current applied). Additionally, different wastewaters contain different buffers (i.e., organic species) in various strength. As demonstrated in Chapter 7, the buffer capacity may present an advantage to increase the current efficiency. The addition of the formed alkaline concentrate back to the influent stream during electrochemical ammonia recovery should be further assessed to understand how this recirculation influences the performance of the system, particularly the current efficiency.

At first sight, the results reported in this thesis indicated that ES would be more suitable for processes in which a full ammonia removal is not desired. As the wastewater is treated, it becomes less concentrated and, consequently, less conductive. This was also demonstrated to have an influence on the energy input

of the system as its resistance changes (ohmic losses increase). Furthermore, the combination with Donnan ('intermittent') mode can decrease the required energy, but not leading to a complete ammonia extraction¹⁹. However, when a high ammonia removal efficiency is strictly necessary, an option is to use a multistage electrochemical systems design. Here, the system could be designed to include two cells (with different sizes), where the first one would remove 80% at a certain energy input (comparable to ANAMMOX, for example) and the second one would be designed to remove the remaining nitrogen at a lowest energy possible input. A multistage was previously presented as an effective solution for desalination and reverse electrodialysis^{20–22}. Therefore, more research should be conducted to evaluate a multistage design as a viable option for ammonia recovery using ES.

c. Inorganic scaling: a bottleneck of electrochemical nitrogen recovery

As demonstrated in Chapters 6 and 7, ammonium was rarely the only specie transported over the cation exchange membrane. This means other cations such as magnesium and calcium present in urine or digestate also accumulate in the concentrate stream. The high pH of this solution will lead to the formation of inorganic precipitates as shown in Figure 1.

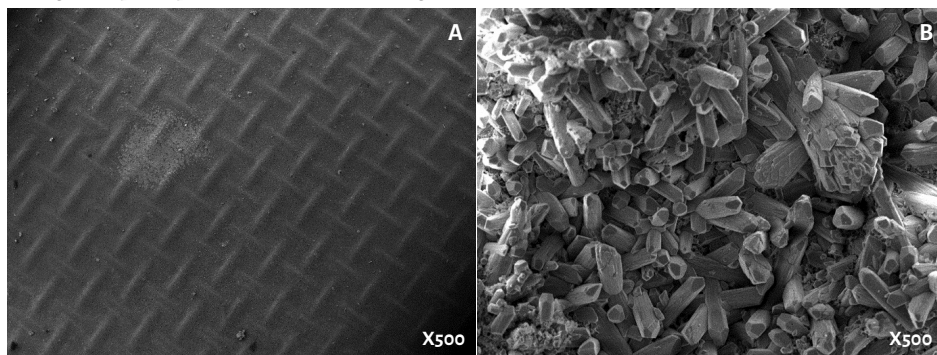


Figure 1. (A) Clean cation exchange membrane (feed side). The small residues were mostly bacteria/organic matter (B) Calcium crystals on the concentrate side of the cation exchange membrane.

Inorganic scaling is a major disadvantage and it is preventing the implementation of different membrane processes, including electrochemical systems^{23–25}. When calcium and magnesium are present in solution, these two cations will be unavoidably transported over the CEM^{23,24}. The alkaline pH of the concentrate solution, necessary for NH_3 extraction, also provides the near perfect conditions for calcium and magnesium salts to precipitate in the form of e.g. CaCO_3 , $\text{Mg}(\text{OH})_2$, $\text{CaMg}(\text{CO}_3)_2$. Donnan dialysis contributed to mitigate this phenomena but was insufficient to completely prevent precipitation²⁴. In Chapter 5, inorganic scaling was addressed with a in situ cleaning strategy using hydrochloric acid and air pressure. The ion

exchange membranes were fully recovered after each cleaning. Nevertheless, this created an additional waste stream that needed to be adequately treated.

Possible pre-treatments should be further investigated in combination with electrochemical nitrogen recovery. This could even lead to the production of other products of interest, such as calcium phosphate ^{26,27}. Furthermore, the pre-treatment should also reduce or prevent the need of cleaning in situ strategy and, therefore, contribute for a chemical-free technology while maintaining the energy consumption.

d. Commodities and consumables of electrochemical nitrogen recovery

d.1. Recovered products

ES recovers nitrogen products. Concentrated ammonium sulphate or ammonium nitrate solutions were previously produced and used for crop growth ^{28,29}. Yet, they are not applied on farmland as fertilizer. Ammonium sulphate is often not the most appealing nitrogen fertilizer, as crops mostly require sulphur during the germination phase, and its market size is smaller than for example urea ¹. Ammonium sulphate is an unavoidable product of other industries; therefore, the market is already saturated, and its commercialization occurs at a reduced cost. Although ammonium sulphate and ammonium nitrate application as fertilizers is quite extensively studied, a few differences can be identified between commercial and recovered fertilizers ¹¹. The recovered fertilizers are less concentrated and often acidic ^{3,28}. This, however, does not represent an issue for crop growth ^{11,29}.

Within the European directive 2003/2003, the admission for fertilizer must include a product with >15 % nitrogen content, produced by an industrial process, free of impurities and organic nutrients of vegetable or animal origin ³. Future research should focus on establishing adequate uses for the generated streams (such as ammonium sulphate or ammonium nitrate) during electrochemical nitrogen recovery. For example, vacuum pumps and gas permeable membranes can allow the recovery of ammonia water instead of recovering ammonium sulphate or nitrate. If the use of recovered nitrogen is proven to be economically unappealing and unsafe for consumers/farmers, other option could be using recovered ammonia as an energy storage molecule ^{17,30,31}. Even though the lower energy density, concentrated ammonia is more easily transported than hydrogen.

Other relevant wastewater constituents include potassium and phosphorus. Potassium could also be concentrated through cation exchange membranes. A part of the phosphorus could be recovered as phosphate through anion exchange membranes or via a pre-precipitation step²⁷. The challenge remains to separate these species from

others in wastewater with the same charge. The implementation of gas permeable membranes only allows the separation of NH_3 . Therefore, two research questions could be further explored: i) can ES be extended to other nutrients recovery (essential nutrients PKN recovery); ii) are these fertilizers possible to be further used.

d.2. Chemical usage

ES excels for being a chemical-free technology ^{32,33}. Nevertheless, as it is currently being employed, the operation of ES must consider the addition of two acidic solutions: hydrochloric acid for inorganic scaling removal (Chapter 5) and sulfuric acid for further ammonia separation over gas permeable membranes. As the production of pure sulfuric acid is also dependent on natural gas and petroleum refining ³⁴, its replacement is crucial. Other configurations including ES with cell triplets or electrodialysis, allow the production of both an acid and an alkaline stream ^{35,36}. However, as all cations and anions in wastewater are further concentrated, the formation of consumable products such as fertilizers is arguable ³⁷. The formed streams may include Cl^- and Na^+ , not ideal for soil application ^{38,39}. Furthermore, AEMs are prone to micropollutants transport, posing a risk to the safety of the acidic stream to be applied in agriculture or protein growth ⁴⁰.

Aside reactive nitrogen, ES can also produce H_2 and O_2 ⁴¹. So far, the electrode production hydrogen and oxygen in electrochemical systems has been neglected. But as all energy should be conserved, their production and re-use should be further characterized.

Lastly, during electrochemical nitrogen recovery, often an acidic effluent is produced. Consequently, if the effluent of the electrochemical cell is too acidic, recycling this stream into biological reactors for further (nutrient) treatment or discharge is more challenging. The presence of buffer in the ES plays a crucial role in keeping the pH of the effluent less acid. Besides, according to the model developed in chapter 7, a buffer regulation could also improve the energy efficiency of the process. This alternative should be further demonstrated experimentally.

This thesis focused mostly on concentrated wastewater streams (between 800 mg/L – 5000mg/L of ammonia). This nitrogen concentration range includes streams such as urine, black water and digestate (supplied in the experiments presented in this thesis), as well as manure and organic waste ^{3,42}. It was predicted ES has potential to treat streams between 60mg/L to 8000mg/L ¹⁰. Therefore, the application of ES is suitable for a wide range of other wastewater streams.

2. Nitrogen recovery in the center of attention of environment challenges

The Planetary boundaries concept, was first evaluated in 2009^{43,44}. Here, the nitrogen cycle was already reported to be significantly affected by human influence and way beyond a safe planetary bound. Nevertheless, little has changed regarding nitrogen recovery over the last decade. Besides the high amounts of energy required to handle the anthropogenic nitrogen cycle, billions of euros are spent to produce and to later remove and convert a small part of the nitrogen back to the atmosphere. The larger part of reactive nitrogen is lost in the environment.

Sustainable development and Net Zero emission predictions forecast that the need of ammonia will increase at least 25% by 2050 (Figure 2). Furthermore, the use of ammonia will likely expand from fertilizers and chemical industry/consumption to power generation and maritime fuel, see Figure 2.

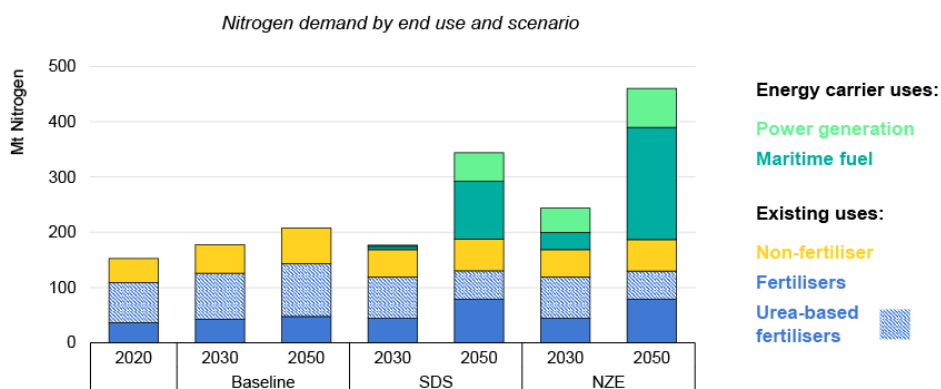


Figure 2. Ammonia demand for fertilizers and other existing uses is predicted to grow by 25% by 2050 in the Sustainable Development (SDS), and Net Zero Emissions (NZE) by 2050 scenarios. Adapted from⁴⁵.

In Chapter 1, two options can be taken for sustainable ammonia production: (i) replace the hydrogen/energy by renewable source or (ii) recover nitrogen^{30,46,47}. Several projects have been making efforts in changing the hydrogen source, to produce ammonia in a renewable, sustainable and carbon-free way^{48,49}. This could also be achieved through electrochemical systems⁵⁰. But one does not come at the expense of the other. As far as treatment is needed in our WWTPs, we should implement recovery technologies as soon as possible. Additionally, as only ~16% of the reactive nitrogen reaches the WWTPs, from which only 15-20% is actually found in reject water (digestate), nitrogen recovery needs to be expanded to much larger nitrogen-rich streams such as manure^{3,51}.

Some of the most important developments regarding nitrogen include: i) the Haber-Bosch development, due to the need of ammonia for both fertilizers and explosives when Germany was fighting World War I, ii) the nitrogen crisis in the Netherlands/Germany during 2018 due to stringent legislation forbidding more activated nitrogen compounds emissions; iii) the (European) natural gas supply is currently under the threat, limiting the feasibility to produce nitrogen from the Haber Bosch process, since Russia invaded Ukraine in February 2022. Thus, it seems with war and strong legislation a strong impulse in recovery or recycling will be given.

3. Concluding remarks

Unlike phosphate, nitrogen is not scarce, and a nitrogen crisis is more difficult to define. However, the nitrogen crisis can be seen from the N_2O emissions point of view, the energy consumption, eutrophication of natural areas giving health problems or water contamination (algae bloom). These points could all be tackled to a certain extent by implementing electrochemical nitrogen recovery. As up-scaling is now demonstrated, ES has potential to be almost immediately included both in our centralized and decentralized WWTPs. Further model development could predict the optimal operation parameters to achieve the required performance/cost and a more efficient energy use. Simultaneously, the products generated by ES must be further characterized and positively presented to stakeholders (incl. society at large).

If we look at the Paris agreement ⁵² established in 2015, more steps need to be taken in order to save our planet. Most countries should recognize how environmental issues do not respect borders. It is all a shared obligation not only to implement directives to protect the environment, but also to support each other financially and create infrastructure to reduce emissions. To manage resources as a whole rather than individually is more sustainable. “We need a global science-policy body on chemicals and waste” ^{53,54}. The nitrogen crisis is no exception, as polluted aquatic ecosystems and nitrous emissions to the atmosphere are global issues. Without efficient and effective nitrogen recovery, mankind will often find itself on an energy/pollution pickle.

References

- (1) Beckinghausen, A.; Odlare, M.; Thorin, E.; Schwede, S. From Removal to Recovery: An Evaluation of Nitrogen Recovery Techniques from Wastewater. *Applied Energy* **2020**, *263* (February), 114616. <https://doi.org/10.1016/j.apenergy.2020.114616>.
- (2) Kuntke, P.; Sleutels, T. H. J. A.; Rodríguez Arredondo, M.; Georg, S.; Barbosa, S. G.; ter Heijne, A.; Hamelers, H. V. M.; Buisman, C. J. N. (Bio)Electrochemical Ammonia Recovery: Progress and Perspectives. *Applied Microbiology and Biotechnology* **2018**, *102* (9), 3865–3878. <https://doi.org/10.1007/s00253-018-8888-6>.
- (3) van Eekert, M.; Weijma, J.; Verdoes, N.; de Buissonjé, F.; Reitsma, B.; van den Bulk, J.; van Gastel, J. On Innovative Nitrogen Recovery. **2012**, 1–56.
- (4) Ukwuani, A. T.; Tao, W. Developing a Vacuum Thermal Stripping – Acid Absorption Process for Ammonia Recovery from Anaerobic Digester Effluent. *Water Research* **2016**, *106*, 108–115. <https://doi.org/10.1016/j.watres.2016.09.054>.
- (5) Cho, S.; Kambey, C.; Nguyen, V. K. Performance of Anammox Processes for Wastewater Treatment: A Critical Review on Effects of Operational Conditions and Environmental Stresses. *Water (Switzerland)* **2020**, *12* (1). <https://doi.org/10.3390/w12010020>.
- (6) Ahn, Y. H. Sustainable Nitrogen Elimination Biotechnologies: A Review. *Process Biochemistry* **2006**, *41* (8), 1709–1721. <https://doi.org/10.1016/j.procbio.2006.03.033>.
- (7) Datawheel. *Nitrogenous Fertilizers*. <https://oec.world/en/profile/hs92/nitrogenous-fertilizers>.
- (8) NationMaster. *Top Countries in Nitrogen Fertilizer Production*. <https://www.nationmaster.com/nmx/ranking/nitrogen-fertilizer-production>.
- (9) Institute for Industrial Productivity. Ammonia. **2011**.
- (10) van der Hoek, J. P.; Duijff, R.; Reinstra, O. Nitrogen Recovery from Wastewater: Possibilities, Competition with Other Resources, and Adaptation Pathways. *Sustainability (Switzerland)* **2018**, *10* (12). <https://doi.org/10.3390/su10124605>.
- (11) Rodrigues, M.; Lund, R. J.; ter Heijne, A.; Sleutels, T.; Buisman, C. J. N.; Kuntke, P. Application of Ammonium Fertilizers Recovered by an Electrochemical System. *Resources, Conservation and Recycling* **2022**, *181*, 106225. <https://doi.org/10.1016/j.resconrec.2022.106225>.
- (12) Radjenovic, J.; Sedlak, D. L. Challenges and Opportunities for Electrochemical Processes as Next-Generation Technologies for the Treatment of Contaminated Water. *Environmental Science and Technology* **2015**, *49* (19), 11292–11302. <https://doi.org/10.1021/acs.est.5b02414>.
- (13) Ye, Y.; Ngo, H. H.; Guo, W.; Liu, Y.; Chang, S. W.; Nguyen, D. D.; Liang, H.; Wang, J. A Critical Review on Ammonium Recovery from Wastewater for Sustainable Wastewater Management. *Bioresource Technology* **2018**, *268* (July), 749–758. <https://doi.org/10.1016/j.biortech.2018.07.111>.
- (14) Liu, Y.; Deng, Y. Y.; Zhang, Q.; Liu, H. Overview of Recent Developments of Resource Recovery from Wastewater via Electrochemistry-Based Technologies. *Science of the Total Environment* **2021**, *757*, 143901. <https://doi.org/10.1016/j.scitotenv.2020.143901>.
- (15) Strathmann, H. Electrodialysis, a Mature Technology with a Multitude of New Applications. *Desalination* **2010**, *264* (3), 268–288. <https://doi.org/10.1016/j.desal.2010.04.069>.
- (16) Thompson Brewster, E.; Jermakka, J.; Freguia, S.; Batstone, D. J. Modelling Recovery of Ammonium from Urine by Electro-Concentration in a 3-Chamber Cell. *Water Research* **2017**, *124*, 210–218. <https://doi.org/10.1016/j.watres.2017.07.043>.

- (17) van Linden, N.; Spanjers, H.; van Lier, J. B. Application of Dynamic Current Density for Increased Concentration Factors and Reduced Energy Consumption for Concentrating Ammonium by Electrodialysis. *Water Research* **2019**, *163*, 114856. <https://doi.org/10.1016/j.watres.2019.114856>.
- (18) Cord-Ruwisch, R.; Law, Y.; Cheng, K. Y. Ammonium as a Sustainable Proton Shuttle in Bioelectrochemical Systems. *Bioresource Technology* **2011**, *102* (20), 9691–9696. <https://doi.org/10.1016/j.biortech.2011.07.100>.
- (19) Rodrigues, M.; Sleutels, T.; Kuntke, P.; Hoekstra, D.; ter Heijne, A.; Buisman, C. J. N.; Hamelers, H. V. M. Exploiting Donnan Dialysis to Enhance Ammonia Recovery in an Electrochemical System. *Chemical Engineering Journal* **2020**, *395* (April), 125143. <https://doi.org/10.1016/j.cej.2020.125143>.
- (20) Veerman, J.; Saakes, M.; Metz, S. J.; Harmsen, G. J. Reverse Electrodialysis: Performance of a Stack with 50 Cells on the Mixing of Sea and River Water. *Journal of Membrane Science* **2009**, *327* (1–2), 136–144. <https://doi.org/10.1016/j.memsci.2008.11.015>.
- (21) Simões, C.; Pintossi, D.; Saakes, M.; Brilman, W. Optimizing Multistage Reverse Electrodialysis for Enhanced Energy Recovery from River Water and Seawater: Experimental and Modeling Investigation. *Advances in Applied Energy* **2021**, *2*, 100023. <https://doi.org/10.1016/j.adapen.2021.100023>.
- (22) Doornbusch, G.; van der Wal, M.; Tedesco, M.; Post, J.; Nijmeijer, K.; Borneman, Z. Multistage Electrodialysis for Desalination of Natural Seawater. *Desalination* **2021**, *505*, 114973. <https://doi.org/10.1016/j.desal.2021.114973>.
- (23) Thompson Brewster, E.; Ward, A. J.; Mehta, C. M.; Radjenovic, J.; Batstone, D. J. Predicting Scale Formation during Electrodialytic Nutrient Recovery. *Water Research* **2017**, *110*, 202–210. <https://doi.org/10.1016/j.watres.2016.11.063>.
- (24) Rodrigues, M.; Paradkar, A.; Sleutels, T.; Heijne, A.; Buisman, C. J. N.; Hamelers, H. V. M.; Kuntke, P.; Donnan Dialysis for Scaling Mitigation from during Complex Electrochemical Wastewater Ammonium Recovery. *Water Research* **2021**, 117260. <https://doi.org/10.1016/j.watres.2021.117260>.
- (25) Ping, Q.; Cohen, B.; Dosoretz, C.; He, Z. Long-Term Investigation of Fouling of Cation and Anion Exchange Membranes in Microbial Desalination Cells. *Desalination* **2013**, *325*, 48–55. <https://doi.org/10.1016/j.desal.2013.06.025>.
- (26) Rathinam, K.; Oren, Y.; Petry, W.; Schwahn, D.; Kashner, R. Calcium Phosphate Scaling during Wastewater Desalination on Oligoamide Surfaces Mimicking Reverse Osmosis and Nanofiltration Membranes. *Water Research* **2018**, *128*, 217–225. <https://doi.org/10.1016/j.watres.2017.10.055>.
- (27) Lei, Y.; Du, M.; Kuntke, P.; Saakes, M.; van der Weijden, R.; Buisman, C. J. N. Energy Efficient Phosphorus Recovery by Microbial Electrolysis Cell Induced Calcium Phosphate Precipitation. *ACS Sustainable Chemistry & Engineering* **2019**, *7* (9), 8860–8867. <https://doi.org/10.1021/acssuschemeng.9b00867>.
- (28) Rodrigues, M.; Lund, R. J.; ter Heijne, A.; Sleutels, T.; Buisman, C. J. N.; Kuntke, P. Application of Ammonium Fertilizers Recovered by an Electrochemical System. *Resources, Conservation and Recycling* **2022**, *181*, 106225. <https://doi.org/10.1016/j.resconrec.2022.106225>.
- (29) Sosulski, T.; Szara, E.; Adam, W.; Sulewski, P.; Szyma, M.; Szymanska, M.; Sosulski, T.; Szara, E.; Was, A.; Sulewski, P.; van Pruissen, G. W. P.; Cornelissen, R. L. Ammonium Sulphate from a Bio-Refinery System as a Fertilizer – Agronomic and Economic Effectiveness. *Energies (Basel)* **2019**, *12* (24). <https://doi.org/10.3390/en12244721>.
- (30) Smith, C.; Hill, A. K.; Torrente-Murciano, L. Current and Future Role of Haber-Bosch Ammonia in a Carbon-Free Energy Landscape. *Energy and Environmental Science* **2020**, *13* (2), 331–344. <https://doi.org/10.1039/c9ee02873k>.
- (31) Giddey, S.; Badwal, S. P. S.; Kulkarni, A. Review of Electrochemical Ammonia Production Technologies and Materials. *International Journal of Hydrogen Energy*. Elsevier Ltd 2013, pp 14576–14594. <https://doi.org/10.1016/j.ijhydene.2013.09.054>.

- (32) Yan, H.; Wu, L.; Wang, Y.; Shehzad, M. A.; Xu, T. Ammonia Capture by Water Splitting and Hollow Fiber Extraction. *Chemical Engineering Science* **2018**, 192, 211–217. <https://doi.org/10.1016/j.ces.2018.07.040>.
- (33) Liu, Y.; Qin, M.; Luo, S.; He, Z.; Qiao, R. Understanding Ammonium Transport in Bioelectrochemical Systems towards Its Recovery. *Scientific Reports* **2016**, 6 (December 2015), 1–10. <https://doi.org/10.1038/srep22547>.
- (34) Matt King, Michael Moats, W. G. D. *Sulfuric Acid Manufacture: Analysis, Control and Optimization*, Second.; Elsevier, Ed.; Elsevier Ltd., 2013.
- (35) van Linden, N.; Bandinu, G. L.; Vermaas, D. A.; Spanjers, H.; van Lier, J. B. Bipolar Membrane Electrodialysis for Energetically Competitive Ammonium Removal and Dissolved Ammonia Production. *Journal of Cleaner Production* **2020**, 259, 120788. <https://doi.org/10.1016/j.jclepro.2020.120788>.
- (36) Pärnamäe, R.; Mareev, S.; Nikonenko, V.; Melnikov, S.; Sheldeshov, N.; Zabolotskii, V.; Hamelers, H. V. M.; Tedesco, M. Bipolar Membranes: A Review on Principles, Latest Developments, and Applications. *Journal of Membrane Science* **2021**, 617. <https://doi.org/10.1016/j.memsci.2020.118538>.
- (37) Christiaens, M. E. R.; Gildemyn, S.; Matassa, S.; Ysebaert, T.; de Vrieze, J.; Rabaey, K. Electrochemical Ammonia Recovery from Source-Separated Urine for Microbial Protein Production. *Environmental Science & Technology* **2017**, 51 (22), 13143–13150. <https://doi.org/10.1021/acs.est.7b02819>.
- (38) Li, X. Z.; Zhao, Q. L. Recovery of Ammonium-Nitrogen from Landfill Leachate as a Multi-Nutrient Fertilizer. *Ecological Engineering* **2003**, 20 (2), 171–181. [https://doi.org/10.1016/S0925-8574\(03\)00012-0](https://doi.org/10.1016/S0925-8574(03)00012-0).
- (39) Maurer, M.; Schwegler, P.; Larsen, T. A. Nutrients in Urine: Energetic Aspects of Removal and Recovery. *Water Science and Technology* **2003**, 48 (1), 37–46. <https://doi.org/10.1017/S000748530002229X>.
- (40) Roman, M.; van Dijk, L. H.; Gutierrez, L.; Vanoppen, M.; Post, J. W.; Wols, B. A.; Cornelissen, E. R.; Verliefde, A. R. D. Key Physicochemical Characteristics Governing Organic Micropollutant Adsorption and Transport in Ion-Exchange Membranes during Reverse Electrodialysis. *Desalination* **2019**, 468 (July), 114084. <https://doi.org/10.1016/j.desal.2019.114084>.
- (41) Kuntke, P.; Rodríguez Arredondo, M.; Widyakristi, L.; ter Heijne, A.; Sleutels, T. H. J. A. J. A.; Hamelers, H. V. M.; Buisman, C. J. N. N. Hydrogen Gas Recycling for Energy Efficient Ammonia Recovery in Electrochemical Systems. *Environmental Science & Technology* **2017**, 51 (5), 3110–3116. <https://doi.org/10.1021/acs.est.6b06097>.
- (42) Provolto, G.; Perazzolo, F.; Mattachini, G.; Finzi, A.; Naldi, E.; Riva, E. Nitrogen Removal from Digested Slurries Using a Simplified Ammonia Stripping Technique. *Waste Management* **2017**, 69 (5), 154–161. <https://doi.org/10.1016/j.wasman.2017.07.047>.
- (43) Li, M.; Wiedmann, T.; Fang, K.; Hadjikakou, M. The Role of Planetary Boundaries in Assessing Absolute Environmental Sustainability across Scales. *Environment International* **2021**, 152. <https://doi.org/10.1016/j.envint.2021.106475>.
- (44) Rockström, J.; Steffen, W.; Noone, K.; Persson, Å.; Chapin, F. S.; Lambin, E. F.; Lenton, T. M.; Scheffer, M.; Folke, C.; Schellnhuber, H. J.; Nykvist, B.; de Wit, C. A.; Hughes, T.; van der Leeuw, S.; Rodhe, H.; Sörlin, S.; Snyder, P. K.; Costanza, R.; Svedin, U.; Falkenmark, M.; Karlberg, L.; Corell, R. W.; Fabry, V. J.; Hansen, J.; Walker, B.; Liverman, D.; Richardson, K.; Crutzen, P.; Foley, J. A. A Safe Operating Space for Humanity. *Nature* **2009**, 461 (7263), 472–475. <https://doi.org/10.1038/461472a>.
- (45) Kevin Rouwenhorst. *IEA publishes Ammonia Technology Roadmap*. <https://www.ammoniaenergy.org/articles/iea-publishes-ammonia-technology-roadmap/>.
- (46) Gilbert, P.; Thornley, P. Energy and Carbon Balance of Ammonia Production from Biomass Gasification. Proceedings of Bio-Ten Conference. *Bio-ten conference* **2010**, 1–9.
- (47) Liu, X.; Elgowainy, A.; Wang, M. Life Cycle Energy Use and Greenhouse Gas Emissions of Ammonia Production from Renewable Resources and Industrial By-Products. *Green Chemistry* **2020**, 22 (17), 5751–5761. <https://doi.org/10.1039/d0gc02301a>.

- (48) Kevin Rouwenhorst. *DEHEMA and Fertilizers Europe: decarbonizing ammonia production up to 2030*. Copyright © 2019 Ammonia Energy Association. <https://www.ammoniaenergy.org/articles/dechema-and-fertilizers-europe-decarbonizing-ammonia-production-up-to-2030/>.
- (49) Julian Atchison. *Accelerating green ammonia import plans for Germany*. Copyright © 2019 Ammonia Energy Association. <https://www.ammoniaenergy.org/articles/accelerating-green-ammonia-import-plans-for-germany/>.
- (50) Kyriakou, V.; Garagounis, I.; Vourros, A.; Vasileiou, E.; Stoukides, M. An Electrochemical Haber-Bosch Process. *Joule* **2020**, 4 (1), 142–158. <https://doi.org/10.1016/j.joule.2019.10.006>.
- (51) Wang, Q.; Fang, K.; He, C.; Wang, K. Ammonia Removal from Municipal Wastewater via Membrane Capacitive Deionization (MCDI) in Pilot-Scale. *Separation and Purification Technology* **2022**, 286 (December 2021), 120469. <https://doi.org/10.1016/j.seppur.2022.120469>.
- (52) *The Paris Agreement*. <https://unfccc.int/process-and-meetings/the-paris-agreement/the-paris-agreement>.
- (53) Wang, Z.; Altenburger, R.; Backhaus, T.; Covaci, A.; Diamond, M. L.; Grimalt, J. O.; Lohmann, R.; Schäffer, A.; Scheringer, M.; Selin, H.; Soehl, A.; Suzuki, N. We Need a Global Science-Policy Body on Chemicals and Waste. *Science (1979)* **2021**, 371 (6531), 774–776. <https://doi.org/10.1126/science.abe9090>.
- (54) Brack, W.; Barcelo Culleres, D.; Boxall, A. B. A.; Budzinski, H.; Castiglioni, S.; Covaci, A.; Dulio, V.; Escher, B. I.; Fantke, P.; Kandie, F.; Fatta-Kassinos, D.; Hernández, F. J.; Hilscherová, K.; Hollender, J.; Hollert, H.; Jahnke, A.; Kasprzyk-Hordern, B.; Khan, S. J.; Kortenkamp, A.; Kümmerer, K.; Lalonde, B.; Lamoree, M. H.; Levi, Y.; Lara Martín, P. A.; Montagner, C. C.; Mougin, C.; Msagati, T.; Oehlmann, J.; Posthuma, L.; Reid, M.; Reinhard, M.; Richardson, S. D.; Rostkowski, P.; Schymanski, E.; Schneider, F.; Slobodnik, J.; Shibata, Y.; Snyder, S. A.; Fabriz Sodr , F.; Teodorovic, I.; Thomas, K. v.; Umbuzeiro, G. A.; Viet, P. H.; Yew-Hoong, K. G.; Zhang, X.; Zuccato, E. One Planet: One Health. A Call to Support the Initiative on a Global Science–Policy Body on Chemicals and Waste. *Environmental Sciences Europe* **2022**, 34 (1), 21. <https://doi.org/10.1186/s12302-022-00602-6>.



Summary



Summary

As the nitrogen boundary for the planet has already exceeded reasonable limits, new challenging environmental issues arise. The nitrogen cycle needs to be improved to ensure food security and maintain biodiversity. Therefore, there is an urgent need to bring forward nitrogen recovery technologies. These new recovery technologies should not only be efficient, but also be environmentally friendly (low energy consumption, scalable, competitive, chemical free, etc.). In this thesis, the study and optimization of electrochemical systems (ES) as an ammonia recovery technology is described. Chapter 1 provides a theoretical background of the working principles and state of the art for ES. In an ES, a cation exchange membrane (CEM) separates a feed from a alkaline concentrated solution. The ammonium is transported from the feed (supplied with wastewater), through the CEM and it is concentrated. Due to the alkaline pH, it is converted to ammonia and can be further recovered.

Donnan Dialysis (DD) can be a good strategy to enhance TAN recovery in batch operation mode since additional ammonium was removed at a lower energy input. In this thesis, the TAN (Total ammonia nitrogen, ammonium and ammonia) removal efficiency was improved by combining ES with DD. In the electrodialysis stage, a concentration gradient of cations builds up between catholyte and feed solution, as current is continuously applied. When current is no longer applied, cations (such Na^+ and K^+) diffuse back through the CEM as a result of the concentration difference. To maintain electroneutrality, DD occurs, meaning these cations will be exchanged for other cations. As the main cations are the newly supplied ammonium ions and protons formed at the electrode reaction, Na^+ and K^+ in the concentrate solution are mostly exchanged with NH_4^+ and H^+ from the feed solution. In Chapter 2, a hydrogen recycling electrochemical system (HRES) was combined with a DD cell to improve the TAN removal efficiency from synthetic urine. When continuously supplied with new influent, DD did not substantially affect the overall TAN removal efficiency of the system. In batch operation however, an additional ten percent removal efficiency was achieved through DD. The successful exchange between sodium and potassium with NH_4^+ was characterized by the transport numbers of the different cations, being NH_4^+ the most transported charge. It was demonstrated that in batch mode, DD indeed exchanges mostly NH_4^+ with Na^+ and K^+ . In continuous mode, however, mostly protons were transported from anode to cathode to compensate for electroneutrality. Furthermore, batch operation with DD consumed less energy (between $7.8 \text{ kJ g}_\text{N}^{-1}$ and $10.1 \text{ kJ g}_\text{N}^{-1}$) than continuous operation.

In Chapter 3, DD was used as a strategy to prevent inorganic scaling of the CEM. A similar combined system (HRES+DD), as in Chapter 2, was supplied with digested blackwater (after phosphate removal). Here, Donnan dialysis was not only used as TAN removal efficiency enhancer but also to prevent scaling and to prolong operation of an electrochemical system for TAN recovery. As wastewater often includes bivalent cations (Ca^{2+} and Mg^{2+}), inorganic scaling is an obstacle for implementing electrodialysis systems including membranes for nutrient recovery. The effect of bivalent cations in synthetic and real digested black water on an electrochemical system with and without an additional Donnan dialysis cell was studied. For the same Load Ratio (nitrogen load vs applied current), the system could be operated for a three times longer period when combined with the Donnan Dialysis cell. Furthermore, more nitrogen was recovered.

In Chapter 4, it was confirmed that bipolar membranes could be used to stack electrochemical systems for ammonia recovery. Efficiency aside, electrochemical systems for ammonia recovery will only be an alternative for conventional nitrogen removal technologies if their treatment capacity is increased. In Chapter 4, it was proposed to stack several cell pairs using bipolar membranes (BPM) and CEMs. The tested bipolar electrodialysis (BP-ED) stack included six cell pairs of feed and concentrate compartments. The effect of current density and load ratio (ratio between applied current to nitrogen loading) on the system performance were investigated. The up-scaled stacked system achieved a TAN transport rate of $1145.1 \pm 14.1 \text{ g}_\text{N} \text{ m}^{-2} \text{ d}^{-1}$ and a TAN removal efficiency of 80% at 150 A m^{-2} and load ratio of 1.2. The TAN removal efficiency was almost constant at different current densities. However, the lowest energy input ($18.3 \text{ kJ g}_\text{N}^{-1}$) was obtained during operation at a load ratio of 1.2 and a current density of 100 A m^{-2} .

Following the knowledge gained in Chapter 4, a bipolar electrodialysis (BP-ED) pilot plant including 3.15 m^2 of cation exchange membrane and bipolar membrane each was developed. This pilot system treated source-separated diluted urine ($\sim 1 \text{ gNH}_4^+ \text{ L}^{-1}$). As previously described, different operation parameters (i.e., LN, Current density, ...) used during the lab-scale experiments were characterized regarding their influence on the pilot plants performance. However, no direct relation was established between these parameter and the pilot plants performance. However, the effluent pH of the BP-ED stack was directly related to the removal efficiency of the system. When set to pH 4, 80% nitrogen removal was achieved. Therefore, a controlling the effluent pH strategy was used to achieve high NH_4^+ removal. This control strategy is important especially when other wastewater types are supplied

or the wastewater composition fluctuates, so the BP-ED stack is not limited in performance by fixed operation conditions. The pilot plant removed up to 88% of the NH_4^+ from urine and recovered around 700 g d^{-1} (from 1 m^3 of urine). The energy consumption was around $13 \text{ Wh g}_\text{N}^{-1}$. Nevertheless, the energy consumption can be further improved if the current efficiency losses are addressed in a improved cell design. Only $\sim 40\%$ of the applied total charge was used for cation transport over the CEM, with most losses caused by parasitic ionic shortcut currents occurring at the hydraulic manifolds of the BP-ED stack.

As the relation between current, ion loading and feed composition was not directly related with the performance of an ES for ammonia recovery in the previous chapters, a model was developed in Chapter 6 and 7 to understand their influence on the performance of ES. Firstly, in Chapter 6, a system including an ion exchange membrane (IEM) used to extract counter ionic species of interest (e.g., ion 1, such as NH_4^+) from a mixture of multiple ions was considered. Here, the species fractions at the membrane and the adjunct boundary layer were dependent of the extraction of ion 1 (concentrated on the cathode side). Hence, the species transport through the electrochemical system (ES) can no longer be described as electrodialysis-like. Furthermore, the system behaves in a dynamic state. Once the boundary layer-membrane interface is depleted, the IEM reaches a maximum current. The operation at maximum current is similar to limiting current, and the boundary layer-membrane ensemble no longer presents selectivity towards ion 1. Therefore, at a current higher than the maximum current, the fluxes of both ion 1 and other competing ions, with the same charge (ion 2, such as Na^+) occurs. As only ion 1 is recovered, the concentration of ion 2 will build up in time (on the concentrated side). Consequently, a steady state is never reached. Ideally, low currents should be applied to ES for nutrient recovery, in order to avoid reaching maximum current region and consequently ion depletion next to the membrane.

In Chapter 7, the model was further extended to illustrate in detail the transport over the CEMs (including the effect of cation loading and buffer). The influence of current, loading, supplied wastewater (ion fraction and buffer presence) were established, first on the ion transport regime and consequently on the performance parameters (removal, energy input, flux and transport number). Four transport regimes were distinguished: 1) transport of only NH_4^+ ; 2) transport of NH_4^+ and Na^+ ; 3) transport NH_4^+ and H^+ and 4) transport of all ions (NH_4^+ , Na^+ and H^+). The characterization demonstrated how a high removal can only come at the cost of more energy (solution depletion), particularly at high current densities. The buffer fraction in solution was also established as crucial parameter affecting the ion

transport over the CEM. Hence, only considering the current and TAN loading is insufficient to predict the performance of an ES and also explains why so far, high removal at low energy consumption for high current densities as illustrated in chapter 4 and 5 are never observed.

ES can be up-scaled and energy efficient. Nevertheless, more research should be further applied in order to guarantee a completely chemical free technology, with usable products (for example fertilizers), and at competitive cost. Additionally, the complete elimination of inorganic scaling during electrochemical ammonia recovery, needs to be achieved. This is included in Chapter 8 with other main outcomes of this thesis. With the gained knowledge, new research challenges were presented for electrochemical ammonia recovery. Additionally on this Chapter, a perspective on the progress of nitrogen recovery is discussed as the planet boundary for nitrogen are significantly surpassed causing severe consequences on the environment. por me deixarem abraçar todas as oportunidades que a vida me deu, por me darem força incondicional e por todo o amor quando as coisas ficaram difíceis. For all who saw me having an AWESOME Ph.D. over the last 4 years, please believe me that it would not be possible without my parents' support and love!

I am better at talking than writing, so hopefully, over the next years, I will better tell you all here listed and everyone else who participated in this journey how important you are. This book and the end of an era would have never happened if I did not have you by my side!



Epilogue

List of Publications

About the Author

Acknowledgments



List of Publications

Rodrigues, M.; Sleutels, T.; Kuntke, P.; Buisman, C. J. N.; Hamelers, B., Effects of Current on the Membrane and Boundary Layer Selectivity in Electrochemical Systems Designed for Nutrient Recovery, *ACS Sustainable Chemistry & Engineering* (2022). <https://doi.org/10.1021/acssuschemeng.2c01764>

Rodrigues, M.; Lund, R. J.; ter Heijne, A.; Sleutels, T.; Buisman, C. J. N.; Kuntke, P., Application of Ammonium Fertilizers Recovered by an Electrochemical System, *Resources, Conservation and Recycling* (2022). <https://doi.org/10.1016/j.resconrec.2022.106225>.

Rodrigues, M.; Paradkar, A.; Sleutels, T.; Heijne, A.; Buisman, C. J. N.; Hamelers, H. V. M.; Kuntke, P., Donnan Dialysis for Scaling Mitigation from during Complex Electrochemical Wastewater Ammonium Recovery, *Water Research* (2021). <https://doi.org/10.1016/j.watres.2021.117260>.

Rodrigues, M.; de Mattos, T. T.; Sleutels, T.; ter Heijne, A.; Hamelers, H. V. M.; Buisman, C. J. N.; Kuntke, P., Minimal Bipolar Membrane Cell Configuration for Scaling up Ammonium Recovery, *ACS Sustainable Chemistry & Engineering* (2020). <https://doi.org/10.1021/acssuschemeng.0c05043>.

Rodrigues, M.; Sleutels, T.; Kuntke, P.; Hoekstra, D.; ter Heijne, A.; Buisman, C. J. N.; Hamelers, H. V. M., Exploiting Donnan Dialysis to Enhance Ammonia Recovery in an Electrochemical System, *Chemical Engineering Journal* (2020). <https://doi.org/10.1016/j.cej.2020.125143>.

Kuntke, P.; Rodrigues, M.; Sleutels, T.; Saakes, M.; Hamelers, H. V. M.; Buisman, C. J. N., Energy-Efficient Ammonia Recovery in an Up-Scaled Hydrogen Gas Recycling Electrochemical System, *ACS Sustainable Chemistry & Engineering* (2018). <https://doi.org/10.1021/acssuschemeng.8b00457>.

About the Author



Mariana Rodrigues was born on the 3rd of September of 1994 in Horta, Faial. But she truly comes from a very small Portuguese island called Pico. Being raised on a small island made her aware from a very young age of the importance of cooperation and sustainability. With this in mind, she started a combined master's degree in Bioengineering at the Engineering Faculty of Porto's University in 2012. During this time, she did several internships, related to wine production/certification at the Wine Institute of Douro and Porto (IVDP) and the Cooperativa Vitivinícola da Ilha do Pico. What seemed to be an almost certain career in the wine industry, shifted, when Mariana did the Erasmus program at Wetsus (Leeuwarden, the Netherlands) in 2017 and she learn the first bits about electrochemical ammonia recovery. Once concluded her Master, she started working in 2018 as PhD student in the Resource Recovery theme at Wetsus. Her project was a cooperation between Wetsus and the Environmental Technology department of Wageningen University and it was integrated within the NEWBIES LIFE-project (including also as partners W&F Technologies, ICRA and EVIDES). The results obtained during her PhD are presented in this dissertation.



Acknowledgments

On the first day of my Ph.D. I was running around in Wetsus, trying to get a Poster done, a proposal written and an experiment starting. The anxiety levels were so high that I believe I got home and said “I want to quit”. A wise soul told me on the phone “it is your first day, the only thing you needed to do was find your desk”. To all the wise and lovely people that kept me sane over these last four years, these words and my eternal gratitude are for you.

First, I want to thank all my supervisors **Philipp, Tom, Bert** and **Annemiek**, and promotor **Cees** for always challenging me to do more and better. Tom with your vague question marks, Annemiek with your calmness, Bert with your opposite way, Cees with your critical way, and Philipp with your detailed attention, all in your unique way of being allowed this stubborn person to grow professionally, personally, and be a truly privileged Ph.D. student. Philipp you were more than a supervisor, you are a friend. Thanks for the motivational talks and the nice gatherings with your beautiful family (**Sandra** and **Tim**).

Second, thank you to **everyone from the Resource Recovery theme**, particularly the ones I worked with directly in the NEWBIES project **Sam, Federico, Pieter, Paula, Ioanna, Lisa, Slawick**, and **Jan**. Sam, thanks for driving me nuts over the last 4 years, I learned tremendously thanks to you (and thanks to **Sanne** for allowing our crazy backyard experiments/meetings). **Michel** thanks for always having an extra moment and an extra cell that I could lend.

I also want to thank all the technical team (**Wim, Jan, John, Ernst, Jan Jurien, Harm**) for all the support in the lab and all the analytical team (**Mieke, Jelmer, Lisette, Jan-Willen**) for the analysis on the great deals of samples I always delivered. A special thanks to Harm for all the patience with my urgent requests and help in building more and more in a madness of a setup.

Thank you to all Wetsus secretaries (**Jeanette, Trienke, Marnejaeike, Roely, Linda, Jannie, Laura** and **Willy**) for the patience with my last-minute meeting changes requests and help, to all human resources people, particularly to **Nynke** for saving my bureaucratic life several times, and communication staff (particularly **Hester**) for sharing our work all the time. Thank you, **Liesbeth** for handling all my Wageningen paperwork and requests with tremendous patience and carefulness.

Thanks to my Ph.D. representative colleagues and **Johannes**, Cees, and Bert for a great experience in bringing our Wetsus a step closer to excellence. Thanks to **the best PV group** that Wetsus ever had, with special attention to **Gerben** and **Catharina** and all our laughs in the borrel time.

A huge thank you to all my students **Thiago, Aishwarya, Gladys, Jens, Joana, Edwin**, and **Thomas**. I am very grateful that you took this project as your own and thought me so much too.

To all my Wetsus people, thank you for 4 great years and awesome memories. For all the uplifting and fun office talks, plenty of tasty dinners, and several adventures I would like to thank the great friends that Wetsus gave me, **Wokke, Sebastian, Sara Pinela, Danielle, Barbara, Marianne, Vania (and Raziel), Ruizhe, Yujia, Gosia, Rita Rebola, Carlo, Raquel, Rik, Mariana Rodriguez**, my old and new office mates **Paulina, Steffen, Maarten, Karine, Nimmy, Stan, Chris, Talie, Alicia, Pamela, Jessica, Cao Vinh**, and **Edward**. With particular thanks to my Dutch parents **Catarina** and **Gijs**, and my “Norths and Souths” **Sanne, João, Qingdian**. Although not listed, during this time I was very happy to belong to two houses Wetsus and Wageningen, and to all my dear colleagues from the ETE a special thanks too.

Another big special thanks to other friends all over the Netherlands, Portugal, and the world, **Quentin, Jean, Sara Morais, Magali, Vanessa, Ben, Advait, Filipe, Inigo, Thaise, Joana, Teresa, Tania, Bruno, Filipe, Emanuel (Pintado), Salomé, Ricardo, Sara Jorge, Daniela**, to all my band friends, **Daniel Jorge, Daniel Garcia, André, Joana (madrinha), Yanyue, Alik**i, for the talks, the support, the trips, the adventures, all the fun gatherings somewhere all over the world. With special attention to the divas (**Marta, Rita**, and **Monica**), **Diana** and **Claudia**, you are always there at my worst and my best.

Margo, Adam, and **Emanuel**, I cannot count the number of times you took my head out of the sand, gave me a glass of wine, and said let’s keep going. I am truly grateful for having you over the last 4 and the next 50 years.



I would like to thank my family. Aos meus padrinhos (**Maria e José**), aos meus avós (**Angelina, Manuel, Iduina e Jaime**) e tia (**Maria Leonor**) por sempre ajudarem na minha educação e ser um pouco de cada um de vocês hoje. Mas eu queria agradecer particularmente aos meus pais (**Jaime e Fernanda**) por me deixarem abraçar todas as oportunidades que a vida me deu, por me darem força incondicional e por todo o amor quando as coisas ficaram difíceis. For all who saw me having an AWESOME Ph.D. over the last 4 years, please believe me that it would not be possible without my parents' support and love!

I am better at talking than writing, so hopefully, over the next years, I will better tell you all here listed and everyone else who participated in this journey how important you are. This book and the end of an era would have never happened if I did not have you by my side!



Epilogue



*Netherlands Research School for the
Socio-Economic and Natural Sciences of the Environment*

D I P L O M A

for specialised PhD training

The Netherlands research school for the
Socio-Economic and Natural Sciences of the Environment
(SENSE) declares that

Mariana Rodrigues

born on 3rd September 1994 in Pico, Portugal

has successfully fulfilled all requirements of the
educational PhD programme of SENSE.

Leeuwarden, 7th October 2022

Chair of the SENSE board

Prof. dr. Martin Wassen

The SENSE Director

Prof. Philipp Pattberg

The SENSE Research School has been accredited by the Royal Netherlands Academy of Arts and Sciences (KNAW)



K O N I N K L I J K E N E D E R L A N D S E
A K A D E M I E V A N W E T E N S C H A P P E N



The SENSE Research School declares that **Mariana Rodrigues** has successfully fulfilled all requirements of the educational PhD programme of SENSE with a work load of 40.7 EC, including the following activities:

SENSE PhD Courses

- o Environmental research in context (2019)
- o Research in context activity: 'Member of the Organizing Committee of ESEE2021'

Other PhD and Advanced MSc Courses

- o Business Development Course, Wetsus (2018)
- o Illustrations for scientific Publication, Wetsus (2018)
- o Data Analysis and Modelling using Python, Wetsus (2018-2019)
- o Bath Electrochemical Winter School, University of Bath (2019)
- o Wetsus Personal Development courses, Wetsus (2019)
- o Scientific Writing, Wageningen Graduate Schools (2020)
- o Introduction to R and Rstudio, PE&RC graduate school (2021)

Management and Didactic Skills Training

- o Supervising four MSc student with thesis (2019-2020)
- o Supervising one BSc student with internship (2021)
- o Assisting practicals of the MSc course 'Biological Wastewater' (2019-2020)

Oral Presentations

- o *Exploiting Donnan dialysis to enhance ammonia recovery in an electrochemical system.* 10th IMSTEC: International Membrane Science & Technology Conference, 2-6 February, 2020, Sydney Australia
- o *Minimal Bipolar configuration for ammonia recovery.* ESEE: European symposium on electrochemical engineering, 13-17th June 2021, Leeuwarden (online), The Netherlands
- o *Scaling up electrochemical ammonium recovery.* Wetsus internal congress, 25 November 2021, Leeuwarden, The Netherlands

SENSE coordinator PhD education

Dr. ir. Peter Vermeulen



This thesis was performed in the cooperation framework of Wetsus, European Centre of Excellence for Sustainable Water Technology (www.wetsus.eu). Wetsus is co-funded by the Dutch Ministry of Economic Affairs and Ministry of Infrastructure and Environment, the European Union Regional Development Fund, the Province of Fryslân, and the Northern Netherlands Provinces. This thesis was also supported by the LIFE-NEWBIES project. The LIFE-NEWBIES project (LIFE17 ENV/NL/000408) has received funding from the LIFE Programme of the European Union. The authors finally like to thank the participants of the research theme “Resource Recovery” for their financial support.

Financial support from Wageningen University and Wetsus for printing this thesis is gratefully acknowledged.

Cover design by Cláudia Medeiros.
Printed by Proefschriftenprinten.nl